



**ISOLATION AND CHARACTERIZATION OF NOVEL BACTERIOPHAGES
AGAINST MULTIDRUG RESISTANT *Enterobacter cloacae* AS
ALTERNATIVES TO ANTIBIOTICS**

MARTIN INDONGOLE INYIMILI

I56/ 81326/2015

BSc. Biology (University of Nairobi)

**A thesis submitted in partial fulfillment for the degree of Master of Science in
Biotechnology in the Department of Biochemistry in the University of Nairobi.**


March, 2022

DECLARATION

This thesis is my original work and has not been presented for a degree in any university.

MARTIN INYIMILI

Registration Number: 156/81326/2015

Signature.......... Date..... 8th November, 2023

This thesis has been submitted for examination with our approval as university and academic supervisors.

Prof. Edward Muge,

Senior Lecturer,

Department of Biochemistry,

University of Nairobi,

Signature..... Date..... 08.11.2023

Dr. Lillian Musila,

Research Scientist,

Kenya Medical Research Institute KEMRI /USAMRD-A

Department of Emerging Infectious Diseases.

Signature.......... Date..... 09.11.2023

Dr. Atunga Nyachio,

Head of Research,

Institute of Primate Research,

National Museums of Kenya,

Signature..... Date..... 09.11.2023

DEDICATION

To my wife Mary Wairimu for the love, encouragement, and dedication to family and for taking care of our kids while I was away.

To my three sons, Ryan Rodney, Ivan Adams and Bryant Collin, and daughter Lindsey Abigail, for the many lessons I have learned along the way.

To my dad John and mum Betty for the immense sacrifices you made to make me what I am today.

ACKNOWLEDGEMENT

This study was carried out under the supervision of Dr. Lillian Musila, Principal Investigator (PI) Antimicrobial Resistance (AMR) at Kenya Medical Research Institute (KEMRI) Headquarters, Dr. Atunga Nyachieo, Senior Research Scientist at the Institute of Primate Research (IPR), Karen and Professor Edward Muge, Lecturer at the Department of Biochemistry, University of Nairobi. I wish to convey my gratitude to my supervisors for their insightful ideas, guidance, suggestions, and encouragement right from the development of the research proposal to the end of this study. I sincerely thank Dr. Musila and Dr. Nyachieo for hosting me in their respective laboratories at Kenya Medical Research Institutes', Centre for Microbiology Research in Mbagathi and at the Institute of Primate Research, Phage Biology Laboratory respectively. Many more thanks to Dr. Musila for funding this work and many thanks to Prof. Wallace Bulimu for linkage to this work, I truly appreciate.

I am greatly indebted to staff in these two laboratories who made this work a success. Specifically, the staff at KEMRI led by Project Manager Mr. Eric Odoyo, Daniel Matano Mbuvi, Fred Tiria, Martin Georges, Cecilia Katunge and Valerie Odundo and staff at IPR led by Assistant Laboratory Manager, Mr Gerishon Deya, Ivy Mutai, Dennis Koti, Angela Juma, and Martin Mulandi.

I am also indebted to my colleagues at the Department of Human Anatomy led by the Chairman of Department Prof. Moses Obimbo, Technologists Ms. Margaret Irungu, Ms. Esther Mburu, Mr. Robert Chemjor, Mr. Jacob Gimongo and Mr. Acleus Murunga for shouldering my responsibilities while I was away. Special thanks to the late Professor Saidi Hassan for encouraging me to take this course and for allowing me time to attend my course work.

I am also grateful to Mr. Accadius Lunayo and Mr. Fernando Noutin for their immense help during analysis and laboratory work respectively and to Mr. Kevin Ochwedo for his help during the formative stages of this work.

I am grateful to my family, especially my wife, Mary Wairimu Mukuwa, for the support, both material and otherwise, for the encouragements, for standing with me throughout this work until you mastered phage work concepts that were completely different from your IT skills and for taking care of the family while I was away. This was not in vain, the future is brighter for both of us. And to my three sons and my only daughter, the lessons along the way have been invaluable, will cherish you always. To Mum and dad, thank you for your encouragements and for pushing me this far.

I will not forget the Almighty God, who granted me health, strength, knowledge and wisdom in putting up all this work, to him I give glory.

TABLE OF CONTENTS

DECLARATION.....	Error! Bookmark not defined.
DEDICATION.....	iii
ACKNOWLEDGEMENT.....	iv
LIST OF Figures.....	ix
LIST OF TABLES.....	x
ABSTRACT.....	xi
CHAPTER ONE.....	1
1.0 INTRODUCTION.....	1
1.1. Background information.....	1
1.2. Research Problem Statement.....	2
1.3. Rationale/Justification.....	3
1.4. Research Question.....	3
1.5 Null Hypothesis.....	4
1.6 Alternative Hypothesis.....	4
1.7 Objectives.....	4
1.7.1 General Objectives.....	4
1.7.2 Specific objectives.....	4
CHAPTER TWO.....	5
2.0 LITERATURE REVIEW.....	5
2.1 History of Antibiotic Resistance.....	5
2.2 Future Threat of Antimicrobial Resistance.....	7
2.3 Description of <i>Enterobacter cloacae</i> ; Occurrence, Morbidity and Mortality.	9
2.4 Epidemiology of <i>E. cloacae</i>	11
2.5 Challenges Posed by Multidrug-Resistant <i>E. cloacae</i>	12
2.6 Global Distribution of MDR <i>E. cloacae</i>	14
2.7 Life Cycle of Phages.....	15

2.7.1	Types of Phages	16
2.8	Phages as alternatives to antimicrobial resistance	18
2.8.1	Historical and current use of phages	19
2.8.2	Advantages and Disadvantages of Phage Use	22
2.9	Current use of Phages in Combating <i>E. cloacae</i>.....	23
CHAPTER THREE		25
3.0	METHODOLOGY.....	25
3.1	Study site and design	25
3.2	Bacteria culture	25
3.3	Sampling strategy	26
3.3.4	Sample collection	27
3.4	Isolation of bacteriophages targeting <i>E. cloacae</i>.	29
3.4.3	First enrichment of potential phages from liquid samples	29
3.4.4	Second enrichment of potential phage from each of the sample collected from the different sources	29
3.5	Isolation of bacteriophages from the enriched media	29
3.6	Phage titration, propagation, cross infection and identification.....	30
3.7	Phage titration and propagation prior to purification.....	31
3.7.3	Phage precipitation and Purification.	31
3.7.4	Host Range Determination.....	32
3.7.5	Multiplicity of Infection (MOI).	33
3.8	Physical characterization of isolated phages.....	34
3.8.3	Phage genomic DNA extraction and sequencing.....	34
3.8.4	PCR and Gel Electrophoresis.....	35
3.9	DNA Library preparation.	36
3.10	Sequencing and Base-Calling.	39
3.11	Genome characterization and Phylogenetic analysis	40
3.12	Scientific and Ethical Approval	40

3.13	Data Analysis	40
3.14	Biosafety	41
CHAPTER FOUR.....		42
4.0	RESULTS.....	42
4.1	Phenotypic confirmation of <i>E. cloacae</i> isolates.....	42
4.2	Morphology of <i>Enterobacter cloacae</i>	43
4.3	Antimicrobial Susceptibility testing.....	44
4.4	Phage Screening.....	46
4.4.1	Spot test results	46
4.4.2	Morphology of phages obtained	47
4.5	Physical characterization.....	48
4.6	Host Range Analysis.....	51
4.7	Test for purity of phage DNA.....	53
4.8	Genomic characterization.....	54
4.8.1	DNA extraction, quantification and library preparation	54
4.8.2	Phage sequencing	55
4.8.3	Sequence assembly, annotation, alignment and analysis	56
4.8.4	Alignment of bacteriophage sequences.....	58
4.9	Phylogenetic Analysis.....	60
5.0	DISCUSSION, CONCLUSION AND RECCOMENDATIONS.....	62
5.1	DISCUSSION	62
5.2	Conclusions and Recommendation	72
5.3	Recommendations.....	73
5.4	Limitations of the Study.....	73
REFERENCES.....		74
APPENDICES		87

LIST OF FIGURES

Figure 2.1: A World Map Showing the Global Distribution of Multidrug-Resistant (MDR) <i>E. Cloacae</i>	14
Figure 2.2: Lytic Cycle of a bacteriophage.....	15
Figure 2.3: Lysogenic Cycle of a bacteriophage.....	16
Figure 3.1: Schematic representation of experimental framework of the isolation, purification selection and characterization of phages against MDR <i>E. cloacae</i>	28
Figure 4.1: <i>Enterobacter cloacae</i> clinical isolate cultured on different types of media. .	43
Figure 4.2 : A micrograph of <i>E. cloacae</i> as seen under the light microscope after Gram's staining.....	44
Figure 4.3 : Spot assay results revealing clear zones indicative of the presence of bacteriophages on the bacterial lawns.....	46
Figure 4.4: Double layer plaque assay revealing plaques of various sizes on the host bacteria.....	47
Figure 4.6: Graphical representation of the phage titres at different pH and Temperature variations.....	50
Figure 4.7: Gel electrophoresis of bacteriophages DNA and respective amplicons of 16S rRNA gene.	53
Figure 4.8: Circular Genome View for vB_Eclo_MII_001.....	57
Figure 4.9 : Circular Genome View for vB_Eclo_MII_002.....	58
Figure 4.10 : Multiple Sequence alignment of the isolated bacteriophages with related sequences from National Center for Biotechnology Information (NCBI) database.....	59
Figure 4.11: Phylogenetic analysis of the sequenced bacteriophages in comparison to those found in databases.....	61

LIST OF TABLES

Table 4. 1: Description of bacterial colonies of <i>E. cloacae</i>	42
Table 4. 2:Antimicrobial susceptibility testing result for <i>Enterobacter cloacae</i> clinical isolates blinded as Bp.....	45
Table 4. 3: Host Range Analysis of the 19 isolated bacteriophages	52
Table 4. 4: Extracted Phage DNA quantification on both Nanodrop and Qubit platforms.	54
Table 4.5: Phage DNA library Preparation prior to sequencing. Results are recorded after each step to attain the required threshold for sequencing	55
Table 4. 6: Sequencing Results	55
Table 4.7: Classification of one of the isolated phages as obtaine from PATRIC.....	60

ABSTRACT

Enterobacter cloacae is a significant nosocomial pathogen, causing bacteremia and infections of the lower respiratory tract, urinary tract, and intra-abdominal cavity. Acquisition of antibiotic resistant genes due to increased pressure on antibiotics use has resulted in emergence of multidrug-resistant (MDR) *Enterobacter* species implicated in hospital acquired infections. Development of antibiotic regimens against MDRs is not at par with bacteria rates of resistance necessitating the need for adoption of alternative strategies among them the use of bacteriophages (phages). The general objective of this study was to identify and characterize bacteriophages that can lyse gram-negative MDR *E. cloacae* bacteria with potential clinical applications. Three environmental water samples from each site were obtained from Kenyatta National Hospital (KNH) sewer, Chiromo River, Mathare River, Kibera slums and Zimmerman and fresh water (Lake Victoria). Host bacteria were obtained from the KEMRI-CMR repository. Spot test and plaque assay were used to screen and quantify the isolated bacteriophages. Isolated bacteriophages were tested for their stability at different temperatures (4, 25, 37, 60 and 90 °C) and pH (2.0, 4.5, 5.5, 7.5, 9.0, 11.5 and 13.0). Host range determination using 28 isolates of *E. cloacae* bacteria and one *Staphylococcus aureus* bacteria as a negative control was done. Whole genome sequencing was done using the Nanopore platform and results analysed using various bioinformatics tools like PhiSiGns programmes, GeneMark, REsFINDER, among others. Nineteen (19) bacteriophages were isolated with all 19 phages lysing 12/28 (42.9%) *E. cloacae* bacteria isolates. The phages were stable at 4, 25 and 37 °C and 4.5, 5.5, 7.5, 9.0, and 11.5 pH. The selected 5 phages had dsDNA genomes with no genes associated with antibiotic resistance or toxicity. Three phages belonged to the family Autographiviridea/Studiivirinae while two could not be assigned. The study identified potentially suitable phage candidates for *Enterobacter cloacae* therapy due to their wide host range against endemic clinical isolates and their lack of genes associated with resistance and toxicity.

CHAPTER ONE

1.0 INTRODUCTION

1.1. Background information

Nosocomial infections are hospital-acquired infections (HAIs) caused by various pathogens among them; bacteria, fungi, viruses, parasites, and other organisms. The predominant HAI are caused by *Enterococcus faecium*, *Staphylococcus aureus*, *Klebsiella pneumoniae*, *Acinetobacter baumannii*, *Pseudomonas aeruginosa* and *Enterobacter* spp; acronymed ESKAPE (Levy & Marshall, 2004). Most of these infections have become resistant to antibiotics which have been conventional medications of choice. Infections by the two bacterial species have become difficult to control or treat due to the transfer and acquisition of antibiotic resistance. Continued application of antibiotics in the management of these diseases has brought about selection of resistance genes in the bacterial populations (Levy & Marshall, 2004). The development of new antibiotics is not moving as fast as these pathogens are gaining resistance hence causing a challenge to health systems.

An alternative to the use of antibiotics in the management of bacterial infections is the use of bacteriophages or simply “phage therapy. Bacteriophages are viruses discovered in the early-20th century (Clokier et al 2011). Their dominant property was their ability to “eat” bacterial cultures by specifically reducing their turbidity and consequently named phage. Phages contain nucleic acids, which can be either DNA or RNA covered in a protein coat whose main function is to protect the phage genome as it moves from one infected cell to another (Levy & Marshall, 2004). Phages replicate via two mechanisms, the lytic phase, and lysogenic phase. In the lytic phase, phages infect the bacterial cell, replicate, and lyse the cell, with phage progeny finding and infecting new host bacterial cells. The lytic phages are suitable for phage therapy, an example being T4 bacteriophage that infects *E. coli* bacteria found in the human gut. The lysogenic phages, also called temperate phages, integrate their genome with that of the host and replicate alongside the host genome. They remain latent until host circumstances decline, perhaps owing to nutritional depletion, at

which point the endogenous phages become active resulting in cell lysis (Levy & Marshall, 2004).

Western countries successfully used the phage therapy however, they halted its use due to emergence of antibiotics (Principi, Silvestri, & Esposito, 2019a). With the growing threat of illnesses associated with multidrug-resistant bacteria and limited availability of newly launched antibiotics for the future, phages, especially lytic bacteriophages, are being investigated as alternative or complimentary therapies.

1.2. Research Problem Statement

The growing challenge of MDR *E. cloacae* in nosocomial infections puts a strain on healthcare systems and the global economy. Some of the repercussions include high mortality and morbidity rates, increased treatment costs, diagnostic ambiguity, and a loss of trust in traditional medicine. According to Gillian (2018), the prevalence of *E. cloacae* in children is 1.6%, with a 0.1% estimated fatality rate in Kenya. With big pharmaceutical companies failing to invest in the development of new antibiotics, there is a need for novel and low-cost techniques of treating MDR bacteria with minimum injury to host cells and interference with natural flora.

Despite the use of phages commencing decades ago, their use in treating MDR bacterial and other nosocomial infections has remained in nascent stages. One of the challenges is paucity of reliable experiments and strict regulations on use of phages to address human health. Phages have been effectively used to manage *E. coli* and other infections (Anand et al., 2020). With increased knowledge in biotechnology, phages use as an alternative to antibiotics is gaining traction. In Kenya, there is no study or clinical experiments that have been documented regarding phage use as an option to antibiotics particularly in managing the infections caused by MDR *E. cloacae*. This study, seeks to find bacteriophages that can be used as an alternative in the management of MDR *E. cloacae* since it is among the leading causative agent in HAIs.

1.3. Rationale/Justification

MDR *E. cloacae* are among important opportunistic bacteria. They have been found to not only contain antibiotic resistant genes, but also possess enzymes such as carbapenemases and Extended-Spectrum-Beta-Lactamases (ESBL) which serve to neutralize the antibiotic effect of a wide of range of antibiotics (Tamma et alro 2019). The prevalence of MDR *E. cloacae* has increased globally because of the increased use of extended-spectrum carbapenems and cephalosporin antibiotics in therapy. Antibiotics administered to patients with infections from MDR bacteria is likely to be unsuccessful(Haney & Hancock, n.d.). The need to have alternative approaches in treatment and management of these infections is evident and phage therapy is a potential solution (Royer et al 2021).

Bacteriophages have many advantages over antibiotics; among them is their abundance in nature in many habitats such as sea water, soil, sewage and fresh water. Bacteriophages target specific bacterial hosts, lyse them, and produce progeny that go on to infect other bacterial cells. Their lytic activity enables them to rapidly kill their bacterial host. Phages are less toxic than antibiotics due to the specificity of their hosts and are less likely to affect human cells or alter the normal bacterial flora of the host. Phages are also known to penetrate the polysaccharide matrix of the bacterial cell membrane which is impenetrable to many antibiotics (Lin et al 2017).

1.4. Research Questions

1. Are there multidrug resistant *E. cloacae* bacteria clinically isolated?
2. What are the therapeutic characteristics of the isolated bacteriophages have against MDR *E. cloacae*?
3. Are the isolated bacteriophages isolated against MDR *E. cloacea* genetically novel?

1.5 Null Hypothesis

There are no lytic bacteriophages in the environment that can lyse MDR *E. cloacae*.

1.6 Alternative Hypothesis

There are lytic bacteriophages in the environment that can lyse MDR *E. cloacae*

1.7 Objectives

1.7.1 General Objectives

To isolate and characterize bacteriophages against MDR *E. cloacae* bacteria for potential clinical applications.

1.7.2 Specific objectives

1. To screen *Enterobacter cloacae* bacteria and select representative strains for bacteriophage isolation
2. To isolate and identify stable lytic bacteriophages from different sources with specific activity against MDR *E. cloacae* bacteria.
3. To genetically characterize the identified phages and select novel phages with broad activity against *E. cloacae* strains.

CHAPTER TWO

2.0 LITERATURE REVIEW

2.1 History of Antibiotic Resistance

Since the introduction of sulphonamides as the first efficient antibacterial medicines in 1935 (Jeśman, Młodzik, & Cybulska, 2011), the establishment of resistance mechanisms has prohibited their use as therapeutic agents. Resistance to sulfonamides was first identified towards the end of the 1930s and early 1940s (Sköld, 2000), and the same mechanisms are still active over 70 years later (Sköld, 2000). Alexander Fleming developed penicillin between 1928 and 1940. Penicillinase was discovered by two members of the Penicillin research team some years before penicillin was approved as a medicinal drug (Bhattacharje, 2016). Resistant strains capable of inactivating penicillin grew common as the medicine became more extensively used, necessitating synthetic efforts to chemically alter penicillin to avoid cleavage by penicillinases. Amazingly, bacterial penicillinases were found long before the use of the antibiotic, according to new results that indicate *r-genes* in bacteria as components of natural microbial populations (Demain, 2014).

Streptomycin was first used to treat tuberculosis (TB; "The Great White Plague") in 1944. During patient therapy, mutant strains of *M. tuberculosis* were found to be resistant to the antibiotic therapeutic dose in use. A similar chain of events has occurred with other antibiotics that have been identified and put into clinical practice (Vilchèze & Jacobs, 2015). Most bacterial infections involved with human illnesses have become multidrug-resistant (MDR) strains as a result of antibiotic usage (Turner *et al.*, 2017). MDR *M. tuberculosis*, for example, is an important disease in both developing, middle income and developed countries, and has evolved into a twentieth-century form of an old pathogen. Nosocomial (hospital-associated) infections with *Acinetobacter baumannii*, *Burkholderia cepacia*, *Campylobacter jejuni*, *Citrobacter freundii*, *Clostridium difficile*, *Enterobacter spp.*, *Enterococcus faecium*, *Enterococcus faecalis*, *Escherichia coli*, *Haemophilus influenzae*, *Klebsiella pneumoniae*, *Proteus mirabilis*, *Pseudomonas aeruginosa*,

Salmonella spp., *Serratia* spp., *Staphylococcus aureus*, *Staphylococcus epidermidis*, *Stenotrophomonas maltophilia*, and *Streptococcus pneumonia* have become a common phenomenon. (Davies, 2010 MMBR,)

Superbugs are microbes that cause increased morbidity and mortality levels because of the many genes and mutations conferring high levels of resistance to antibacterial drugs that are primarily recommended for their intervention; treatment strategies for these superbugs are limited, and hospitalisations have become longer and much more expensive. Super-resistant bacteria have improved virulence and transmissibility in some circumstances. In reality, antibiotic resistance might be regarded as a virulence factor (Tanwar *et al.*, 2014). Antibiotic use in the treatment of the most common Gram-negative bacteria, like *E. coli*, *S. enterica*, and *K. pneumoniae*, which are responsible for a range of human and animal illnesses, has been linked to the rise in antibiotal resistance during the previous half-century. This has been observed in the classes of β -lactam and β -lactamases of antibiotics, which are related-inactivating-enzyme antibiotics. Several other groups and classes of resistance-related β -lactamases have been found, totalling up to 1,000 (Davies, 2010).

P. aeruginosa has progressed from a minor infection of burn wounds to being a serious nosocomial danger in hospital-acquired infections. Coincidentally, antibiotic resistance mechanisms for *P. aeruginosa* have emerged with the advent of novel antiobiotic therapies that include the highly therapeutic interventions (such as β -lactams and aminoglycosides) and thus becoming a serious worry for patients with cystic fibrosis due to its ability to persist as well as avoid human immune defense mechanisms. Antibiotic resistance has been linked to lengthy periods of antibiotic use in cystic fibrosis patients (Laxminarayan *et al.*, 2013; Horrevorts, 1990).

A. baumannii on the other hand is a relatively modern Gram-negative microbe that is mostly nosocomial. Similar to *Pseudomonas*, this pathogen possesses *r-genes* and pathogenicity determinants, resulting in increased death and morbidity rates (Peleg, 2008). *Acinetobacter*'s infectious qualities are assumed to be derived from its ability to survive

and biodegrade within the environment; also, majority of the variants are innately proficient for DNA absorption and therefore have increased rates of adaptive evolution. Additionally, *A. baumannii* is quickly changing, with current sequenced genomes revealing about 28 genomic islands that contain determinants of antibiotic resistance, with over 50% of the inserts encoding for functions of virulence type IV secretion systems (Barbe, 2004).

Although *E. cloacae* complex species are widespread all-natural habitats, they are also known disease infection agents, with *E. cloacae* and *E. hormaechei* being common and usually identified in patient clinical samples. It is therefore by no surprise that, *E. cloacae* has not only been identified as one of the most prevalent *Enterobacter* sp. responsible for nosocomial diseases over the last decade, but one of the microbes whose profile regarding its antibiotic resistance has been widely published. Despite its relevance in nosocomial infections, the pathogenicity processes as well as determinants leading to sickness related with the ECC are not well characterized; partly because of lack of understanding and its dispersion. Its pathogenicity is determined by its capacity to build biofilms and produce several cytotoxins among them enterotoxins, hemolysins, as well pore-forming toxins (Mezzatesta et al 2012). Although clonal outbreaks involving variants of the ECC were uncommon, numerous variants and races recently demonstrated relationships with patients clinical materials, notably urine and sputum (Izdebski et al., 2015)(Izdebski et al., 2014). Because of the widespreading of ESBL and carbapenemases genes in *E. cloacae* this species has lately evolved to be the third-most *Enterobacteriaceae* spp implicated in HAIs after *E. coli* and *K. pneumonia* (Potron et al 2013).

2.2 Future Threat of Antimicrobial Resistance

Several factors contribute to the rising public health issue of antimicrobial resistance (AMR). Appropriate and improper use of anti-infective medications for human and animal health, food production, as well as insufficient efforts to limit infection transmission have been most cited. Recognizing the public health threat caused by AMR, various states,

international agencies, and other organizations throughout the world have taken steps to combat it through initiatives implemented in animal and human sectors (Dramowski et al., 2017).

AMR poses a huge challenge to the global society in terms of depth, breadth, and complexity (Marshall, 2018). Resistance to antibiotics jeopardizes strides in health care, production of food, as well as life expectancy. Combating these dangers entails preventing infections in the first place, lowering resistance development through better antibiotic use, and slowing resistance dissemination once it has occurred (CDC, 2019).

AMR reports are frequently based on laboratory data on microorganisms acquired from human patients. Despite informed decisions on individual patient treatment and as evidence for policies at the local, national, and international levels, cases of AMR have become pervasive in the public health, raising concerns about whether authorities will be able to manage these threats in the event of pandemics (WHO, 2012).

Public health organizations are concerned about the challenges that AMR would present, as well as the cost of treating a range of common infections, which would result in delays in adequate treatment or, in the worst-case scenario, an inability to deliver appropriate treatments. Many recent medical developments, such as cancer treatments and organ transplantation, are contingent on the availability of anti-infective medications (Pharell *et al.*, 2012). Resistance results in increased morbidity, extended sickness, a higher risk of complications, and higher fatality rates. This results to an economic impact that includes lost productivity (loss of income, decreased worker productivity, time spent with family) and increased diagnostic and treatment costs (consultation, infrastructure, screening, equipment costs, medications) (“Global Action Plan on Antimicrobial Resistance,” 2015) (WHO, 2015). The health and economic repercussions of AMR are significant and costly, but they are difficult to measure precisely because available data in many countries is insufficient. There is also a major human burden connected with it (pain, changes in everyday activities, and psychological costs) (Holmes *et al.*, 2016).

2.3 Description of *Enterobacter cloacae*; Occurrence, Morbidity and Mortality.

In recent years, *E. cloacae* has been the most often isolated species of *Enterobacter*, a genus within the *Enterobacteriaceae* family that has caused infections in hospitalized and immunocompromised individuals. *E. cloacae* bloodstream infection (EcBSI) is a new nosocomial pathogen with rising antibiotic resistance (Huang, 2013). HAI are major sources of morbidity and mortality across the world (Bao *et al.*, 2012). The typical members of the gastrointestinal tract flora, *Enterobacter* species, are major pathogens for a range of illnesses, including wound infections, urinary tract infections, pneumonia and bacteremia, particularly in HAI. *Enterobacter* species seldom cause illness in healthy children; nevertheless, in patients with underlying disorders, particularly preterm babies, they often cause bacteremia (Unlemahn *et al.*, 2019).

Enterobacter cloacae may be found both on land and in water environments. This bacterium can also be found in human and animal digestive systems as commensal microflora. Additionally, *E. cloacae* can be found colonising both insects and plants as a pathogenic agent. Genetically *E. cloacae's* is diverse as reflected in the varied environments it inhabits. (Mezzatesta *et al.*, 2012). Epidemiological data from MLST and PFGE techniques has shown clonal complexes of *E. cloacae* responsible for the widespread pandemics around the globe. Primarily, *E. cloacae* is a common nosocomial pathogen, causing bacteremia, endocarditis, inflammatory arthritis, osteomyelitis, skin/soft tissue infections, lower respiratory tract infections, urinary tract infections, and intra-abdominal infections (Fata *et al.*, 1996). It has also been shown that *E. cloacae* may colonize a wide range of medical, intravenous, as well as other healthcare equipment (Dugleux *et al.*, 1991). Colonization of surgical instruments as well as operational cleaning solutions have all been linked to nosocomial infections (Wang *et al.*, 2000). *E. cloacae* has been routinely documented as a hospital acquired pathogen in newborn facilities for over a decade, with various outbreaks of infection (Fernández-Baca *et al.*, 2001) (Pestourie *et al.*, 2014).

Gastrointestinal disorders, life-threatening infections, malignancies, preterm, central venous catheter placement, ventriculostomy, placement of a ventriculoperitoneal shunt catheter, extended antibiotic therapy, parenteral nutrition, and immunosuppressive medication are all risk factors for *Enterobacter* bacteremia. *E. cloacae* accounted for 3.9 percent of all hospital acquired bloodstream infections, according to a large-scale survey done in the USA. At the same time, there was a considerable increase in *E. cloacae* antibiotic resistance rates (Annajhala *et al*, 2019; Izdebski *et al.*, 2015)

According to a research done by (Chen & Huang, 2013), *E. cloacae* was the most prevalent species in the United States, accounting for 78 occurrences (81.3%). The isolation rate of *E. cloacae* has grown in a Taiwanese hospital since 1995, according to a study conducted by (Xia *et al.*, 2016), and this increased prevalence was connected to increased mortality rates from *E. cloacae* illnesses.

In the United Kingdom on the other hand, epidemiological research on *E. cloacae* indicated a rising prevalence coupled with high fatality rates of 24/79, which translates to 34.3% (Eichenberger & Thaden, n.d.) (Josh, 2012). WHO noted in its first global antimicrobial resistance monitoring report in 2014 that resistance to antimicrobial drugs was rising in all six WHO regions in Africa. In Sub-Saharan Africa, *Enterobacter* species account for 20% of all-age mortality and 33% of morbidity. In South Africa, a significant rise in ESBL synthesis as well as carbapenemase variants in *K. pneumoniae* and *E. cloacae* is noted (Annajhala *et al.*, 2019a).

During a 4-year period in Senegal, the detection rate of carbapenemases among *E. cloacae* blood isolates from public laboratories was 1.9 percent, and the death rate was estimated to be 0.1 percent (Dia *et al.*, 2016). Multidrug-resistant bacteria were to blame, including *E. cloacae*, which secretes broad-spectrum betalactamase, MRSA, and *Pseudomonas aeruginosa*. Establishment of an infection control program in a teaching hospital was successful in lowering the rate of *E. cloacae* from 5.8 to in 2003 to 2.8% in 2006 in Nigeria (Brady *et al.*, 2013).

Few investigations on the morbidity and mortality of *E. cloacae* have been undertaken in Kenya. However, Saleem *et al.* (2010) found elevated numbers of *E. cloacae* infections. This study discovered that coagulase-negative *Staphylococci* (CoNS) were isolated as the prevalent organism (30.1 percent), followed closely by *E. cloacae* (21%), *Citrobacter* spp (14%), *Klebsiella* spp (11%), *Enterococcus* spp (9%), *Escherichia coli* (7%), *S. aureus* (4%), and *Proteus* spp (4%). (1 %). According to Gillian (2018), the prevalence of *E. cloacae* in children is 1.6 percent, with a 0.1 % estimated fatality rate.

2.4 Epidemiology of *E. cloacae*

Increased morbidity and an estimated 40% mortality have resulted from multidrug resistance among clinically relevant gram-negative bacteria (GNB) such as *Escherichia coli*, *Klebsiella pneumoniae*, *Enterobacter* spp., *Pseudomonas aeruginosa*, and *Acinetobacter baumannii* (WHO, 2014). Last-resort medications like tigecycline in use for the control and treatment of infections arising from these infections have proved unfavourable and costly. One significant β -lactam medication class that is used to treat serious bacterial infections that are resistant to many drugs is carbapenems (Founou, Founou, & Essack, 2017). Consequently, it has been determined that the worldwide rise in carbapenem resistance (CR) poses a serious risk to public health (WHO, 2014).

Chromosomally-encoded or plasmid-encoded carbapenemases, which are classified into three classes, are the main mediators of CR: Class A, which includes, *K. pneumoniae* carbapenemases (KPC); Class B, which includes, New Delhi Metallo- β -lactamase (NDM), the Verona integrin-encoded Metallo- β -lactamase (VIM), and Imipenemase (IMP); and Class D, which includes OXA-48 and -181 (Martínez *et al.*, 1999). The constitutive over-production of AmpC and alterations in permeability brought on by the loss or down-regulation of porins are secondary mechanisms for CR. (Bauernfeind, 1986). The frequency of carbapenem resistance in GNB varies from less than 1% to 60%, which is a developing concern in Africa (Annavajhala, Gomez-Simmonds, & Uhlemann, 2019b). According to recent research conducted in Tanzania and Uganda, the prevalence may

reach 22.4–35%, with *K. pneumonia* and *P. aeruginosa* being the main carriers of the CR genes blaVIM, blaOXA-48, blaIMP, blaKPC, and blaNDM-1 (Mushi, Mshana, Imirzalioglu, & Bwanga, 2014)(Okoché, Asiimwe, Katabazi, Kato, & Najjuka, 2015). Only the carbapenemase genes blaNDM-1, blaOXA-23, blaSPM, and blaVIM-2 have been found in Kenya, and they are found in the bacteria *K. pneumoniae*, *P. aeruginosa*, and *A. baumannii*. Nairobi, Kiambu, Kilifi Kisumu, Kericho and Kisii are the six Kenyan counties where these are from hospitals. Kenya's high concentrations of ESBL-producing Enterobacteriaceae have led to an increase in the usage of carbapenem, which has coincided with a rise in CR, hence close monitoring(Musila Id et al., 2021).

2.5 Challenges Posed by Multidrug-Resistant *E. cloacae*.

Both acquired and inherent antibiotic resistance processes have decreased the number of viable therapies available for *E. cloacae* infections. *E. cloacae* is innately immune to β -lactam antibiotics and 1st - and 2nd generation cephalosporins because of the low-level expression of chromosomal ampC genes that encode for an inducible AmpC-type Bush group 1 (class C) cephalosporinase. AmpD mutations that cause constitutive hyperproduction (derepression) of AmpC can result in resistance against 3rd-generation cephalosporins and aztreonam (Cheng *et al.*, 2017).

The rising incidence of *E. cloacae* is one of the most significant issues in MDR. Most penicillins are resistant, with their mechanisms of resistance conferred by β -extended-spectrum -lactamase (β - ESBL) genes (Cheng *et al.*, 2017). Discovery of plasmid encoding genes in *E. cloacae* was made in 1989. Since then, the incidence of ESBL-encoding *E. cloacae* has grown, notably in nosocomial settings and among patients who have previously received antibiotics. Resistance to β -lactam is now often mediated by both ESBL and AmpC, resulting in near-pan-resistance(Chavda *et al.*, 2016).

Another challenge of MDR *E. cloacae* is the spread of carbapenem-resistant *E. cloacae* complex (CREC) aided by genetic variables. Carbapenem resistance is defined by one or more pathways, including carbapenemase synthesis. Carbapenemases, which can

hydrolyze carbapenem drugs and other β -lactam antibiotics, have the highest antibiotic resistance (Liu *et al.*, 2019). *K. pneumoniae* carbapenemase (KPC) is one of the most prevalent causes of resistance against carbapenem in *K. pneumoniae*, and can spread widely due to its presence on numerous plasmids (Adler *et al.*, n.d.). KPC enzymes are a large family of class A serine carbapenemases generated mostly by *K. pneumoniae*. In *Enterobacteriaceae*, β -lactamase resistance is most often linked with the overproduction of enzymes from inducible or de-repressed chromosomal genes (though AmpC can also be plasmid-based), whereas ESBLs are usually invariably carried by plasmids. Carbapenemase genes may be carried on either chromosomes or plasmids.

Given that these genes can be found on plasmids, their horizontal transfer between species as is seen in *Enterobacteriaceae* where *K. pneumoniae* and *E. cloacae* fall is feasible. In *Enterobacteriaceae*, KPC is the most common cause of carbapenem resistance (Codjoe & Donkor, n.d.). Other genetic factors associated with MDR include blaKPC genes that may contribute to CREC's rapid development. ST171 and ST78 include many lineage-specific genomic islands that code for systems against toxin-antitoxin as well as cell stress response systems, respectively. Genes encoding for toxin-antitoxin systems as well as those encoding for heavy metal resistance have been found to exist on MDR plasmid in CREC isolates. These characteristics may also contribute to the organism's success, particularly in nosocomial situations (Chen *et al.*, 2014).

According to current research, the formation and dissemination of CREC is attributable to the vast variety of clonal lineages and carbapenemases. A recent research that drew on two worldwide monitoring systems revealed the amazing spread and diversity of carbapenemase genes in the *E. cloacae* complex (ECC). CREC can also exist as low-virulence microorganism with particular mutations enabling it to flourish in nosocomial environments (Gomez-Simmonds *et al.*, 2018). Several factors, among them, cross-class antibiotic resistance, horizontally acquired carbapenem- and fluoroquinolone-resistance genes, suggest that pressure on antibiotic use in hospitals, and not merely the increase in virulence, played a bigger role in CREC ST171 spread in the USA (Cheng *et al.*, 2017).

2.6 Global Distribution of MDR *E. cloacae*.

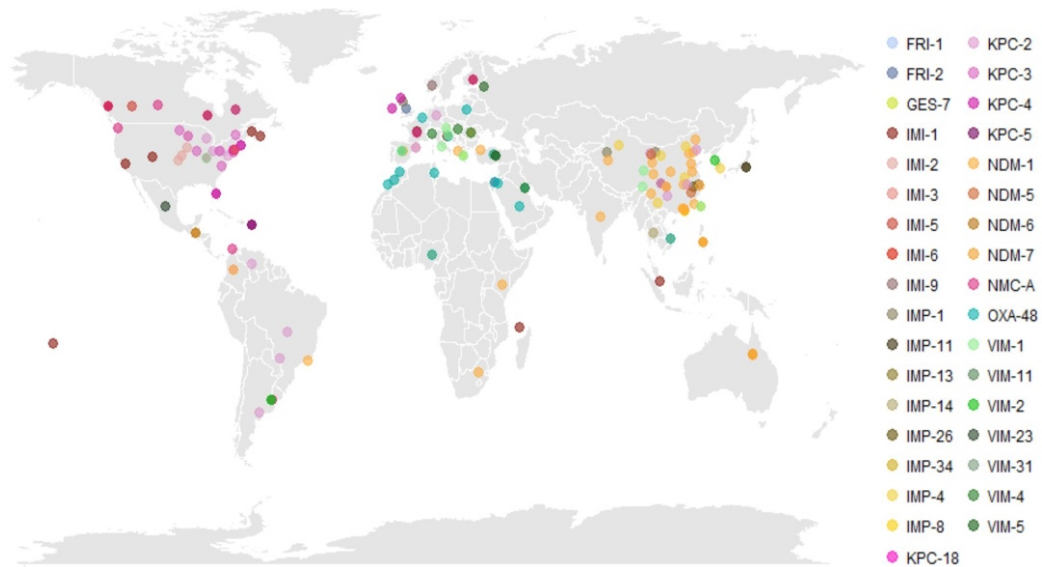


Figure 2.1: A World Map Showing the Global Distribution of Multidrug-Resistant (MDR) *E. cloacae* (Kempf et al., 2015).

In the US and Canada, *E. cloacae* that is primarily blaKPC-positive has been discovered, with just a few instances of organisms that have genes encoding for IMI- and NMC-A. In Kenya, NDM-carrying isolates have been discovered (“Detection of NDM-1-Producing *Klebsiella pneumoniae* in Kenya,” n.d.)(Musila et al., 2021). Positive blaKPC isolates have also been found in South America and among European countries. blaNDM and blaNDM-1 alleles are widespread in India and the surrounding countries and across Eastern China hospitals respectively.

IMP-alleles exist around several S.E Asian nations while VIM gene variations, on the other hand, are more common in Europe, with only a few examples found in S. America and S.E Asia. Additionally, carbapenemases OXA-48-like genes are believed to have originated in Turkey then to the Arab subcontinent, Europe, and eventually to the Northern Africa region (Kempf et al., 2015).

2.7 Life Cycle of Phages

The life cycle of a phage begins with infection, where a bacteriophage attaches itself onto a bacterial cell surface via the tail fibers and injects its genetic material into the cell. Thereafter, a phage typically goes through either of the two life cycles: lytic (virulent) or lysogenic (temperate) (Thung *et al.*, 2018). Lytic phages (Fig. 2.3) use the cell's machinery to generate phage components. The phage in turn exploits its host machinery, directing it to produce proteins needed in the construction new phage particles. The new viral heads and their tail sheaths are built separately, followed by insertion of the new synthesized genetic material into the viron heads and eventual assembly of new daughter viron particles being formed. (Ml Haq *et al.*, 2012). During this stage, phage enzymes weaken host cells progressively, leading them to burst and release between 100-200 new daughter progeny bacteriophages within the environment that go on to infect other host cells.

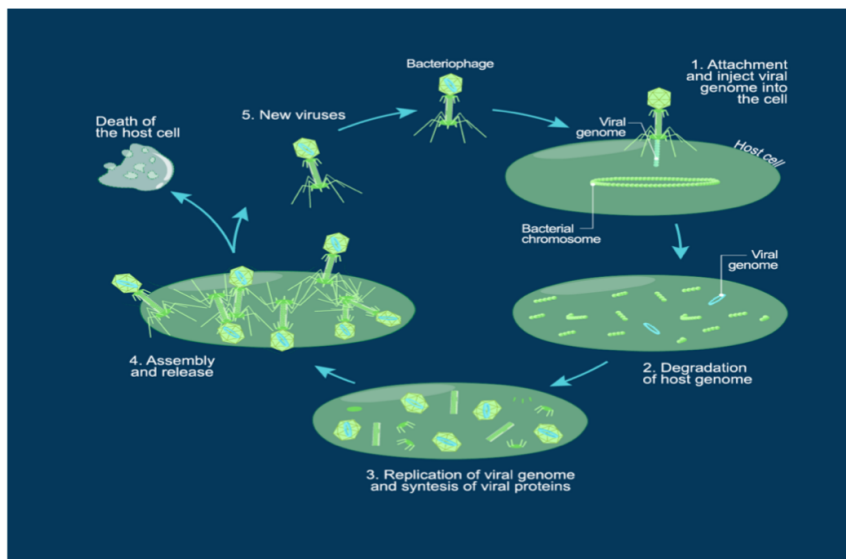


Figure 2.2: Lytic Cycle of a bacteriophage (Steward, 2018).

The lysogenic cycle (Fig. 2.4) does not destroy the host cell, instead exploiting it as a haven in which it can dwell dormant. After injection, the bacteriophage integrates its

DNA into the host cell genome via the help of the intergrases encoded by the phage. This changes the phage into a prophage. It follows then that the intergrated genome is passively replicated alongside its host. Owing to the fact that phage genomes are small, the intergrative event has nimal effect on the overall performance of the host cell. (MI Haq *et al.*, 2012). However, lysogeny state is temporal and under certain conditions, prophages can enter the lytic phase.

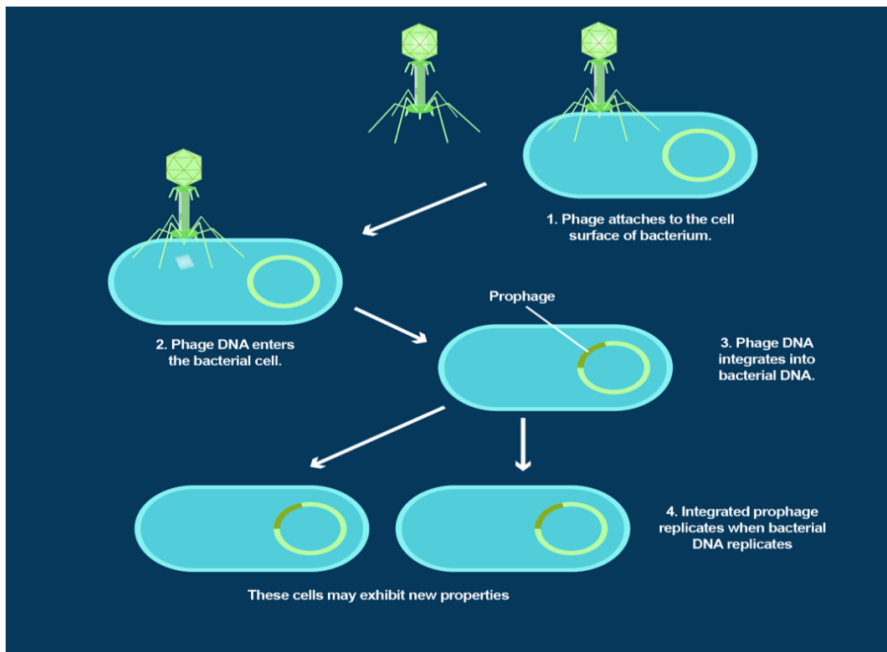


Figure 2.3: Lysogenic Cycle of a bacteriophage (Steward, 2018).

2.7.1 Types of Phages

Although various phages have been identified, knowledge on their nature may be insufficient since the discovery and usage of phages is still in its early stages. *Ackermannviridae*, *Myoviridae*, *Siphoviridae*, and *Podoviridae* are among bacterial phage families identified (Shang *et al.*, 2021).

Phages in the *Ackermannviridae* family are non-enveloped and possess head-tail configurations. Their head is icosahedral with a diameter measuring around 93nm. They

feature a base plate and a neck with no collar. Their tail is contractile and is roughly 140nm in diameter and 20nm in length. Their fibers are linked onto the tail and measure around 38nm long. *Ackermannviridae* phages replicate virally in their cytoplasm (Steward, 2018; Loh *et al.*, 2020).

Myoviridae phages feature heads that are elongated (about 110nm in length), collars with long tails (about 114nm), spiked base plates, and six long fiber tail. Their genome is linear, around 33–244 kb long and encodes 40–415 proteins. They employ cytoplasmic replication, they are lytic, and do not contain genes needed for transit to lysogeny phase, making them among the finest for phage treatment (Dion, 2020).

Bacteriophages of the *Siphoviridae* family attack both archaea and bacteria. Most of the bacteriophages in this family are categorized as unclassified and with no genus, yet, most of these phages have been identified as targeting *Lactobacillus*, *Mycobacterium*, *Streptococcus*, and other bacteria. Currently this family has about 313 species, divided into 47 genera. They also lack an icosahedral enclosed head. Distinguishing features of this group of bacteriophages is their non-contractile cross-banded tails. They have double-stranded or linear genomes (about 50kb in length), with 70 genes. Bacteriophages of *Siphoviridae* family utilise cytoplasmic viral replication, and have a lytic lifecycle suitable for phage treatment (Addy *et al.*, 2019; Turner *et al.*, 2017).

The *Podoviridae* (Addy *et al.*, 2019) family has 50 species divided into 20 genera. The distinguishing feature of bacteriophages in this family is their extremely small but non-contractile tail, which has six short sub-terminal fibers. They have a thick tail that is constructed to resemble stack-like disks, reaching about 17nm in length. They have an icosahedral head and are non-enveloped. They have a diameter of 60nm and 72 capsomers. Bacteriophages in this family have a linear dsDNA genome of about 40-43kb in length and encoding 55 genes. Their genome contains the genetic information for nine structural proteins. They adhere to the bi-directional replication of DNA process. Cytoplasmic viral replication is used by these bacteriophages (Turner *et al.*, 2016).

2.8 Phages as alternatives to antimicrobial resistance

Phage treatment, which employs bacteriophages in treatment of bacterial illnesses, can be traced back nearly a century. The widespread fall in antibiotic efficacy has sparked considerable interest in reconsidering this method. Phage treatment is traditionally based upon their natural existence as phages infect and lyse their host at their point of infection. Advances in technology, specifically biotechnological techniques, has served to expand the repertory of phages as therapeutic agents with techniques such as bio-engineering of phages and purification of phage lytic proteins being incorporated in their isolation (Kakasis & Panitsa, 2019) (Principi *et al*, 2019b).

Recent studies particularly on the use of whole phages or their extracted lytic proteins, especially those targeting MDR bacterial illnesses, shows that bacteriophage therapy can be utilized instead of or in addition with antibiotic regimens. Antibacterial treatment, whether phage- or antibiotic-based, has benefits and drawbacks. As a result, several factors must be considered while creating novel therapeutic techniques for use in preventing and/or treating infections caused by MDR bacteria. Despite the fact that little is known about the factors that come into play during interactions between bacteriophage, host bacteria and human host, the time to seriously investigate phage therapy is approaching quickly (Ghosh *et al*, 2019).

The UN General Assembly met in 2016 to deliberate on antibiotic resistance, which was rated as "...biggest and most serious global concern." One of the most common approaches for alternative prevention and management of bacterial illnesses includes resurrecting the old practice of bacteriophage treatment. Advocates of phage treatment point to numerous significant benefits possessed by phages against those of antibiotics, including and not limited to host-specificity, self-amplification abilities, abilities to invade and destroy biofilm formation by bacteria, and their low toxicity towards human cells (Ghosh *et al.*, 2019). The science of phage biology is gaining maturity due to the advent of analytical methods that can investigate very minute biological entities (about 25-200 nm lengthwise), including next-generation sequencers as well as electron microscopy.

These technical breakthroughs have brought about renaissance in phage treatment research, as seen in the current surge in human and animal trials (Pires, Melo, Vilas Boas, Sillankorva, & Azeredo, 2017).

Phages have the capacity to activate both innate and adaptive immune cells, which may impact the outcome of phage treatment. There are three primary areas of phage-immune interaction that have been identified. First, immunological detection via pattern recognition receptor (PRR), which is a mechanism for phagocyte recruitment to the infection site. When PRR detects phage-derived DNA and RNA, phages can facilitate triggering of inherent immune cells. However the degree of immune activation varies with phage type, phage dosage, and *in vivo* nucleic acid synthesis activity (Criscuolo *et al.*, 2017) (Nagel *et al.*, 2016).

Phages can be used as mixtures, commonly known as “phage cocktails”, is a significant benefit of phage therapy over traditional therapies for avoiding resistance development. Phage cocktail refers to employment of many phages, each targeting a different receptor and belonging to a distinct genetic lineage, and is believed will improve the capacity to compensate against adsorption loss or host genetic protective mechanisms (Malik *et al.*, 2017). Additionally, genetic engineering of phages can be used not only as a means of increasing the variety of hosts per phage but also increase phage targeting efficiency in order to avoid host resistance to the cell. Another factor to consider is that bacterial changes that give phage resistance frequently cost the resistant bacterium fitness (Ghosh *et al.*, 2019). The function of the indigenous gut phageome in human health and illness should also be considered when assessing the feasibility of phage treatment.

2.8.1 Historical and current use of phages

For more than a century, phage use in treating bacterial illnesses has been established, but it is gaining popularity because of the advent of multidrug-resistant organisms. The distinct lysis zone attributed to phage infection was recorded by Frederick Twort in 1915, although it was Felix d'Herelle who recognized this phenomenon, attributing the plaques

to viruses that feed on bacteria thus coining the name "bacteriophage" (meaning, "bacteria-eater") Ghosh *et al.*, 2019). D'Herelle was also responsible for the first known clinical trial of phages, which occurred Paris in 1919 at the Hôpital des Enfants-Malades. In this clinical use of phages four juvenile incidences of diarrhoea arising from bacteria infection were successfully treated. Poor controls were one of the reasons that undermined d'Herelle's early trials, leading to strong protests from the scientific community (Torres-Barcelo & Hochberg, 2016).

Despite this, d'Herelle continued to develop bacteriophage treatment in the early twentieth century, employing a network of bacteriophage therapy clinics and manufacturing companies found all over Europe and India for production of phages to treat dysentery, cholera, and bubonic plague. In 1931 research using phage therapy as a cholera cure in India's Punjab area, d'Herelle saw a 90% decrease in mortality, with about 74 fatalities in the control group and only 5 in the experimental group (Chanishvili, 2012; Lin *et al.*, 2017)

Bacteriophages are being used in the clinical therapy of bacterial infections with remarkable success. Lehman and Donlan (Lehman & Donlan, 2015) reported *in vitro* investigations of urinary tract infections (UTIs) with isolated bacteriophages on particular pathogens using cocktail to cover a larger host range to prevent resistance. Among the prevalent causes of UTIs are *E. coli* and *K. pneumoniae* (Yang *et al.*, 2010). In 1981-1986 in Poland, 550 patients were included in a number of reviews conducted by physicians at Hirsfeld Institute of Immunology and Experimental Therapy in Wroclaw for conditions caused by bacteria with 70 to 100% cure rates. Suppurative skin infection caused by *E. coli*, *Klebsiella*, *Proteus*, *Pseudomonas* and *Staphylococcus*, of the 31 patients under study, 23 cases showed marked improvement with treatment by bacteriophages (Yin *et al.*, 2021; Abedon *et al.*, 2011). In another case, cerebrospinal meningitis caused by *K. pneumoniae*, following unsuccessful treatment with antibiotic therapy, a new-born was successfully treated with orally administered phage (Furfaro *et al.*, 2018).

In Brazil and US, additional medical entrepreneurs commercialized phage manufacturing with formulations for *Staphylococcus*, *Streptococcus*, *E. coli*, and other infections caused by bacteria. Willing doctors were given the concoctions, but therapy was greeted with uneven results; this lack of dependability contributed significantly to Western medicine's preference for antibiotics. The errors made in the formative days of phage treatment were ascribed to a lack of knowledge about the biological interactions of phages. The use of crude purification and preservation techniques produced very low titers of viable phage. Contaminants mainly from bacterial antigens as well as bacteriophages with no infectivity were utilized in the treatment thus undermining the effects of the target bacterial host cells (Principi *et al*, 2019; Ul Haq *et al*, 2012).

Presently, there exists no bacteriophage treatment products licensed for use in human in the European Union or the US. However, various commercial phage formulations are employed in the food sector for the biocontrol of bacterial diseases. Approval for such formulations has been granted by the Food and Drug Administration (FDA) as "generally recognized as safe" mainly for treatment of *Salmonella* spp., *Listeria monocytogenes*, *Mycobacterium tuberculosis* among others (Torres-Barceló, 2018).

There were approximately 48 million incidents related to food poisoning in US in 2011(Scallan *et al.*, 2011). Evidence shows bacteriophage biocontrol being an effective strategy in enhancing food safety at several phases of producing and processing meat, as well as reducing contamination caused by bacteria in fruits and vegetables as well as dairy products (Moye *et al.*, 2018) (Endersen & Coffey, 2020) (Fernández *et al.*, 2018)

Advancement in technology, among them, CRISPR/Cas gene editing tool have opened a plethora of new possibilities for phage treatment. For example, a bioengineered phage might be used to transfer a CRISPR/Cas designed to break antimicrobial resistance genes thus rendering antibiotic resistant plasmids susceptible. Such genetically engineered phages might be used to minimize the occurrence and spread of antibiotic resistance genes on hospital surfaces (Salmond & Fineran, 2015; Ghosh *et al.*, 2019). However, the area

of bioengineered phages is still in its early stages, it is expected to produce several breakthrough technologies that will improve the usage of phage therapy.

2.8.2 Advantages and Disadvantages of Phage Use

Bacteriophage treatment offers varied significant advantages that make it an appealing alternative/supplement to antibiotics. In contrast to antibiotics, that are known to have broader scope, phages are very unlikely to induce dysbiosis or cause secondary infections (e.g., fungal infections). Furthermore, it has been demonstrated that bacteriophages have no substantial side effects or known toxicity to mammalian cells. In addition, the process of isolating and selecting for new bacteriophages has been proven to be less expensive and time consuming than the process of developing an efficient antibiotic, which typically takes several years and millions of dollars to create (Torres-Barceló & Hochberg, 2016). Bacteriophages have the capacity to spread widely throughout the human body when administered systemically, as well as self-replicate within the host, traits that many antibiotics lack. Phages, unlike other antibiotics, may cross the blood–brain barrier (Torres-Barceló, 2018). Some phages can also enter and disturb the biofilms that many microbes live in naturally and are protected from antibiotics and disinfectants (Alves et al., 2016) (Abedon, 2015).

Bacterial resistance to phage treatment is less relevant than antibiotic resistance since phage mixtures may be regulated by phage replacement, pressure brought about by *in vitro* evolutionary or genetic engineering. Phages also evolve to evade bacterial resistance. Phages can also be used successfully in treatment of MDR bacteria since they attack cells through many methods (Torres-Barceló & Hochberg, 2016).

Despite its benefits, the use of phages has some disadvantages. These, however, are mostly due to information gaps that in future may be overcome. There exists scarcity of detailed information on therapeutic application of bacteriophages to treat illnesses caused by bacteria. When compared to conventional medicines, scientists face even greater obstacles in gaining necessary regulatory clearances for phage-based therapeutics (Reindel & Fiore,

2017). More research and less stringent clinical rules, on the other hand, can help to alleviate this problem (Abedon, 2017). Furthermore, phage genetic biosafety is difficult to measure. Genes coding for toxins or virulence genes, and those coding for antibiotic resistance genes, or those with ability to transfer genes horizontally in the human microflora must not be present in phages utilized for treatment (Kutter *et al.*, 2010). While whole genome sequencing is a useful platform for assisting in investigations, the functionality of all phage encoded genes remain unknown. This is likely to be solved in the future by phage genetic engineering (Y. Chen *et al.*, 2019). The reticuloendothelial system may drastically lower phage concentrations during therapy or be neutralized by antibodies, reducing their antibacterial efficacy. The effect of phage-neutralizing antibodies, on the other hand, may be minimized by fine-tuning dosage regimens as well as engineering or selecting for phages that can elude the immune system (Crisuolo *et al.*, 2017).

2.9 Current use of Phages in Combating *E. cloacae*

To address the issues raised by multidrug-resistant *E. cloacae*, a more effective alternative treatment approach is needed. Phages are excellent bio-degraders that consume bacteria. They are regarded as viable option in the suppression of bacterial proliferation within the environment as well as diseases control. Monohar *et al* in 2018 (Manohar *et al.*, 2018) employed *E. cloacae* strain el140 obtained from health facilities in Tamil Nadu region of India, in their *in vivo* study in larvae el140 and ELP140 of the *Enterobacter* phage belonging to the *Podoviridae* and *Myoviridae* families, respectively. This *Enterobacter* phage ELP140 was shown to be less efficient in treating infected larvae with a single dosage of the phage in this investigation.

This study proved that the efficiency of phage treatment is governed only by the particular phage's capacity to lower bacterial burden, rather than the complexity of phage manufacturing. Aminov *et al* in 2019 (Aminov *et al.*, 2019) discovered that *E. cloacae* phages lacked genes that would limit their usage for phage treatment. The phages were

particularly lethal to *E. cloacae* isolates from left-ventricular assist device (LVAD) infections, where the disease might well have originated in the skin. Only one phage was effective in killing UTI *E. cloacae* isolates. Additional isolates from different locations be investigated to establish whether bacterial site of origin influences efficiency of phage killing.

CHAPTER THREE

3.0 METHODOLOGY

3.1 Study site and design

The study was a laboratory based experimental study conducted at the Kenya Medical Research Institute (KEMRI) and Institute of Primate Research (IPR) in Nairobi, Kenya. Phage isolation and characterization was conducted at IPR laboratories while extraction of phage DNA and sequencing was done at the KEMRI Centre for Microbiology Research laboratories. The general flow of the work is shown in Figure 3.1 and a detailed description of each procedure provided hereafter.

3.2 Bacteria culture

Standard control strains of *E. cloacae* (ATCC 50398) and de-identified archived multidrug resistant clinical isolates (from protocol SERU#2767) were cultured on sheep blood agar (SBA) and/or MacConkey agar plates then sub-cultured on Mueller Hinton Agar (MHA) to obtain pure cultures. This was followed by catalase and oxidase tests for all the bacterial isolates. In catalase, 3% hydrogen peroxide was poured in a test tube and using a sterile wooden applicator stick, a colony of an 18-24 hours of bacteria was immersed in the hydrogen peroxide and observed for bubbling. In the oxidase test, the swab method was used in which a swab was dipped into Kovac's oxidase reagent. The wet swab was then used to touch a colony of an 18-24-hour bacteria and a colour change observed in 5-10 seconds. Identity and antimicrobial susceptibility patterns were confirmed on an automated Vitek2 platform and documented. The clinical isolates used for this study were selected based on the confirmed antimicrobial susceptibility test (AST) patterns and the degree of multidrug resistance.

3.3 Sampling strategy

Sampling was done from several environmental sources providing the diversity of phages needed to increase the chances of obtaining the targeted bacteriophages from the environment which include:

3.3.1 Fresh water (Lake Victoria).

Studies of marine environment suggest that sea water is a rich source of bacteriophages having about 10 phages per bacteria/archaeal cell. Fresh water has been shown to have a similar bacteriophage abundance (Levy & Marshall, 2004). Because phages have been known to co-exist with bacteria, areas of human activities were considered for sampling, in this case samples were collected from Dunga beach in Kisumu County.

3.3.2 Hospital sewage.

Sewage was obtained from the Kenyatta National Hospital with a bias for sewer line originating from the hospital wards. The hospital serves a population of about 1.1 million patients in a year with varied infections many of whom are on antibiotics. Due to the antibiotic use and nosocomial infections which are typically more multidrug resistant than community strains, the hospital sewer was presumed to be a rich environment from which to isolate the target bacteriophages. Specific bacteriophages are found in environments where their host bacteria are abundant (Levy & Marshall, 2004).

3.3.3 Urban effluent.

Combined Sewer Overflows (CSOs) are a primary source of faecal pollution indicators to urban settlements receiving waters from streams and rivers. The discharge in-streams, accumulation of sediments from CSOs constitute a bacterial reservoir fielding a continuous inoculation to the receiving waters. (LauraBaronea, 2019). Nairobi Rivers and streams receive sewage effluents from residential and commercial. This forms a rich source of

phages and hence Chiromo River at Museum Hill, Mathare River, Kibera slums and the sewage plant at Kariobangi were considered for sampling.

3.3.4 Sample collection

Samples from the Lake Victoria, KNH sewage and urban effluent including Mathare River, Kibera slums, Kariobangi, Chiromo River and Zimmerman Estate were collected in sterile 500 ml bottles. Samples were then transported in cool boxes on ice to the laboratories at the IPR for processing. 500 mls of water samples were collected in triplicates.

EXPERIMENTAL FRAMEWORK

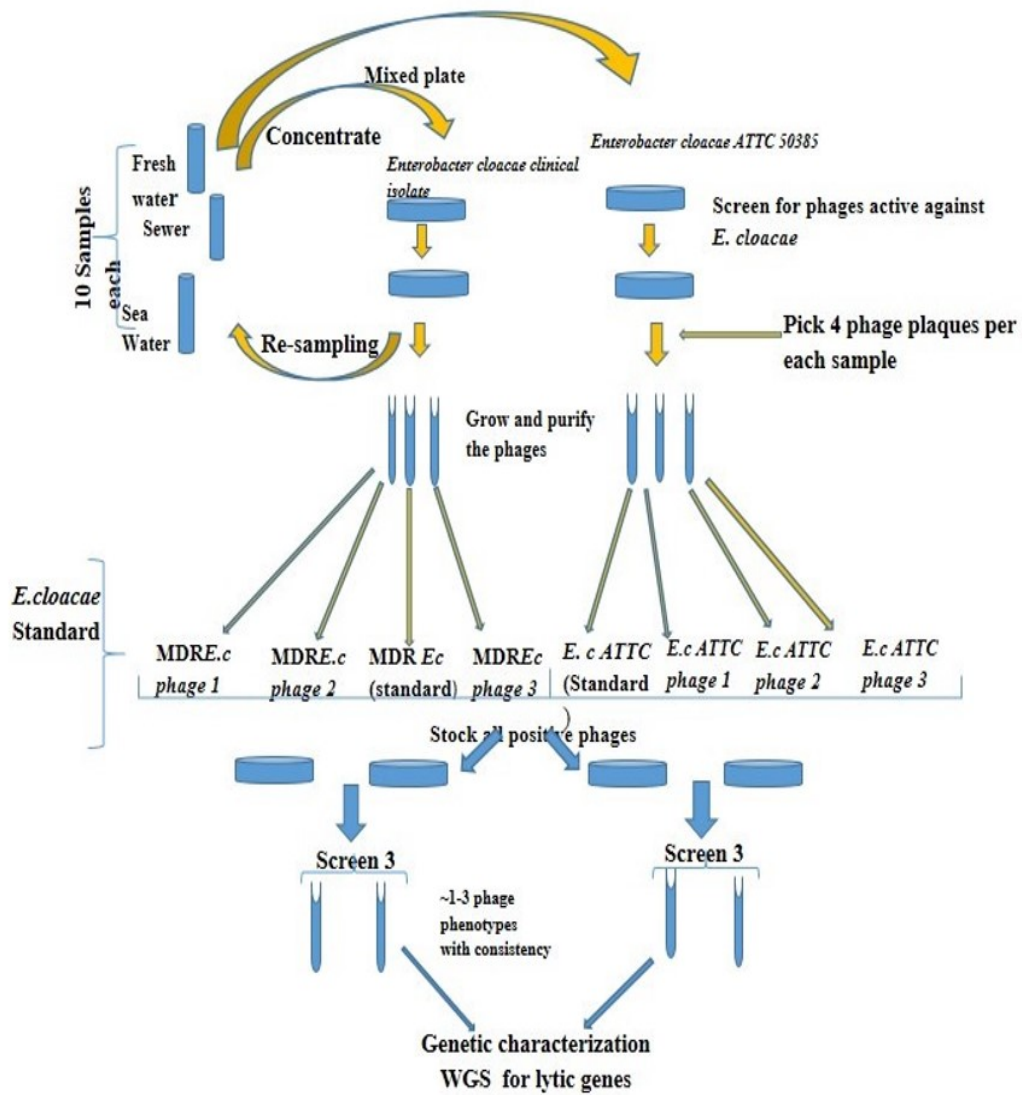


Figure 3.1: Schematic representation of experimental framework of the isolation, purification selection and characterization of phages against MDR *E. cloacae*

3.4 Isolation of bacteriophages targeting *E. cloacae*.

3.4.3 First enrichment of potential phages from liquid samples

Each of the collected liquid samples were centrifuged at 10000g for 15 minutes at 4 °C. 15 ml each of the supernatant was used in the enrichment step and the volume topped up using double strength (2x) Tryptone Soy broth (dsTSB) (Casein peptone [pancreatic] 17.0g, Soya peptone [papain digest] 3.0g, NaCl 5.0g, Dipotassium hydrogen phosphate 2.5g, Glucose 2.5g, dH₂O 1litre, final pH 7.3 +/- 0.2 at 25 °C) to make 30 ml of solution. A 100 µl suspension of control strains of *E. cloacae* bacteria were then added into separate labelled tubes containing 30 ml of the dsTSB and liquid sample solution. The enrichment was cultured overnight at 37 °C on a shaker (Model No. 3525-1, Lab-Line Instruments, Lab-Line Plaza, Melrose Park, Illinois, USA.) set at 120 rpm. This procedure was followed by a second and final enrichment step.

3.4.4 Second enrichment of potential phage from each of the sample collected from the different sources

The target bacterial cells in the first enrichment were obtained through centrifugation for 15minutes at 10,000g and 4 °C followed by filtration using a 0.45 µm filter membrane (CHMLAB, Spain). A volume of 2.5 ml of each filtrate was then transferred into labelled sterile 15 ml tubes and further enrichment of potential phages done overnight by addition of 2.5 ml dsTSB broth and 50 µl of the control strains of *E. cloacae* for the test and a negative control (sterile water) was also included. The enrichment was done overnight at 37 °C on a shaker (Model No. 3525-1, Lab-Line Instruments, Lab-Line Plaza, Melrose Park, Illinois, USA.).

3.5 Isolation of bacteriophages from the enriched media

After the overnight incubation, each phage suspension from the second enrichment stage was centrifuged for 15 minutes at 10000g and at 4 °C. Obtained supernatant was filtered using a 0.22µm membrane filter (CHMLAB, Spain) and stored as stock phage lysate 4 °C.

Tryptic Soy Agar (TSA) (Casein peptone [pancreatic] 17.0g, Soya peptone [papain digest] 3.0g, NaCl 5.0g, Dipotassium hydrogen phosphate 2.5g, Glucose 2.5g, Agar 15 g, dH₂O 1litre, final pH 7.3 +/- 0.2 at 25 °C) plates were then prepared (0.04% w/v) and 100 µl of each respective bacteria spread onto the agar plates to create a bacterial lawns. This was followed by spreading of 5 µl supernatant from each of the second enrichments. The plates were labelled and incubated at 37 °C overnight then examined the following day for the presence of plaques in each bacterial lawn. Four (4) individual plaques were selected from each environmental source for each target organism and transferred into labelled sterile bottles containing 500µl of TSB media and incubated for 37 °C overnight as an initial phage stock.

3.6 Phage titration, propagation, cross infection and identification

A 1:10 serial dilution of the initial phage stock was made to determine the number of infective phage particles through a double-layer plaque assay. Using a sterile pipette, 900 µl each of SM buffer (NaCl 100mM, NaSO₄.7H₂O 8mM, Tris-Cl [1M, pH 7.5] 50mM, Gelatin [2%, w/v] 0.01%, H₂O to 1 litre, final pH adjusted to 7.5) was added into eppendorf tubes and labelled from 10⁻¹ to 10⁻⁸. A 100 µl phage stock of each respective bacteria was serial diluted from 10⁻¹ to 10⁻⁸. Bacterial lawns were prepared in 7% soft agar and 100 µl of respective target bacteria added and swirled by rubbing between palms before pouring the mixture onto TSA plates. The agar plates were then allowed to set before spotting 5 µl each of the serially diluted phage stock each at the respective diluted factor. The plates were then allowed to dry before incubating overnight and plaque forming units (PFU) observed thereafter. Dilutions with 30-300 PFU were picked for plaque assays. For plaque assay, 100 µl of target bacteria and 100 µl of phage at the dilution factor with 30-300 PFU were added to soft agar, swirled between palms and the mixture poured onto labelled TSA plates. The plates were then allowed to settle followed by an overnight incubation at 37 °C. Plates were observed for plaques the following morning.

3.7 Phage titration and propagation prior to purification

Each plate was examined for plaques and each plaque picked based on its morphological appearance. The picked plaques were re-suspended in 1 ml of Sodium-Chloride-Magnesium-Sulphate-Gelatin (SM buffer) in eppendorf tubes and vortexed gently between palms then incubated for one hour at RT. The tubes were centrifuged at 10,000g for 15 minutes at 4 °C. The supernatant was filtered through a 0.22 µm membrane (CHMLAB, Spain) and stored as phage stock at 4 °C. A volume of 100 µl each filtered phage and target bacteria were then mixed in 0.7% soft agar and overlaid on agar plates. They were then incubated overnight at 37 °C and those with plaques of similar morphology scrapped off the agar plate and mixed with 3 ml of SM buffer. This was followed by incubation for half an hour at RT, centrifuged at 10000 g for 15 minutes at 4 °C followed, then filtration through a 0.22 µm membrane (CHMLAB, Spain) before storage as phage clone for each target bacteria.

3.7.3 Phage precipitation and Purification.

Phage lysates ($\geq 10^8$ or 10^9 PFU/mL) were propagated in a large volume, concentrated, and cleaned up in the presence of NaCl and polyethylene glycol (PEG) as described elsewhere <https://cpt.tamu.edu/phage-links/phage-protocols/>, Guittierez *et al.*, 2018. Briefly, a single colony of *E. cloacae* was inoculated in a sterile 10 ml tube that contained 5 ml of sterile TSB media. The bacterial culture was incubated at 37 °C on a shaking incubator (150 rpm) for 18-22 h overnight. From the overnight bacterial culture, 500 µl was added to 50 ml sterile TSB in a sterile 100 ml conical flask (1% v/v of the *E. cloacae* overnight culture). The bacterial culture was then incubated at 37 °C with shaking (150 rpm) until the exponential growth phase ($OD_{600}=0.4-0.7$) was achieved. Subsequently, the exponentially growing bacteria was transferred to four sterile 50 ml Falcon tubes, one for the control and three for phage propagation with three different multiplicity of infections (MOIs) (0.1, 1 and 10). The tubes were incubated at 37 °C in shaking incubator (Model No. 3525-1,

Lab-Line Instruments, Lab-Line Plaza, Melrose Park, Illinois, USA.) for 2-3 hours or until observation of complete lysis of the phage treated cultures (transparent tube) in comparison to the control tube (turbid tube) by visual inspection.

Each phage lysate was centrifuged, filtered and titrated using spot tests and plaque assays. The optimal MOI in this study was 1 and the propagation protocol was repeated to scale the volume of phage lysate stock with highest titer ($\geq 10^9$ PFU/mL). The final propagation was performed using 250 ml bacterial culture at its exponential growth phase and until complete lysis of the bacterial cultures. The suspensions were then centrifuged at 10,000g, 4°C for 10 minutes with the supernatants being transferred to new sterile culture bottles using serological pipettes. The final phage lysate stock was filtered through 0.22 μ l membrane filter (CHMLAB, Spain), treated with RNase (40 μ g/ml final concentration) and DNase (40 μ g/ml final concentration) to digest bacterial nucleic acid followed by incubation at room temperature for half an hour. An aliquot of 8 ml filter-sterilized EDTA solution was added to the suspension and finally, the lysate was concentrated by addition of NaCl (0.5 M final concentration) and polyethylene glycol (PEG 7.5% final concentration). The mixture was divided into sterile Falcon tubes and centrifuged for 40 minutes at 13,000 x g, supernatant discarded and precipitate dried by spinning for 3 minutes at 4,000 x g to form a clear pellet at the bottom of the centrifuge tube. Each phage pellet was suspended in 500 μ l SM buffer, into new sterile centrifuge tubes and centrifuge for 10 minutes at 21,000xg. The supernatant was then filtered through 0.22 μ l membrane filter (CHMLAB, Spain) and the precipitated phage suspension sub-cultured on solid culture medium (TSA) to check for the presence of bacterial contamination. The phage precipitate titer was determined and then stored at + 4 °C.

3.7.4 Host Range Determination

Using a sterile pipette, 100 μ l of each of the five *E. cloacae* phage stocks were pipetted into a sterile 15 mL tubes containing 100 μ l of the MDR strains. The MDR strains included reference and clinical isolates to ensure activity against a broad range of pathogenic and

S. aureus strains. A volume of 3 ml semisolid TSB agar (1.5% agar), was added to the mixture before pouring on labelled TSB agar plate. The soft agar medium was then allowed to solidify, before incubating at 37 °C for 18 hr. The procedure was conducted in triplicate together with a control plate. The phenotypes of the plaques for each phage were documented to ensure stability of the lytic phenotype and consistency of the size of the plaque. Bacteriophages (~5 each) with stable activity against the two MDR bacteria were selected for genomic characterization.

3.7.5 Multiplicity of Infection (MOI).

TSB media (25 ml) was inoculated with 250 µl of 24 hr old host bacteria in a 50ml sterile conical flask and incubated in a thermoshaker (Model No. 3525-1, Lab-Line Instruments, Lab-Line Plaza, Melrose Park, Illinois, USA.) at 100 rpm and 37°C until OD 600 reached 0.4 (approximately 10⁸ CFU/ML at 3 hours). An Elisa plate was labelled for serial dilution, each well containing 180 µl of Phosphate buffered saline (PBS) and 20 µl of the host bacteria. An aliquot (100ul) of the serially diluted host bacterial was transferred to agar plate and spread until the liquid dried. The plates were then incubated for 18-24hrs at 37 °C. Plates with colony counts of between 30-300 were chosen for calculating the CFU/ml using the equation; $CFU/mL = N \times 1/DF \times 1/V$

Where N = counted number of colonies

DF= dilution factor

V= sample volume spread.

Once the host bacteria reached exponential growth phase, 900 µl of the bacterial culture was dispensed in sterile eppendorf tubes and labelled 0s, 30s, 1 minute, 5, 10, 15, 30 and 60 minutes in triplicate. Into each tube, 100 µl of phage lysate of specific titer added followed by incubation of the tubes at 37 °C for the respective times indicated on the tubes. For the first three time points, the tubes were stored on ice because of the proximity of the timings. At each point, samples were removed and centrifuged at 10,000 x g for 15

minutes, filtered and stored at 4 °C until all time points were completed. A serial dilution of the supernatant was done to determine phage titres through spot and plaque assay using the bacterial host as the indicator strain. MOI was then calculated using the MOI calculator at <http://moicalculator.phage.org>.

3.8 Physical characterization of isolated phages

The thermal (heat) and pH stability of the isolated bacteriophages was performed as described previously by Luo *et al.*, 2013. The phages were incubated at different temperature range of 4, 20, 25, 37, 60 and 90 °C respectively and at pH 7.5 for 2 hours and immediately cooled in ice water. Serial dilution was then done and the surviving phages spotted on soft agar overlay and plates incubated overnight at 37 °C. pH stability of the phages was determined by subjecting the phages to different pH values of 2, 4.5, 5.5, 7.5, 9.0, 11.5, and 13. Briefly after adjusting SM buffer to the required pH value using 0.1 M NaOH or 0.1 M HCl, an aliquot of 100 µl of phages were suspended in 100 µl of each of the adjusted pH SM buffers for 2 hours at 25 °C. Serial dilution was done followed by spotting on double layer overlay on agar plates and an overnight incubation at 37 °C. These plates were done in triplicate with the surviving plaques enumerated and recorded.

3.8.3 Phage genomic DNA extraction and sequencing

A high-titre ($>10^9$ pfu/ml) phage lysate (1000 µl) was used for DNA extraction. A commercial DNA extraction kit Norgen Biotek Corporation Phage DNA Isolation Kit Cat 46800 was used following the manufacturer's instructions. Briefly, the starting material was clarified phage supernatant. A working concentration of Wash solution A was prepared by adding 90 mls of ethanol (96-100%) to the bottle containing wash solution A, giving a final volume of 128 mls. A water bath and a heating block were then preheated at 65 °C. The starting material for the phage was 1ml of phage supernatant containing at least 1×10^{10} PFU. The 1ml of the phage lysate was transferred to a 15mls tube. To eliminate any bacterial host genomic DNA, 10 µl of DNase1 (Norgen RNase-free DNAase

kit, product #25710) was added and the tube incubated for 15 minutes at RT, followed by DNase inactivation at 75 °C for 5 minutes. 500uL of Lysis buffer B was added and the tube vortexed vigorously for 10seconds. 4 µl of Proteinase K (20mg/ml) was added and the tube incubated at 55°C for 15 minutes. This step helped increase the DNA yield by breaking down the capsular proteins to release the DNA. The tube was then incubated at 65 °C for 15 minutes with occasional mixing 2-3 times during the incubation. 320 µl of isopropanol was added to the lysate and briefly vortexed.

The spin column was assembled with one of the collection tubes. 650 µl of the lysate was applied to the column and centrifuged at 6000g for 1 minute. The flowthrough was discarded, the column reassembled again and the process repeated until all the lysate had gone through the column. The column was then washed thrice with 400 µl of Wash solution A and spun at 6000g for one minute. The column was then spun at 14000g for 2 minutes to thoroughly dry the resin. The flowthrough was discarded. The column was then placed into a fresh 1.7mL Elution tube. 75 µl of Elution buffer B was added to the column and centrifuged at 6000g for one minute. The extracted DNA was first quantified on a NanoDrop 1000 (ThermoFisher Scientific, 5225 Verona Rd, Madison, WI 53711, USA) followed by Qubit Fluorometer (Quantus™ Fluorometer, E6150, ProMega Corporation, Madison WI 55711-5399, USA,) all according to manufacturer's instructions. The elution buffer used during DNA extraction was used as a blank. The concentration of DNA was measured in ng/ul. The purified DNA sample was then stored at -20 °C for a few days awaiting sequencing.

3.8.4 PCR and Gel Electrophoresis

Phage DNA extraction was done using the Norgen Biotek Corporation Phage DNA Isolation Kit Cat 46800. To further confirm the absence of contaminating bacterial DNA, all phage DNA samples were screened using conventional PCR with primers that target the 16S ribosomal RNA specific to bacteria. The forward primer 27F: AGAGTTTGATCCTGGCTCAG, the reverse primer 1492R:

TACGGTTACCTTGTTACGACTT, and One Taq Hot Start 2X Master Mix (New England BioLabs, Massachusetts, USA) (He *et al.*, 2016) was used. The PCR mastermix contained 7 μ l of nuclease free buffer, 1 μ l (to make a final concentration of 0.2 μ M) of each primer, 2.5 μ l of 2x Master Mix and 1 μ l (1000ng) of template. Amplification was done with the following thermal cycler conditions: Initial denaturation for 1min at 95°C and 35 cycles of amplification consisting of 20 s at 95°C, 1 min at 51°C for annealing and 1 minute at 68°C for extension and a final extension for 5 min at 72°C. PCR products were separated by electrophoresis on a 1% agarose gel (AmpliSize; Bio-Rad Laboratories) using 1 \times TAE Buffer (40 mM Tris, 20 mM acetic acid, and 1 mM EDTA.) containing GelRed Nucleic Acid and visualized on the UV transillumination (Velber Gel Documentation Systems- E-Box CX5 Edge, Fisher Biotec, Australia). O'GeneRuler 1kb DNA Ladder, 0.1 μ g/ μ L (# N3232S, New England BioLabs, Massachusetts, USA) was used as a DNA size marker. In addition, a negative control with master mix and DNase free water as template was also included.

3.9 DNA Library preparation.

At the start of the library preparation for sequencing, DNA was quantified via Qubit Fluorometer (Quantus TM Fluorometer, E6150, ProMega Corporation, Madison WI 55711-5399, USA,) according to manufacturer's instructions to get a more accurate DNA reading. The required amount of DNA for WGS is >50 micrograms

The DNA library was prepared using the Nanopore Native barcoding genomic DNA (EXP-NBD104, EXP-NBD114, and SQK-LSK 109) (Oxford Nanopore Technologies, UK). First, the NEBNext FFPE DNA Repair mix and NEBNext Ultra II End repair/dA-tailing Module reagents were prepared according to the manufacturer's instructions and stored on ice. 1 μ g (about 100-200fmol) of genomic DNA was transferred into a 1.5ml Eppendorf DNA LoBind tube and volume adjusted to 48 μ l with nuclease-free water, mixed well by flicking the tube, spun down, and stored on ice.

DNA (48 μ l), 3.5 μ l NEBNext FFPE DNA Repair Buffer, 3.5 μ l Ultra II End pre-reaction buffer, 3 μ l Ultra II End-prep enzyme mix, and 2 μ l NEBNext FFPE DNA Repair Mix were pipetted into a 0.2 ml thin-walled PCR tube, spun down, and incubated at 20 °C for 5 minutes and 65 °C for 5 minutes using a thermal cycler. The DNA sample was then transferred to a clean 1.5 ml Eppendorf DNA LoBind tube, and 60 μ l of resuspended AMPure XP beads were added, mixed by flicking the tube, and incubated for 5 minutes at room temperature on a Hula mixer (rotator mixer). After that, the sample was spun down and pelleted on a magnet until the eluate was clear and colorless.

The pellet was washed twice with 200 μ l of newly made 70 percent ethanol in nuclease-free water after the supernatant was pipetted off. The sample was spun down, re-magnetized, and any remaining ethanol pipetted off. It was then allowed to dry naturally, but not completely. The tube was then withdrawn from the magnet, and the pellet was resuspended in 25 μ l Nuclease-free water, spun down, and incubated at room temperature for 2 minutes. After that, the beads were pelleted on a magnet until the eluate was clear and colorless. The 2.5 μ l eluate was transferred to a clean 1.5ml eppendorf DNA LoBind tube. On a Qubit fluorometer, a 1 μ l aliquot of the end-prepped DNA was quantified.

The native barcodes were thawed at room temperature (RT), pipetted together, and put on ice. From the 24 available, a unique barcode was chosen. The end-prepped DNA sample to be barcoded was diluted to 22.5 μ l in nucleases free water at a concentration of 500ng. 2.5 μ l native barcode and 25 μ l Blunt/TA Ligase Master Mix were added to it and mixed by flicking, spun down, and incubated for 10 minutes at room temperature. AMPure XP beads (50 μ l) were then added, pipetted, and incubated on the Hula mixer for 5 minutes at room temperature. After that, the material was spun down and pelleted on a magnet. The supernatant was then pipetted off, and the sample was washed twice with 70% of freshly prepared ethanol.

The sample was spun down, put on a magnet, and allowed to air-dry but not crack. The tube was removed from the magnet, and the pellet was resuspended in 26 μ l of Nuclease-free water for 2 minutes at room temperature. After that, the pellet was put on the magnet

until the eluate was clear and colorless. The eluate DNA (26 μ l) was collected and deposited in a clean 1.5 Eppendorf LoBind tube, with a microlitre of it utilized to quantify the DNA on the Qubit fluorometer.

The pooled sample (700 ng) was diluted in Nuclease-free water (65 μ l). Elution buffer (EB) and NEBNext Quick Ligation Buffer (5x) were thawed at room temperature, vortexed, spun down, and placed on ice. T4 Ligase and Adapter Mix II (AMII) were chilled after being spun down. One tube of Short Fragment Buffer was thawed at room temperature, vortexed, spun down, and stored on ice to preserve DNA fragments of various sizes. Adapter mix II (5 μ l), NEBNext Quick Ligation Buffer (5x), and 10 μ l Quick T4 DNA ligase were added to the 65 μ l 700ng pooled barcoded DNA sample, gently mixed by flicking, spun down, and incubated for 10 minutes at room temperature. The reaction was then pipetted with resuspended AMPure beads (50 μ l), mixed, and incubated on the Hula mixer for 5 minutes at room temperature. After that, the tube was placed on a magnet and the beads were allowed to pellet. The supernatant was pipetted off, the sample washed twice with 250 μ l of Short Fragment Buffer, the beads were flicked to resuspend, spun down, and then returned to the magnet to pellet.

The supernatant was withdrawn and discarded. The tube was then spun down and put on a magnet, with any remaining supernatant pipetted out. After 30 seconds, the tube was removed from the magnet and the pellet was resuspended in 15 μ l of Elution Buffer. The tube was spun down and incubated at room temperature for 10 minutes. After pelleting the beads on a magnet until the eluate was clear and colorless, 15 μ l of the eluate containing the DNA library was pipetted and deposited in a clean 1.5 Eppendorf DNA LoBind tube. On the Qubit fluorometer, one microlitre of adapter-ligated and barcoded DNA was utilized to quantify the library prep. The constructed library was kept at 4 °C until it was time to be sequenced.

3.10 Sequencing and Base-Calling.

Whole genome phage DNA sequencing was performed on an Oxford Nanopore MiniION sequencer. At room temperature, the Sequencing Buffer (SQB), Loading Beads (LB), Flush Tether (FLT), and Flush Buffer (FB) were thawed. SQB, FLT, and FB were mixed by vortexed, spun down, and placed on a rack at RT. The lid of the MinION MK1B was opened, and the flow cell slipped beneath the clip. To open the priming port, the priming port cap was turned clockwise. Under the lid, a little air bubble was tested, and a small volume was pulled to eliminate any bubbles. A P1000 with a capacity of 200 μl was inserted into the priming port, and the wheel was turned until the dial read 220-230 μl , or until a small volume of buffer was seen entering the pipette tip.

Flow cell priming mix was made by simply adding 30 μl of frozen and mixed Flush Tether (FLT) to a tube of thawed and mixed FB and vortexing at RT. The priming mix (800 μl) was then loaded into the flow cell through the priming port, which prevented the entrance of air bubbles. The flow cell was incubated at room temperature for 5 minutes. Pipetting was used to fully mix the contents of the LB before loading it. 37.5 μl of SQB, 25 μl of LB (mixed immediately before usage), and 12 μl of DNA library prep were combined in a fresh tube. The flow cell priming was completed by gently raising the SpotON sample cover, allowing access to the SpotON sample cover. The priming mix (200 μl) was loaded into the flow cell through the priming port, which prevented the entrance of air bubbles. The prepared library was gently mixed by pipetting up and down before loading 75 μl of the sample dropwise into the flow cell via the SpotON sample port, ensuring that each drop flows into the port before adding the next. The SpotON sample cover was carefully reinstalled, making sure the bung entered the SpotON port, before closing the priming port and replacing the MinION Mk1B lid.

The MinION Mk1B was then connected to the server using a UBS connection, and the sequencing settings were configured. Sequencing was performed for 5 hours.

3.11 Genome characterization and Phylogenetic analysis

To identify important phage signatures and motifs of the chosen phages and to conduct comparative genomic analysis against other bacteriophage sequences in public databases, whole genomes were analyzed using PhiSiGns programs (<http://www.phantome.org/phisigns/>; <http://phisigns.sourceforge.net/>); The ORFs were predicted using the GeneMark program (<http://exon.gatech.edu/>) and ORF Finder (<http://www.ncbi.nlm.nih.gov/gorf/gorf.html>) and REsFINDER was used to search for potential allergens, virulence and antibiotic resistance genes in virulence factor and allergen databases (<http://www.allergenonline.com>, <http://www.mgc.ac.cn/VFs>) (Chen *et al.*, 2012) and ResFinder (<http://cge.cbs.dtu.dk/services/ResFinder/>) (Kleinheinz *et al.*, 2014). The translated DNA sequences of the sequenced bacteriophages were matched with homologous sequences from phages in the same family using the ClustalW2 tool for phylogenetic analysis. To confirm the phenotypic traits of the chosen phages, the PHACTS tool (<http://www.phantome.org/PHACTS/upload.php>) that predicts if the bacteriophage is temperate or lytic in its lifestyle was utilized.

3.12 Scientific and Ethical Approval

Ethical clearance for this study was obtained from the KEMRI ethical review board. Approval reference; KEMRI/SERU/CMR/P00111/3953.

3.13 Data Analysis

All laboratory data obtained was recorded in the laboratory note book and/or entered in excel sheets in a password protected computer backed-up on external drives. Computational data utilized institutional server and web-based programs and stored on password protected folders on shared drives.

Data analysis was done using various bioinformatics tools such as PhiSiGns, GeneMark, REsFINDER and ClustalW2 as specified in the materials and methods section to characterize the bacteriophages and to compare genome sequences against reported

sequences in databases and conduct phylogenetic analysis of translated DNA sequences of ORFs.

3.14 Biosafety

Laboratory Safety was strictly observed in that all experiments were performed under sterile conditions on a clean bench and/or in a laminar flow hood to not only protect staff but also contain any spillage of the test organisms which are pathogenic. All the two laboratories at KEMRI and IPR are biosafety laboratory level II with Biosafety cabinets level II. Personal protective equipment that includes gloves, laboratory coats and masks were also be used to protect any personnel involved in handling infectious materials. All media and cultures were disposed of by autoclaving at 121 °C for 15 minutes in an autoclavable bag or by incineration. Surfaces were decontaminated using 10-20 % bleach solution for 10 minutes or 70% isopropyl alcohol for 15 minutes.

CHAPTER FOUR

4.0 RESULTS

4.1 Phenotypic confirmation of *E. cloacae* isolates.

These isolates were acquired from the KEMRI repository and sub-cultured on MacConkey agar, Sheep Blood agar and Mueller Hinton agar. There were four clinical isolates blinded as BPa, BPb, BPc and BPd, with an ATTC control as *E. cloacae* 50398. They were all tested for Gram stain, the result of which was gram negative rods. Two biochemical tests (catalase and oxidase) were done for all the isolates, with all the bacteria turning positive for catalase test and negative for oxidase test. The results for both clinical and ATTC isolates of *E. cloacae* are summarised in Table 4.1. while their growth is shown in Figure 4.1

Table 4. 1: Description of bacterial colonies of *E. cloacae*

Characteristic/ biochemical tests	Colony #1 ID <i>E. cloacae</i> 50398(ATTC)	Colony #2 ID BPa	Colony #3 ID BPb	Colony #4 ID BPc	Colony #5 ID PPd
Shape	Circular	Circular	Circular	Circular	Circular
Margin	Entire/smooth	Entire/smooth	Entire/smooth	Entire/smooth	Entire/smooth
Size	Medium	Small	Medium	Medium	Medium
Surface/ texture	Smooth and shiny	Smooth and shiny	Smooth and shiny	Smooth and shiny	Smooth and shiny
Elevation	Raised/convex	Raised/convex	Raised/convex	Raised/convex	Raised/convex
Colour	White/cream	White/cream	White/cream	White/cream	White/cream
Lactose	Negative	Negative	Negative	Negative	Negative
Heamolysis	N/A	N/A	N/A	N/A	N/A
Motility	Non-swarming	Non-swarming	Non-swarming	Non-swarming	Non-swarming
Catalase test	Positive	Positive	Positive	Positive	Positive
Oxidase test	Negative	Negative	Negative	Negative	Negative
Gram's stain	Negative				
Isolate ID:	BPA				
Comment:	For Vitek® 2 platform				

4.2 Morphology of *Enterobacter cloacae*

Phenotypic confirmation and morphology of *E. cloacae* as seen on agar plates of different types of media.

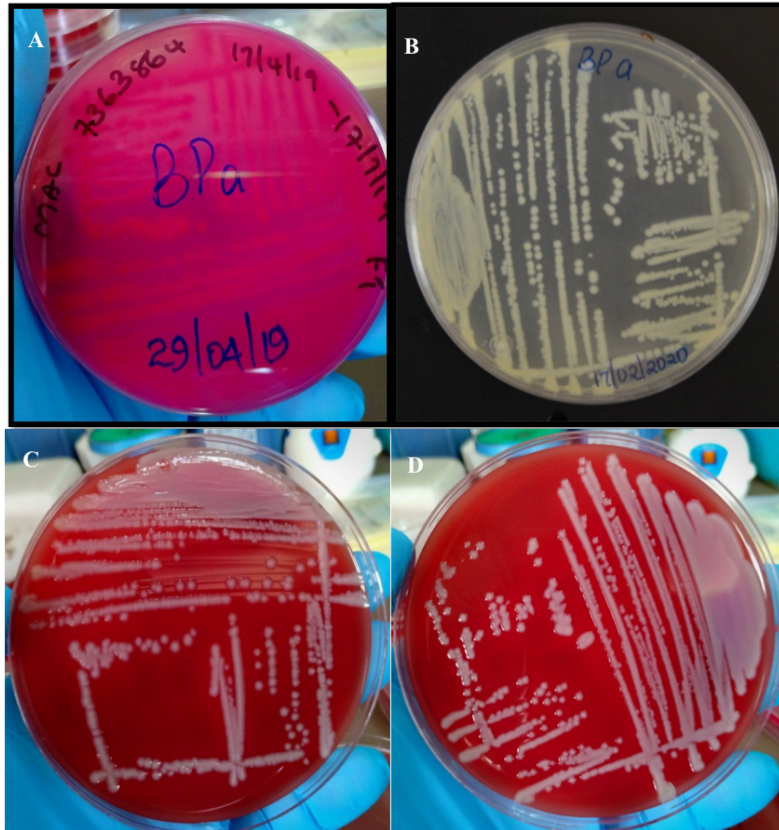


Figure 4.1: *Enterobacter cloacae* clinical isolate cultured on different types of media. A= MacConkey; B= Mueller Hinton Agar; C & D= Sheep Blood Agar (SBA)

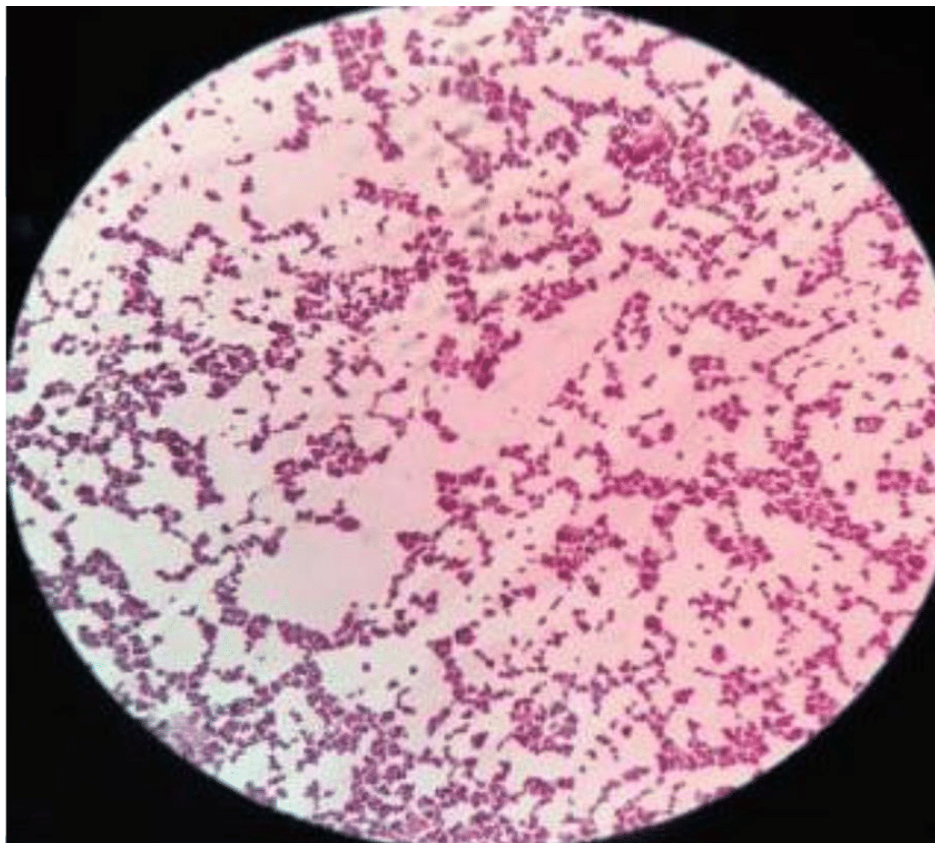


Figure 4.2: A micrograph of *E. cloacae* as seen under the light microscope after Gram's staining. **Magnification X1000.** The bacteria retains the colour of the counter stain thus appearing red, rods in shape and in chains.

4.3 Antimicrobial Susceptibility testing.

After physical and biochemical test of the MDR *E. cloacae* clinical isolates, the Vitek® 2 platform was used to ascertain the AST profile of the different clinical isolates. The results are as indicated in the Table 4.2.

Table 4. 2: Antimicrobial susceptibility testing result for *Enterobacter cloacae* clinical isolates blinded as Bp.

Ticarcillin/Clavulanic Acid MIC TCC	Piperacillin PIP2	Cefuroxime MIC CXM	Cefuroxime Axetil CAE	Cefixime MIC CFM	Ceftriaxone MIC CTX	Cefepime MIC FEP	Aztreonam MIC ATM	Meropenem MIC MEM	Levofloxacin MIC LVX	Moxifloxacin MIC MXF	Minocycline MIC MNO	Tetracycline MIC TCY	Tigecycline MIC TIG	Chloramphenicol MIC C	Colistin MIC COL	Trimethoprim MIC TMP	#R	ID	
R	R	R	R	R	R	R	R	S	R	R	R	R	S	R	S	R	14	Bpa	*
R	R	R	R	R	R	R	R	S	R	R	R	R	S	S	S	R	13	Bpb	
R	R	R	R	R	R	R	R	R	S	S	S	R	S	R		R	12	Bp3	
S	R	R	R	R	R	R	R	S	R	R	R	R	S	S		R	12	Bpc	
I	R	R	R	R	R	R	R	S	S	S	R	R	S	R	R	R	12	BPd	*
R	R	R	R	R	R	R	R	S	S	S	I	R	S	R		R	11	BP2	
R	R	R	R	R	R	R	R	R	S	S	R	R	S	I		S	11	Bp1	

R = Resistance S = Susceptible I = Intermediate susceptibility

Clinical isolates of *Enterobacter cloacae* were subjected to Vitek® 2 platform for confirmation results on the bacterial identity and antimicrobial resistance profile. Seven clinical isolates were classified as MDR as they were resistant to more than 3 classes of antibiotics: BPa, BPb, BPC, BPd, BP1, BP2, and BP3. (BPb and BPC) were susceptible to four antibiotics, that is, Meropenem, Tigecycline, Chloramphenicol and Colistin and Ticarcillin/Clavulanic acid, Meropenem, Tigecycline and Chloramphenicol respectively. BPa was susceptible to only three types of antibiotics; Meropenem, Tigecycline, and Colistin while BPd was susceptible to Levofloxacin, Moxifloxacin and Colistin. Bpa was selected as the most resistant clinical isolate to be used for bacteriophage hunting due to its resistance profile.

4.4 Phage Screening

4.4.1 Spot test results

BP_a and ATTC isolates were screened against samples from all the sources by spot test. Lytic activity was detected only against isolates from Mathare, Zimmerman, Kibera and Chiromo, some of the results are shown in Figure 4.3 as bacterial lawns.

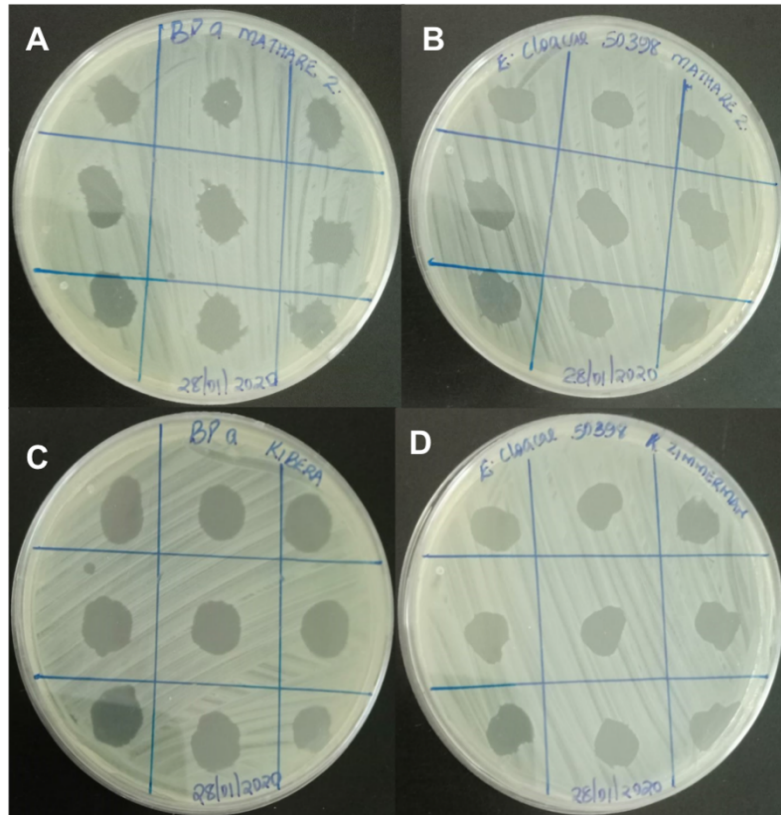


Figure 4.3: Spot assay results revealing clear zones indicative of the presence of bacteriophages on the bacterial lawns. Plates A & C are bacteriophages from Mathare River and Kibera tested on clinical isolate BP_a. Plates B and D are bacteriophages from Mathare river 2 and Zimmerman tested on the ATTC isolate.

4.4.2 Morphology of phages obtained

The isolated phages were characterized by plaque assay, the results shown in Figure 4.4 produced bacteriophages of different sizes as formed on host bacterial lawns of both the ATTC and clinical isolate BPa.

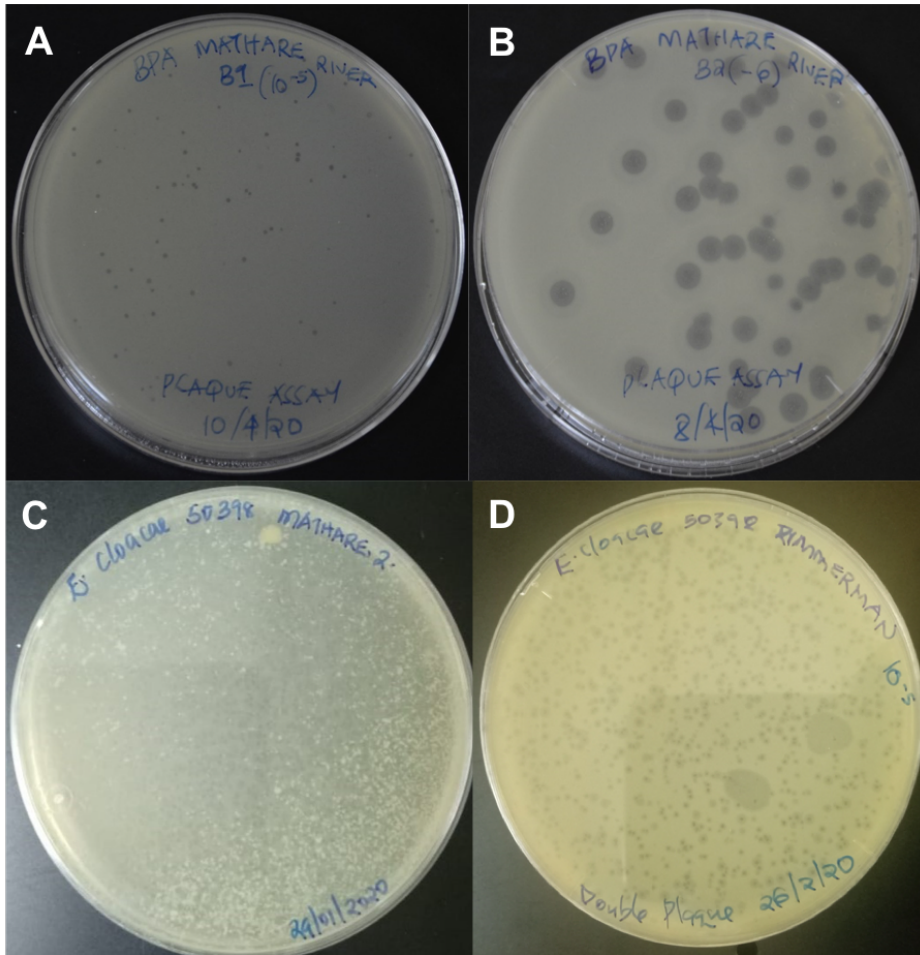


Figure 4.4: Double layer plaque assay revealing plaques of various sizes on the host bacteria. Plates A & B are bacteriophages from Mathare River n lawns of BPa as host while plates C and D were plaques formed by bacteriophages from Mathare river and Zimmerman on lawns of ATTC as the host.

4.5 Physical characterization.

Physico-chemical properties have been known to influence the stability of bacteriophages both in terms of survival and persistence. The isolated phages were subjected to temperature and pH variations to assess not only their therapeutic potential but to simulate their survival in storage conditions. Temperature has been shown to play a pivotal role in phage attachment to host bacterial cell, genetic material injection into the host and eventual phage multiplication. Phages were subjected to various temperature conditions at pH 7.5, with 4°C as control, 25°C as room temperature, 37°C as normal body temperature, while 60°C and 90°C to test the highest temperature the phages can survive. The phages were stable after an hour in a water bath at 4°C, 25°C and 37°C, showing a concentration of about 7 log PFU.mL⁻¹. At 60°C phage titer dropped to half at about while at 90°C, the phage lost their titer to nearly zero. pH tolerance was also assessed for the isolated phages, ranging from pH 2 as acidic, pH 4.5, pH 5.5, pH 7.5, pH 9.0, pH 11.5 and pH 13 as basic. The phages tolerated a wide range of pH. At high acidic pH of 2.0 and high basic pH of 13.0, the phage titers were almost at zero while at pH 4.5 to pH 11.5, the phage remained stable with pH 7.5 being the optimal pH for the phages. Results are shown in Figure 4.5 for clinical isolate BP_a Mathare river bacteriophages on plate A for pH while for temperature the phages against ATTC isolate from the Mathare river are shown in plate B

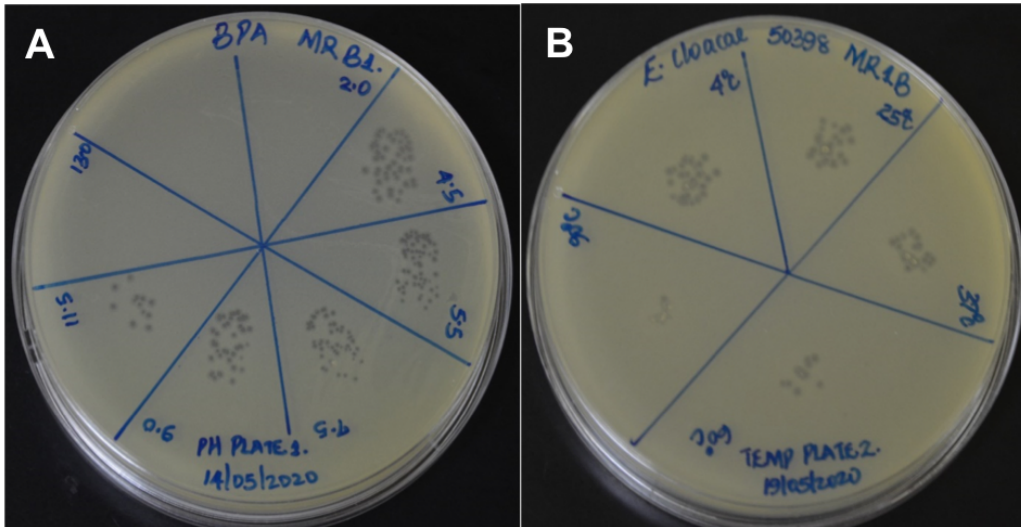


Figure 4.5: Thermal and pH stability of isolated phages. A]: This phage BPA MRB1 exhibited activity at all pH evaluated except at pH 2 and 13. Efficiency increased with increasing pH from pH 4.5 to 9, dropping to nearly half at pH 11.5. Optimal pH was 7.4 hence acting as the control. B]: This phage BPA MRB1 exhibited activity at all temperatures evaluated except at 90 °C. Phage BPA MRB1 has high stability with high efficiency at 4 °C to 37 °C with an optimal temperature being 37 °C. Efficiency at 60 °C reduced to nearly half and to zero at 90 °C.

Isolated bacteriophages were tested for pH tolerance. The phages showed high tolerance to a range of pH values with no significant change noticed between pH 4.5 and pH 9.0, with pH 7.5 being the ideal pH for the phages. At pH 11.5, the phages viability decreased to nearly half while at lower pH of 2.0 and higher pH of 13.0, the phages completely lost their viability (Fig 4.6A). The phages were able to tolerate different temperature conditions with no significance loss of viability at temperatures 4 °C, 25 °C and 37 °C. However, when the phages were treated at 60 °C for 1 hour, they lost their viability which decreased sharply to nearly half while the infective ability of the phages was completely lost when subjected to 90 °C for 1 hour (Fig 4.6B).

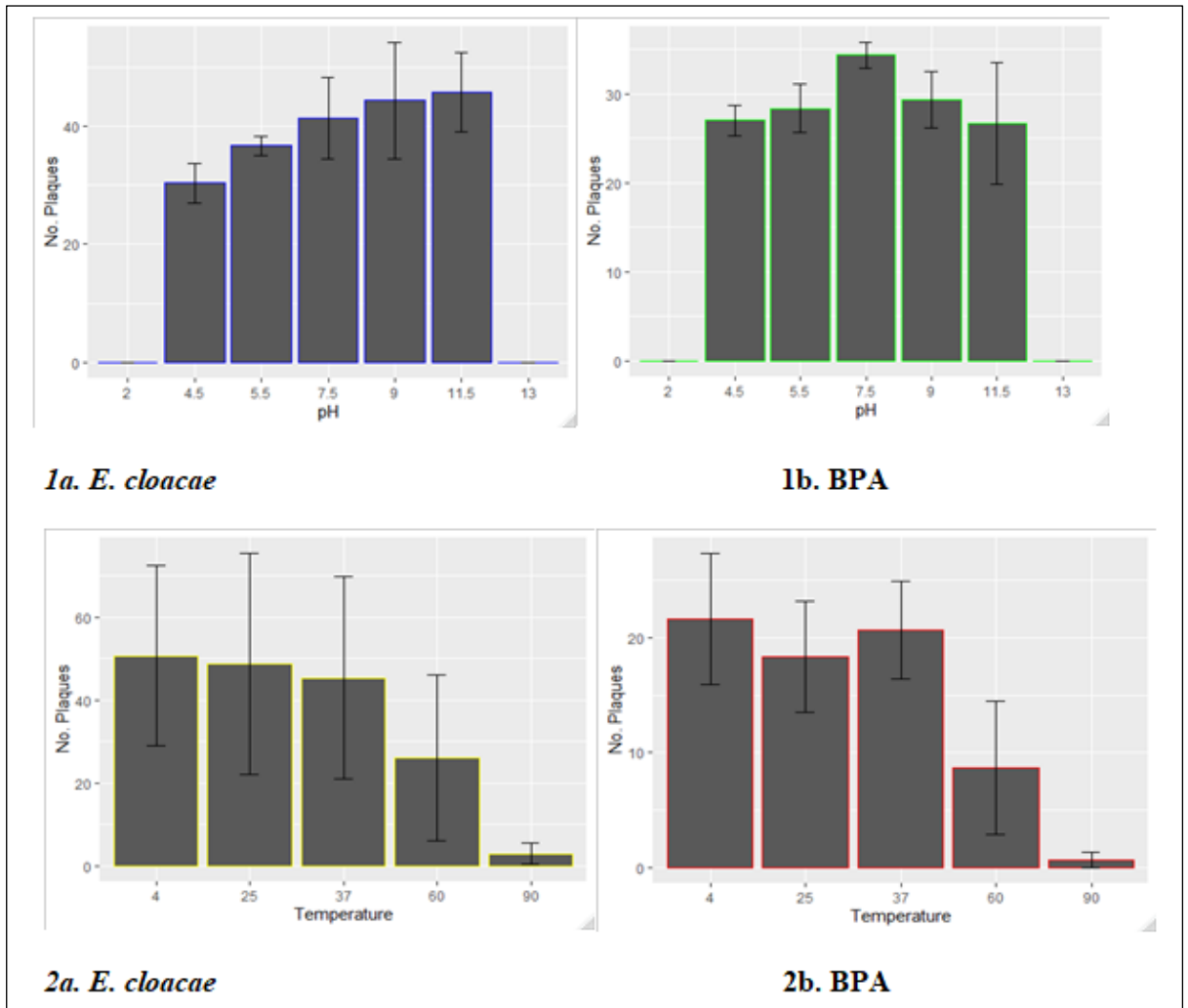


Figure 4.6: Graphical representation of the phage titres at different pH and Temperature variations
 There was little or no activity at pH 2 and 13 (1a). This phage increased in activity from pH 4.5 to 11.5 (1b). The phage had little or no activity at pH levels of 2 and 13, but rose steadily from 4.5 to 11.5, with optimal activity experienced at pH value of 7.5. Figure 2a and 2b represent phage titres at different temperature values. The phages level of activity increased with increasing temperature up to 37 °C, at 60 °C it dropped to nearly half while at 90 °C activity drops to almost zero.

4.6 Host Range Analysis.

Results for host range analysis in which the 19 isolated were tested against 32 *E. cloacae* bacterial isolates and one *S. aureus* as a negative control were analysed and presented in the Table 4.3.

A total of 19 bacteriophages were isolated, majority of which were from environmental samples, mainly from sewage water flowing into Nairobi River. Sewage water is believed to contain a variety of microbes due to contaminations from hospital drainage water and municipal wastes.

The isolated bacteriophages were found to be extremely lytic, as evidenced by their clear plaque-forming behavior, resulting in distinct plaques (of between 1 to 5 mm) Figure 4.3. The phages, showed a wide host range, with all the 19 phages lysing 12 out of the 32, (32 *E. cloacae* and 1 *S. aureus*) bacterial isolates they were subjected to (Figure 4.3) and displaying a lytic range of between 15-23 bacterial isolates. This was a 63.16% of the phages showing 100% lysis of the isolates subjected to. 7/33 (36.84%) of the bacterial isolates were not lysed by any of the 19 phages. There was no lysis on the *S. aureus* negative control plates by all the 19 phages. Host range is an important factor in determining how the phage is used in phage therapy

Table 4. 3: Host Range Analysis of the 19 isolated bacteriophages

Bacterial isolates	#2	#4	#1	#14	#19	#7	#5	#10	#13	#9	#15	#3	#11	#12	#16	#17	#18	#8	#6	Total # of phages that lyse the bacterial strains
<i>Enterobacter cloacae</i> #1	+	+	+	+	+	+	+	+	+	+	+	+	+	+	+	+	+	+	+	19
<i>Enterobacter cloacae</i> #2	+	+	+	+	+	+	+	+	+	+	+	+	+	+	+	+	+	+	+	19
<i>Enterobacter cloacae</i> #4	+	+	+	+	+	+	+	+	+	+	+	+	+	+	+	+	+	+	+	19
<i>Enterobacter cloacae</i> #5	+	+	+	+	+	+	+	+	+	+	+	+	+	+	+	+	+	+	+	19
<i>Enterobacter cloacae</i> #7	+	+	+	+	+	+	+	+	+	+	+	+	+	+	+	+	+	+	+	19
<i>Enterobacter cloacae</i> #10	+	+	+	+	+	+	+	+	+	+	+	+	+	+	+	+	+	+	+	19
<i>Enterobacter cloacae</i> #12	+	+	+	+	+	+	+	+	+	+	+	+	+	+	+	+	+	+	+	19
<i>Enterobacter cloacae</i> #14	+	+	+	+	+	+	+	+	+	+	+	+	+	+	+	+	+	+	+	19
<i>Enterobacter cloacae</i> #16	+	+	+	+	+	+	+	+	+	+	+	+	+	+	+	+	+	+	+	19
<i>Enterobacter cloacae</i> #22	+	+	+	+	+	+	+	+	+	+	+	+	+	+	+	+	+	+	+	19
<i>Enterobacter cloacae</i> #27	+	+	+	+	+	+	+	+	+	+	+	+	+	+	+	+	+	+	+	19
<i>Enterobacter cloacae</i> #23	+	+	+	+	+	+	+	+	+	+	+	+	+	+	+	+	+	+	+	19
EBx1	-	+	+	+	+	+	+	+	+	+	+	+	+	+	+	+	+	+	+	18
EBx2	-	+	+	+	+	+	+	+	+	+	+	+	+	+	+	+	+	+	+	18
<i>Enterobacter cloacae</i> #26	-	+	+	+	+	+	+	+	+	+	+	+	+	+	+	+	+	+	+	18
<i>Enterobacter cloacae</i> #30	-	+	+	+	+	+	+	+	+	+	+	+	+	+	+	+	+	+	+	18
<i>Enterobacter cloacae</i> #11	-	+	+	+	+	+	+	+	+	+	+	+	+	+	+	+	+	+	+	18
<i>Enterobacter cloacae</i> #6	+	-	+	+	+	+	+	+	+	+	+	+	+	+	+	+	+	+	+	18
<i>Enterobacter cloacae</i> #9	-	+	+	+	+	+	+	+	+	+	+	+	+	+	+	+	+	+	+	18
<i>Enterobacter cloacae</i> #21	+	+	-	+	+	+	+	+	+	+	+	+	+	+	+	+	+	+	+	18
<i>Enterobacter cloacae</i> #28	+	-	+	-	-	+	+	+	-	-	+	-	-	-	-	+	+	+	+	10
<i>Enterobacter cloacae</i> #17	-	+	-	-	-	-	-	-	-	+	+	+	+	+	+	-	-	+	+	8
<i>Enterobacter cloacae</i> #20	-	-	-	-	+	+	-	-	-	-	-	-	+	+	+	+	+	+	+	9
<i>Enterobacter cloacae</i> #3	-	-	-	-	-	-	-	-	-	-	-	-	-	-	-	-	-	-	-	0
<i>Enterobacter cloacae</i> #8	-	-	-	-	-	-	-	-	-	-	-	-	-	-	-	-	-	-	-	0
<i>Enterobacter cloacae</i> #13	-	-	-	-	-	-	-	-	-	-	-	-	-	-	-	-	-	-	-	0
<i>Enterobacter cloacae</i> #19	-	-	-	-	-	-	-	-	-	-	-	-	-	-	-	-	-	-	-	0
<i>Enterobacter cloacae</i> #24	-	-	-	-	-	-	-	-	-	-	-	-	-	-	-	-	-	-	-	0
<i>Enterobacter cloacae</i> #25	-	-	-	-	-	-	-	-	-	-	-	-	-	-	-	-	-	-	-	0
<i>Enterobacter cloacae</i> #31	-	-	-	-	-	-	-	-	-	-	-	-	-	-	-	-	-	-	-	0
<i>Staphylococcus aureus</i>	-	-	-	-	-	-	-	-	-	-	-	-	-	-	-	-	-	-	-	0
Total # of bacterial strains that the phages lyse	15	20	20	20	21	21	21	21	21	21	21	22	22	22	22	22	22	23	23	

KEY: + phage susceptible; - phage resistant

Nineteen phages isolated were tested for host range analysis on 33 bacteria (33 *E. cloacae*) and *S. aureus* as a negative control. Twelve (63.15%) out of the nineteen (19) bacteriophages exhibited 100% lysis by spot assay to the *E. cloacae* bacterial species. There was no lysis on the negative control (*S. aureus*) by all the bacteriophages tested against it, a characteristic high specificity phenomenon exhibited by most bacteriophages.

4.7 Test for purity of phage DNA

For us to establish that host bacterial DNA was not present in our phage DNA samples before DNA library preparation, the extracted DNA as well as PCR amplicons of 16S rRNA were run on 1% agarose gel. The extracted phage DNA was present and there was no band equivalent to 16S rRNA, a good indication that the phage DNA did not contain host genome. These results are as displayed in figure 4.7 below

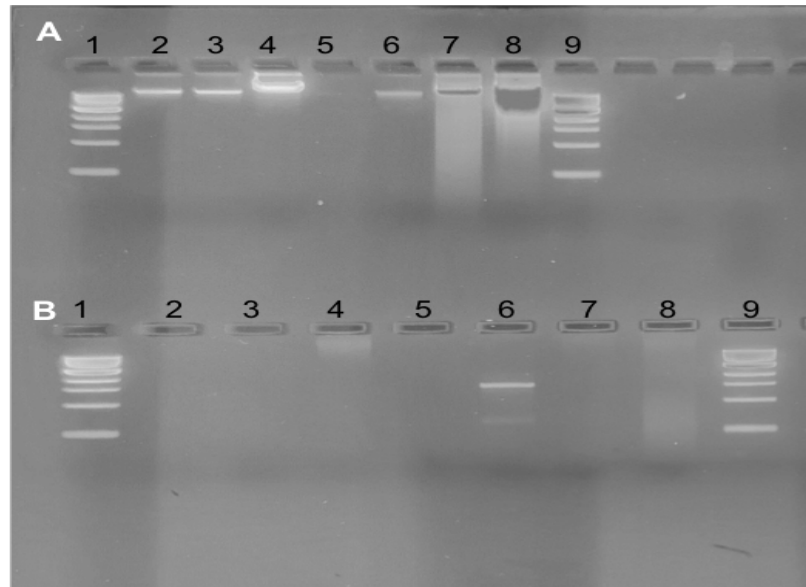


Figure 4.7: Gel electrophoresis of bacteriophages DNA and respective amplicons of 16S rRNA gene. **A:** Wells 2, 3, 6, 7, and 8 represent phage genomic DNA, wells 4 and 5 represents the positive control (phage DNA for *K. pneumoniae*), negative control (Nuclease free water) respectively. **B:** Wells 2, 3, 4, 5 and 8 represent PCR amplicons of 16S rRNA gene. Wells 6 represents the positive control (amplified 16S rRNA gene of *K. pneumoniae* DNA) and well 7 the negative (Nuclease free water) control Molecular weight marker 1Kb; Thermo Scientific™ GeneRuler™ DNA Ladders, was loaded in wells 1 and 9.

4.8 Genomic characterization.

4.8.1 DNA extraction, quantification and library preparation

The extracted DNA was measured on NanoDrop 1000 (ThermoFisher Scientific, 5225 Verona Rd, Madison, WI 53711, USA) followed by Qubit Fluorometer (Quantus TM Fluorometer, E6150, ProMega Corporation, Madison WI 55711-5399, USA.), the results which are displayed in table 4.4.

Table 4. 4: Extracted Phage DNA quantification on both Nanodrop and Qubit platforms.

Sample No	Sample ID	Before extraction	Nanodrop dsDNA Assay			Qubit dsDNA readings
		OD 600nm PFU/ml	ng/μl	A260:280	A260:230	ng/μl
1	EC 50398 MR2	N/A	123.6	1.86	1.33	41.0
2	EC 50398 ZM	N/A	125.5	1.82	1.20	35.0
3	BPA MR E3	N/A	217.2	1.82	1.34	92.0
4	BPA MR KB	N/A	136.2	1.83	1.37	40.0

**A260:230 gives the levels of salt impurities in the DNA samples that is supposed to be below 1.88, an indication that the the extracted DNA was of good quality. Qubit readings indicate the quantity of DNA in the sample.

Phage DNA library preparation was done according to Nanopore sequencing guidelines and results were as displayed in table 4.5.

Table 4.5: Phage DNA library Preparation prior to sequencing. Results are recorded after each step to attain the required threshold for sequencing

Sample No	Sample ID	Before end repair ^a (ng/ul)	1 (or 2) ug DNA ^b	Adjusted to 48ul	After end prep conc ^c	Vol for 750ng/ul ^d	Adjusted to 22.5ul	Barcode no ^e	After barcoding conc ^f	Equimolar pooling 700ng total ^g
1	EC 50398 MR2	85.8	23.3	24.7	59.4	12.6	9.9	NB09	24.8	3.5
2	EC 50398 ZM	93.6	21.4	26.6	47.6	15.8	6.7	NB10	32.4	2.7
3	BPA MR E3	72.4	27.6	20.4	51.8	14.5	8.0	NB11	22.4	3.9
4	BPA MR KB	54.2	36.9	11.1	54.4	13.8	8.7	NB12	30.6	2.9

4.8.2 Phage sequencing

Sequencing was done via Oxford Nanopore sequencing platform. Five phages which had stable lytic phenotypes were sequenced. A total of 349.1K of reads were generated with 140.45 Mb passed bases. Generated FASTQ files were assembled via Canu v2.2 and flye v2.9. These results are as indicated in Table 4.6

Table 4. 6: Sequencing Results

Internal Phage ID	Host Strain	Sequencing QC	Genome size (bp)	Family
vB_Eclo_MII_001	<i>Enterobacter cloacae</i>	Pass	61kb	Autographiviridea/ Studiervirinae
vB_Eclo_MII_002	<i>Enterobacter cloacae</i>	Pass	77kb	Autographiviridea/ Studiervirinae
vB_Eclo_MII_002_1	<i>Enterobacter cloacae</i>	Fail	28kb	Not Determined
vB_Eclo_MII_003	<i>Enterobacter cloacae</i>	Fail	40kb	Not Determined
vB_Eclo_MII_004	<i>Enterobacter cloacae</i>	Pass	39kb	Autographiviridea / Studiervirinae

Bacteriophage DNA was isolated using Qiagen kit. Quantity and quality of the extracted DNA was measured via nanodrop and qubit respectively sequencing was done via Oxford Nanopore sequencing platform. Prepared DNA library was barcoded with NED104 loaded to a flow cell FA023769 and kit SQK-LSK109 and run over the server for 5 hours via MiniKNOW version 21.06.0 with a MiniKNOW core of 4.3.4 and a Beam of 6.2.5. Base-

calling was done via Guppy 5.0.11 at High-accuracy base-calling and barcodes were trimmed on both ends. A total of 349.1K of reads were generated with passed bases at 140.45 Mb. Generated FASTQ files were assembled via Canu v2.2 and flye v2.9.

4.8.3 Sequence assembly, annotation, alignment and analysis

The genome characteristics of the three analysed bacteriophages were as follows. vB_Eclo_MII_001, vB_Eclo_MII_002 and vB_Eclo_MII_004 was composed of a double stranded DNA molecule ranging between 42 kb and 72 kb. vB_Eclo_MII_001, vB_Eclo_MII_002 and vB_Eclo_MII_004 had a genome size of 61,441 bp, 77,825bp and 38,913bp respectively. The GC content was 48.63%, 49.42% and 52.35% respectively.

vB_Eclo_MII_001 had a total of 156 CDSs with two repeat regions out of which 58 sequences code for proteins with functional assignments while 98 sequences coded for hypothetical proteins. Of the proteins with functional assignment, when the genome of this bacteriophage was annotated, it revealed CIII, CII and CoR 2 genes. Figure 4.8 is a gene representation of the bacteriophage vB_Eclo_MII_001, one of the sequenced bacteriophages with annotations showing the presence Cro, CI, CII and CIII genes that are associated with the lysogenic lifecycle of bacteriophage.

vB_Eclo_MII_002 had 422 CDSs, 15 repeat regions and 3 tRNAs, out of this, 216 CDSs code for proteins with functional assignments while 206 code for hypothetical proteins. Of the sequenced phages, vB_Eclo_MII_002 (Figure 4.9) had the most genes that mapped to sequenced phages in databases. It contained genes encoding proteins responsible for the phage lysis system: endolysin, holin, antiholin, and spanin. (Jiangtao Zhao, 2019).

Among the phage structural proteins revealed in the sequenced phage genomes were terminase large subunit, major capsid, baseplate, and tail fiber proteins. (Li *et al.*, 2016)

vB_Eclo_MII_004 on the other hand had 97CDSs with 2 repeat regions. Out of this 65 CDSs codes for proteins with functional assignments while 32 code for hypothetical proteins.

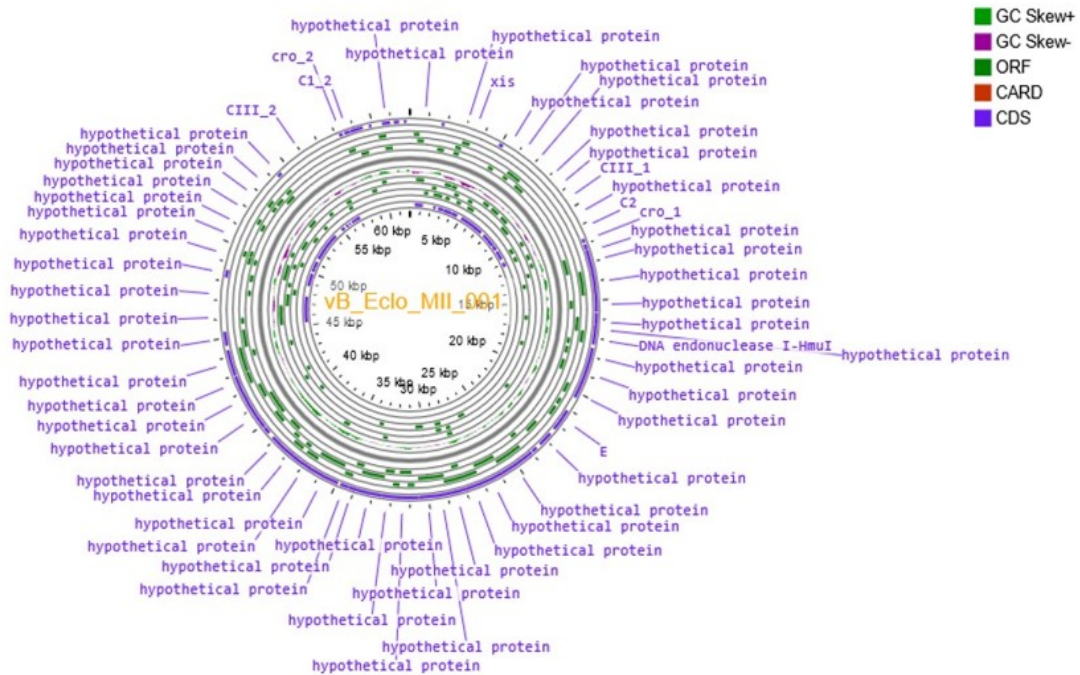


Figure 4.8: Circular Genome View for vB_Eclo_MII_001. The outermost ring represents the contig of the phages. The adjacent three rings represent the CDSs of the linear vB_Eclo_MII_001 genome: Green = positive strand, Purple = Negative strand, Light blue= repeat regions. Orange ring represents tRNA; the inner ring; Light purple represents the GC content while the innermost ring; Brown represents the GC Skew.

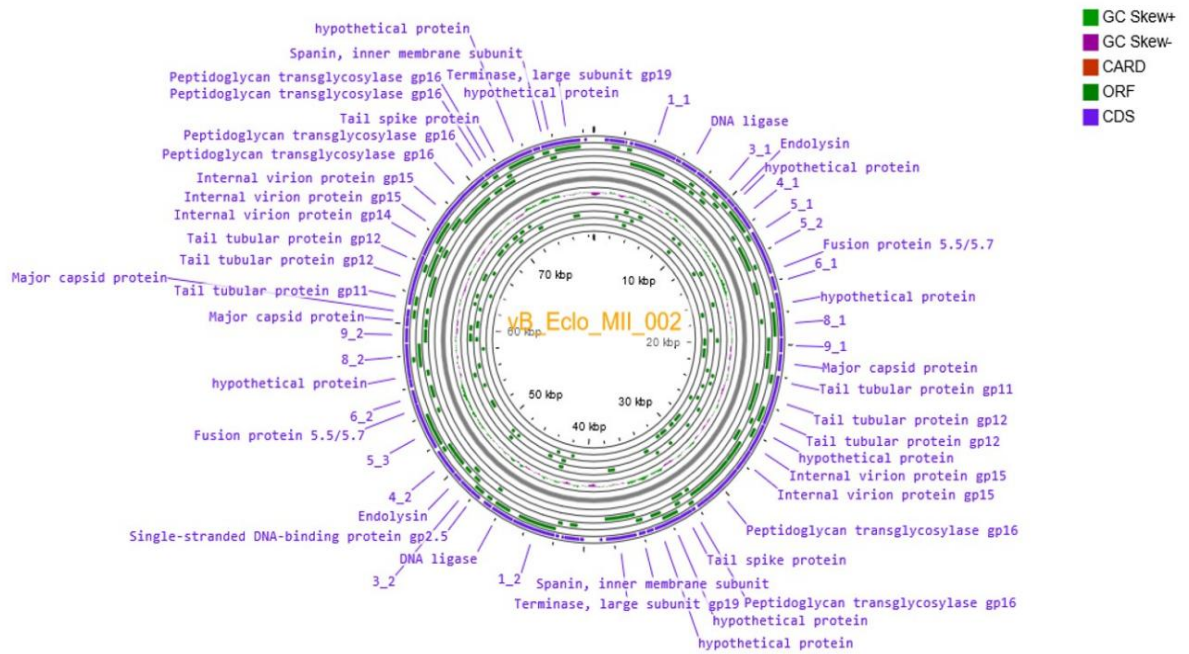


Figure 4.9: Circular Genome View for vB_Eclo_MII_002. The outermost ring represents the contig of the phages. The adjacent three rings represented the CDSs of the linear vB_Eclo_MII_003 genome: Green = positive strand, Purple = Negative strand, Light blue= repeat regions. The inner ring; Light purple represents the GC content while the innermost ring; Brown represents the GC Skew.

4.8.4 Alignment of bacteriophage sequences.

The sequenced bacteriophages were analysed against those sequences downloaded from databases to find areas of similarity that may be the result of functional, structural, or evolutionary links between the sequences. Rows of a matrix were used to represent aligned sequences of nucleotide. Gaps are placed between the residues to align identical or similar characters in succeeding columns. A multiple sequence alignment of the bacteriophage sequences for the sequenced bacteriophages (Figure 4.10).

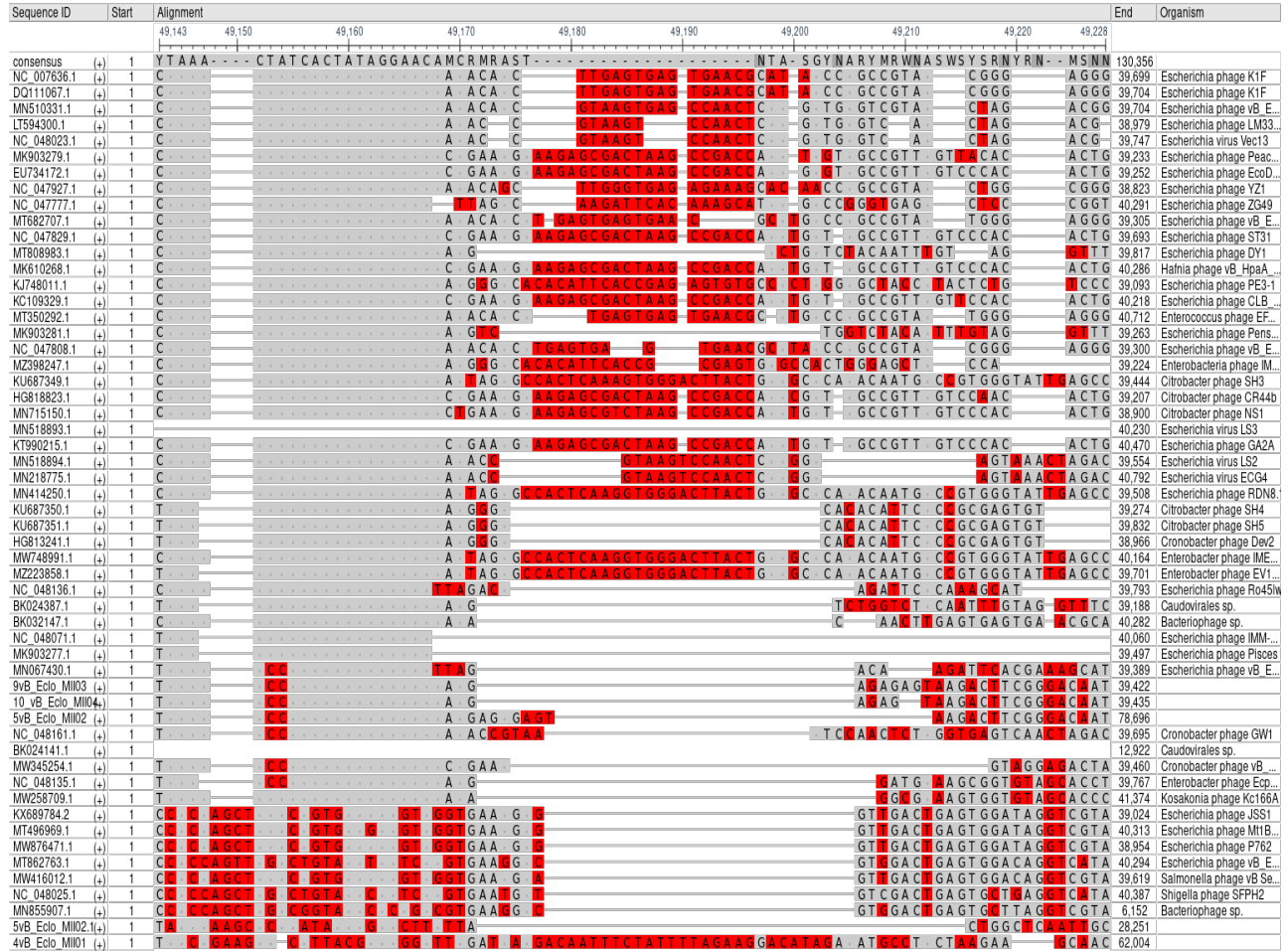


Figure 4.10: Multiple Sequence alignment of the isolated bacteriophages with related sequences from National Center for Biotechnology Information (NCBI) database. The colouring scheme shows bases in regions that are conserved. Gray areas show conserved areas within the genomes of the bacteriophages while the red coloured areas are non-conserved areas of the bacteriophages.

One typical application of open reading frames (ORFs) is as evidence to aid in gene prediction. Long ORFs are frequently employed, in conjunction with other data, to identify possible protein-coding or functional RNA-coding sections in a DNA sequence. Here, ATG was set as the start codon and possible ORF calculated at an interval of between 1 and 50000 nucleotide sequences. The results were displayed, with the longest ORF highlighted.

4.9 Phylogenetic Analysis

To study the evolutionary relationship of the isolated bacteriophages, their genomes were compared with previously sequenced phages deposited in GenBank. Multiple alignment (Fig 4.12) of these phages with those in database clearly indicated that these phages align well with other phages in this family thus should be treated as members of the family Autographiviridea/ Studiervirinae. (Hongyu Ren1, 2020) Classification of one of the bacteriophages

Table 4.7: Classification of one of the isolated phages as obtained from PATRIC. This phage was classified as belonging to class Caudoviricetes and family autographiviridae/studiervirinae

Pct Coverage	Fragments in Clade	Fragments in Taxon	Rank	NCBI Taxon ID	Scientific Name
100.00	1	0	R	1	
100.00	1	0	D	10239	Viruses
100.00	1	0	D1	2731341	Duplodnaviria
100.00	1	0	D2	2731360	Heunggongvirae
100.00	1	0	P	2731618	Uroviricota
100.00	1	0	C	2731619	Caudoviricetes
100.00	1	0	O	28883	Caudovirales
100.00	1	0	F	2731643	Autographiviridea
100.00	1	0	F1	2731653	Studiervirinae
100.00	1	0	G	2732686	Kayfunavirus
100.00	1	0	S	2733639	Escherichia virus IMM002
100.00	1	1	S1	2041760	Escherichia phage IMM-002

A phylogenetic tree based on the blast search was constructed and the topological robustness of the tree was evaluated using percentages of the posterior probabilities. Figure (4.16) shows the phylogenetic tree for sequenced bacteriophages in relation to sequences of other bacteriophages downloaded from databases.

BLASTn analysis of the five phages was performed. vB_Eclo_MII_001, vB_Eclo_MII_002, vB_Eclo_MII_003 and vB_Eclo_MII_004 genomes were highly similar to phages in the family Autographiviridea/ Studiervirinae (similarity approximately 75%).

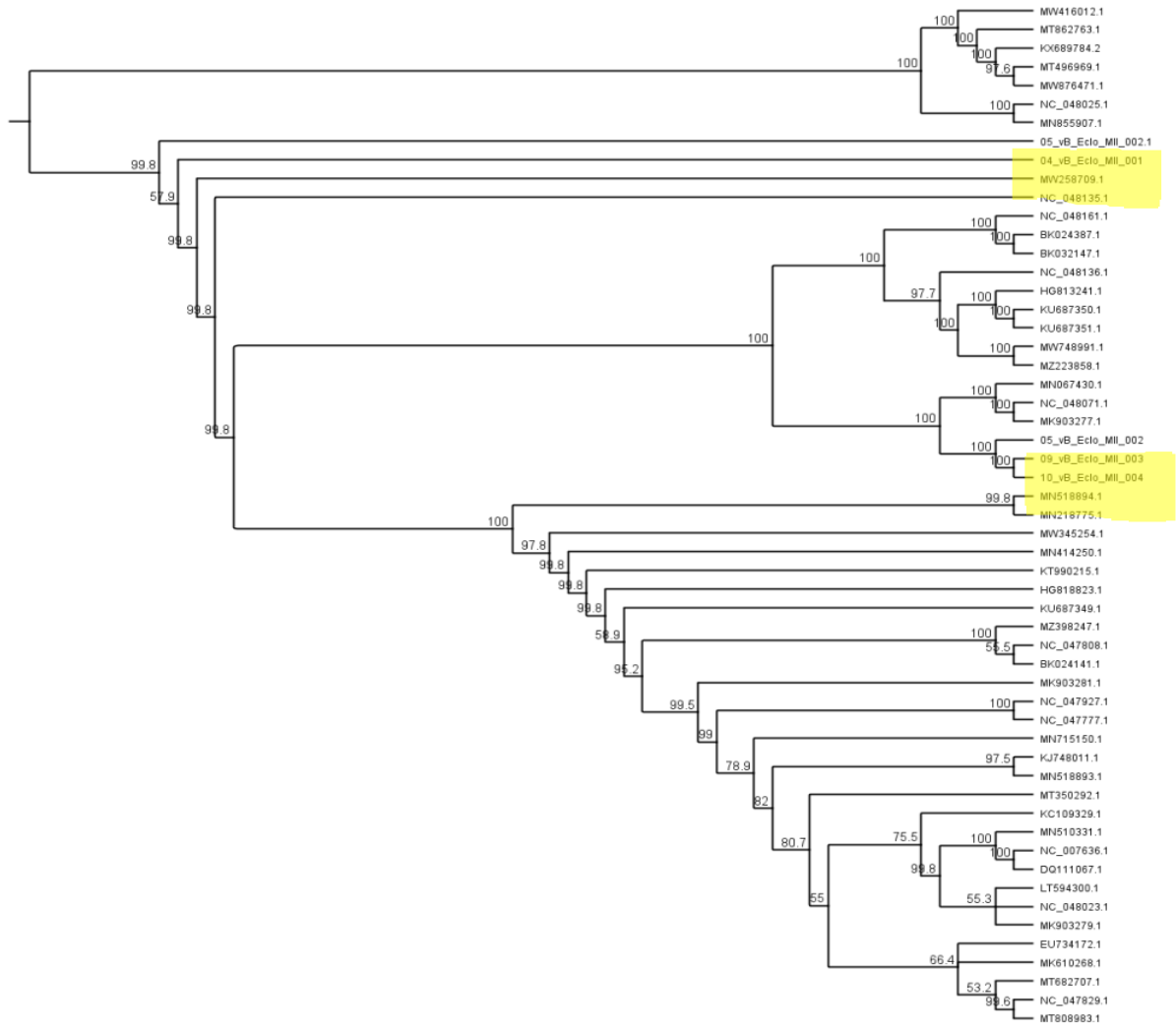


Figure 4.11: Phylogenetic analysis of the sequenced bacteriophages in comparison to those found in databases. Notice that three bacteriophages are in one cluster/cled while two are in one cluster.

CHAPTER FIVE

5.0 DISCUSSION, CONCLUSION AND RECCOMENDATIONS

5.1 DISCUSSION

The rise in multidrug resistance in *Enterobacter cloacae* due to pressure exerted on antibiotics makes it increasingly difficult to treat. This study set out to identify phages against clinical isolates of MDR *E. cloacae* from Kenya with potential as alternatives to antibiotics for clinical therapy. The first objective was to identify MDR isolates for use to screen for phages from an existing repository. A panel of clinical isolates were confirmed by phenotypic and biochemical assays and finally on a Vitek® 2 platform to be *E. cloacae*.

AST results were done for all clinical isolates available. It was noted that among the clinical isolates tested, there were several MDR strains, resistant particularly to penicillins as well as to 1st, 2nd and 3rd generation cephalosporins, confirming that *E. cloacae* can be a human pathogen of concern to physicians because the remaining antibiotics are not readily available for therapy. The potential for having extensively or completely drug resistant isolates exists as has been shown in figure 2.1, with CREC in circulation in different sections of the globe (Capelo, Sahl, Uhlemann, Annavajhala, & Gomez-Simmonds, 2019). *E. cloacae* has been shown to produce chromosomally derived AmpC beta-lactamase (Rottman *et al.*, 2002), as a result, they are innately resistant to aminopenicillins and 1st- and 2nd-generation cephalosporins (Tamma *et al.*, 2019). ESBL-producing *Enterobacter* species on the other hand, arose as a result of the abuse of third-generation cephalosporins (Pfaller & Segreti, 2006; Rawat & Nair, 2010). Treatment options are becoming less available since ESBL-producing isolates have been shown to hydrolyze penicillin, cephalosporins, and monobactams (Gutiérrez-Gutiérrez & Rodríguez-Baño, 2019; Essack, 2000).

BPa as the most resistant isolate susceptible to only three 3 drugs; that is, Meropenem, Tigecycline and Colistin which are among the last line of drugs to be administered to patients in critical care. These drugs are not readily available or affordable in Kenyan public hospitals and some like colistin are nephrotoxic and not in common use. An infection caused by an isolate of this kind could qualify for alternate more available therapies like phage therapy.

The second objective was to screen for lytic phages against this MDR bacterial isolate Bpa. Bacteriophages from different sources that included Kenyatta National Hospital sewer line, Kariobangi waste water treatment plant, waste water from Zimmerman estate and Kibera slums, Nairobi river water with sampling at Museum hill, Chiromo and Mathare slums as well as fresh water from Lake Victoria were isolated. Both BPa as the clinical isolate as well as ATCC 50398 were used in screening of the phages by spot test from all the sources. Lytic activity was observed only against phages from Kenyatta National Hospital, Zimmerman, Kibera, Kariobangi, Mathare, and Chiromo. There was no activity against samples from Lake Victoria and Museum Hill. It was hypothesised that this is due to evolutionary dynamics between phages and their hosts. Phages are found in environment where their hosts exist. These differences could have arisen due the fact that in the environment where there were no bacteriophages sampled, there could be variations to warrant isolation or no isolation of a phage within that locality.

Further characterisation of the bacteriophages meant subjecting them to plaque assay so as to establish their morphology on the plates using bacterial lawns. Bacteriophages of different sizes, small, medium and large plaques were obtained, both for ATCC and the clinical isolate, BPa. Surprisingly, phages that had been obtained by spot assay from KNH, Lake Victoria and Museum Hill failed to form plaques on the bacterial lawns perhaps due to low phage titre numbers that were outgrown by the host bacteria especially after serial dilution.

The isolated phages were subjected to physical characterization, which is temperature stability as well as pH. Physiochemical properties have been known to influence the stability of bacteriophages both in terms of survival and persistence. For therapeutic applications in the developing worlds, phage preparations should be stable at room temperature to minimize transportation logistics and be stable at wide range of pHs to account for minor variations in preparations.

The isolated phages were subjected to temperature and pH variations to assess not only their therapeutic potential but to simulate their survival in storage conditions. Temperature

has been shown to play a pivotal role in phage attachment to host bacterial cell, genetic material injection into the host, the length of the latent period especially for lysogenic phages and eventual phage multiplication. Fewer phages can participate in the proliferation phase because less bacteriophage genetic material enters bacterial host cells at lower temperatures. Higher temperatures might cause the dormant stage to last longer. Temperature also has an impact on bacteriophage abundance, survivability, and storage (Jończyk, Kłak, Międzybrodzki, & Górski, 2011).

Temperature has been demonstrated to be important in phage attachment to host bacterial cell, genetic material injection into the host and eventual phage multiplication. Of the physical parameters assayed, temperature stability of the vB_Eclo_MII_001 remained stable between 4 °C – 37 °C. Infectivity of the phages on the other hand was observed to decrease to nearly half the titres at temperatures 60 °C, with infectivity decreasing to almost zero at temperatures 90 °C (Figure 4.6). Similarly, the phages viability remained stable at pH ranges of 4.5 - 11.5 with the ideal pH being 7.5.

At pH lower than 4.5 and greater than 11.5, the infectivity rates of the phages dropped to nearly zero, an indication that the phages titres decreased in extreme pH levels. These results were similar to those reported by (Zhao *et al.*, 2019; Melo *et al.*, 2019). The ability of bacteriophages to survive in extreme levels of pH has been linked to their ability to acquire nonreversible mutations when incubated at those pH levels. In a survey set out to find the linear relationship between phage mutations and low pH incubation periods conducted by Strack *et al.*, it was shown that phages can acquire mutations to survive in acidic environments.

In this study however, the isolated phages did not survive in pH lower than 4.5. Likewise, our phages were stable at alkaline pH, showing no loss of viability at 7.5, 9.0 and 11.5. At pH 13.5, the viability of these phages reduced drastically to nearly zero, with few phages surviving at this pH. The reduction in phage titers might be associated with the dissociation of the capsid protein in high quantities of hydrogen and hydroxyl ions in the solution (Feng *et al.*, 2003). The capacity of the isolated bacteriophages to survive under

severe pH levels is extremely useful in a variety of applications in animal and food industries. Oral phage formulations need to survive the GIT low pH of between 1-5. Phages can also be employed as biocontrol in acidic foods like fruit juices and fermented foods like pickles (Raya *et al.*, 2006).

High temperatures have been proven to inactivate phages because nucleic acids, both DNA and RNA, and proteins are denatured. Yamaki *et al.*, were able to show that Myoviridea phages decreased in activity after 60 minutes of incubation at 60 °C. In this investigation, it was found out that there was significant loss in activity detected at 60 °C for 60 minutes to nearly half, with no activity detected at 90 °C. Additionally, phages respond to effects of temperatures differently, with some phages being susceptible to high temperatures while others tend to tolerate. Development of heat resistance can be attributed to mutations or strong protein interactions by the phages which can explain the survival of one the isolated phages at 90 °C albeit at low titres (Figure 4.5B).

Some phages may be preserved in solution or dry form for lengthy periods of time under neutral pH (6 to 8). (Jonczyk *et al.*, 2011). In general, bacteriophage titers fall gradually with pH. For example, when pH was dropped from 6.19 to 5.38 between 4 and 6 h, *S. aureus* phage titer reduced by 2 log (Garcia *et al.*, 2009). When the pH falls below 4.5, the multiplication of numerous phages is controlled, but the danger of harmful bacteria food contamination is also lowered. T4 phage of Myoviridae family, for example, is unstable at pH <5. After 1 hour at pH 5.0 and 37°C, Phage PM2 (Corticoviridae family) loses all activity.

In the case of phage oral injection, however, stomach acid can have a deleterious influence on phage survival, potentially leading to treatment failure (Watanabe *et al.*, 2007). These results appeared similar to those observed by (Luís D. R. Melo, 2019) in which comparison of two bacteriophages belonging to *Siphoviridea* and *Podoviridea* revealed a high tolerance of the phages to both temperature and pH ranges. There was no significant loss of phage viability of the phages isolated in the study at 4 °C, 25 °C and 37 °C, even for longer storage at 4 °C. Survival of these phages under different temperature conditions

indicates their long shelf life and broad storage conditions (Warren & Hatch, 1969) ideal for the local setting. It was thus found that not only are these phages thermostable at temperatures between 4-37 °C, they were also stable at pH 7.5 – 11.5.

Bacteriophage host specificity is an important factor to consider while developing a bacteriophage application. As previously mentioned, the greater the breadth of the target pathogen species' host range (how many diverse strains of a species are infected), the more probable it is that a specific phage will be used for any individual infection by that target pathogen. As previously stated, host range is identical with productive host range as described by (Hyman & Abedon, 2010), i.e, bacteria capable of supporting phage infections that create new phage virions. The phages in this investigation were shown to have a confined host range, infecting solely *E. cloacae* strains, with the negative control of *S. aureus* not lysed, results that coincides with recent phage research that had shown that phages had high selectivity for the cell surface receptors presented by their hosts (De Melo *et al.*, 2019). A restricted host-specific bacteriophage appeared to be an appealing property, especially when used in the GIT system to target certain host bacterial cells since bacteriophage's narrow host range might not harm many endogenous microbes (Viazis *et al.*, 2011; Drulis-Kawa *et al.*, 2012).

A phage should not infect other taxa, primarily for two reasons, it may lyse non-pathogenic bacterial cells in the natural flora and it may reduce the phage's optimum dose toward the targeted bacterium, albeit the problem becomes complicated if the infections are productive. Not all the 19 phages isolated could lyse all the clinical isolates subjected them to, partly because of the limited resources and because phages evolve with bacteria in the same environment and thus, as bacteria evolve to gain resistance to phages within that environment, phages too evolve to counter-attack bacterial cell. Thus, there needs to be a wide scope to screen phages for all clinical bacterial isolates. Furthermore, multiple kinds of restricted host range bacteriophages can be mixed in a cocktail composition to inhibit harmful bacteria *in vitro* more effectively (Tanji *et al.*, 2004; Mapes *et al.*, 2016; Bai *et al.*, 2019).

While it is frequently assumed that host range is driven by the presence of the proper receptor on the target bacterium, other restrictions include microbial anti-phage defences mechanisms like CRISPR/Cas systems, restriction enzymes, as well as toxin-antitoxin processes (Labrie *et al.*, 2010; Hyman & Abedon, 2010). Because phages have countering mechanisms, host range is not a static feature but rather a dynamic one that is capable of changing over duration of time (Laanto *et al.*, 2017; Buckling & Brockhurst, 2012).

Although most phages lysed a majority of the clinical isolates, some microbial isolates were not lysed by any phages indicating that more phages would have to be screened for to cover all endemic *E. cloacae* strains. The study postulates that these bacterial cells that could not be lysed by any of the phages isolated have become resistant to the phages. Bacterial defense mechanisms evolve phage resistance under phage selection pressure (Rohde *et al.*, 2018). Phages, on the other hand, evolve counteradaptations against bacterial antiphage processes in this scenario. As a result, phages and bacteria can co-evolve indefinitely through phage infection and antiphage defensive mechanisms (Hall, Scanlan, Morgan, & Buckling, 2011).

Bacterial phage resistance strategies include both non-specific as well as specific adaptation mechanisms (Rohde *et al.*, 2018). Non-specific bacterial defense systems also known as innate immune systems that can counteract phage infection include attachment-inhibition by the phage, phage genome entry prevention, secondary phage infection restriction; (also referred to as superinfection exclusion), endonucleases and methyltransferases activation (also called restriction-modification system), and suicide induction in infected cells (also called abortive infection system)(Rohde *et al.*, 2018).

Phage-specific bacterial defense mechanisms (adaptive immune mechanisms), like CRISPR/Cas proteins, represent a secondary antiphage defense mechanism(Goldfarb *et al.*, 2015). Growth rate, membrane permeability, capsular polysaccharide (CPS) synthesis, phage-binding receptor, pathogenicity, and antibiotic sensitivity are all altered in phage-resistant bacteria(Barrangou & Oost, 2015). Adsorption, penetration, synthesis, assembly, and release are antiphage mechanisms created in bacteria to combat phage invasion

phages(Stern & Sorek, 2011). For these reasons, the study hypothesised that screening of bacteriophages from diverse environments against these phage resistant bacteria and better still, incorporating them into cocktails can help in reducing resistance.

Other antiphage defense mechanisms include: Phage binding based mechanisms in which the predominant defensive strategy is the attachment blocking mechanism that prevents infection by the phage; prevention of phage attachment and entry in which adsorption of phage is blocked by modification of surface cell receptors, extracellular polysaccharides production or synthesis of receptor-binding protein analogs that result in phage resistance; superinfection exclusion systems in which a prophage already integrated in the host genome blocks the assimilation of phage DNA, otherwise referred to as superinfection immunity; inhibition of virion synthesis and assembly where the synthesised phage genome is destroyed at various levels of replication, transcription, translation and assembly by restriction-modification mechanisms (R-M) as well as CRISPR-Cas system; restriction modification mechanism that consists of restriction endonucleases (REases) as well as methyltransferases (MTases) that serve to degrade unmethylated phage genomes and methylated host bacterial DNA that serves to protect host chromosomal DNA from cleavage by REases; CRISPR-Cas systems which is an adaptive immunity with abilities to remember past infections hence serving to degrade the injected bacteriophage genome; abortive infection systems in which the main metabolic functions of replication, transcription and translation in infected bacterial host cell is blocked thus protecting surrounding uninfected bacterial cells of the population from attack by the phage; toxin-antitoxin systems that contains two genes, toxin gene that serves to block major metabolic cellular activities like replication, translation and cellwall reconstruction and toxin-diminishing antitoxin gene that serves to neutralize the cognate toxins(Goldfarb et al., 2015)(Stern & Sorek, 2011).

The third objective was to perform genomic characterization which was the hallmark of this study. Of the 19 phages isolated, sequencing was done on the five best performing phages due to limited resources. The high titre phage suspensions gave high yield DNA

on extraction which was quantified on both Nanodrop and Qubit platforms and was found by 16srRNA PCR to have no bacterial host genome contamination.

Sequence assembly and annotation of vB_Eclo_MII_001 revealed CIII, CII and Cro among genes with functional assignment. These genes have been shown to have lysogeny effect on the bacteriophage. In lambdoid bacteriophage, CIII protein has been shown to be involved in lysogenization process of bacteriophage. Its function is to stabilize the CII, a transcriptional modulator, which in turn induces the transcription of the repressor (cI) and integrase genes while repressing the expression of the late genes.

Overproduction of CIII protein has also been found to cause the heat shock response, most likely by stabilizing the heat shock-specific subunit of RNA polymerase. However, CIII's method of stabilizing these proteins is not clear. The lambda (λ) cIII gene has complicated translational requirements, according to research. Previously, it was discovered that the host protein RNase III is essential for effective cIII translation (Häuser *et al.*, 2012). Furthermore, genetic and biochemical evidence revealed that the area around the cIII ribosome-binding site exists in two different conformations, only one of which is translated (Govind *et al.*, 2009) and hypothesized that these characteristics are related to cIII expression regulation at the translational level. In line with this and given the result obtained in figure 4.8, it is hypothesised that this phage is a lysogenic phage.

vB_Eclo_MII_002 had most of the genes that compared to sequenced phages in databases (Figure 4.9). It contained genes responsible for phages' lysis system consisting of four proteins: endolysin, holin, antiholin, and spanin. (Jiangtao Zhao, 2019). Endolysin acts on the bacterial peptidoglycan layer of the cell wall. Endolysin must pass from the cytoplasm to the periplasm to reach its target. Endolysin employs a variety of mechanisms to do this. The holin–endolysin cell lysis system is one of the most prevalent and well-studied systems that utilizes holin. Holin is a tiny transmembrane protein with one to three transmembranes (Bläsi & Young, 1996; Young, 2002; Reddy & Saier, 2013; Savva *et al.*, 2014). When holin oligomerizes at a precise period, it generates holes in bacteria's cytoplasmic membrane, allowing passive passage of endolysin from the cytoplasm to the

periplasm, prompting cell lysis (Park *et al.*, 2006; Wang *et al.*, 2008). Among the phage structural proteins revealed in the sequenced phage genomes were terminase large subunit, major capsid, baseplate, and tail fiber proteins. (Li *et al.*, 2016)

vB_Eclo_MII_004, on the other hand, had 97CDSs with 2 repeat regions. Out of this 65 CDSs coded for proteins with functional assignments while 32 code for hypothetical proteins. Of the five bacteriophages sequenced, vB_Eclo_MII_002_1 and vB_Eclo_MII_003 were not determined in terms of family while vB_Eclo_MII_001, vB_Eclo_MII_002 and vB_Eclo_MII_004 were determined to belong to Autographiridea/Studiervirinea family.

All three bacteriophages, that is vB_Eclo_MII_001, vB_Eclo_MII_002 and vB_Eclo_MII_004, lacked considerable sequence resemblance to known antibiotic resistance, pathogenicity, or toxin proteins. TnphoA and Tn10d-*bla* transposons (Barondess & Beckwfh, 1990; Reidl & Mekalanos, 1995) are genetic tools produced to help in finding phage factors that encode for virulence. Since PhoA and Bla need to be secreted to be active, screening fusion libraries for transducible PhoA or Bla activity allows for the quick discovery of secreted, phage-encoded potential virulence factors like *E. coli's lom* and *bor* genes (Barondess & Beckwfh, 1990) and *Vibrio cholerae's* phage K139-encoded *glo* gene (Reidl & Mekalanos, 1995). It is worthy noting that phage-encoded genes are not always transmissible, owing to the fact that technological limitations exist in detecting transduction or because integrated prophages frequently fail. Presently, analysis of bacterial pathogen genome sequences swiftly reveals whether virulence factors are linked to phage-like DNA sequences, irrespective of the fact that they could transmissible.

Non-transmissible (Strockbine *et al.*, 1988) *stx* genes found in *S. dysenteriae*, for example resemble sequences found in lambda phage, though they are interrupted by many insertion sequences, pointing to the fact that genes encoding for toxin are located in a prophage whose sequences are faulty due to the presence of insertion sequences. Furthermore,

virulence gene transduction is inadequate proof that virulence gene is located in a phage genome.

Currently, the most common direct as well as sensitive technique used in detecting if virulence genes relate to phage-like sequences is to analyze the sequences around virulence factor genes. While this method can determine if virulence genes are linked to phage sequences, it is unable to determine whether the gene belongs to the prophage transducing it or the gene is affecting its expression. (Waldor & Mekalanos, 1996)

A whole-genome comparison of the phages to those found in databases indicated that they were closely linked to Autographiviridea/Studiervirinae phages (Figure 4.14). ORFs were mostly classified as proteins associated with DNA metabolism, proteins related with cell lysis as well as structural proteins (Figures 4.12, 4.13 and 4.14).

DNA metabolism and replication accounted for a significant fraction of the putative proteins. The phage genomes also contained seven proteins that comprise the primary replisome that functions as a biological motor capable of driving the replicating fork across templates at speed similar to those found in vivo (Miller *et al.*, 2003).

BLASTn analysis of the phages vB_Eclo_MII_001, vB_Eclo_MII_002, vB_Eclo_MII_003 and vB_Eclo_MII_004 genome with other sequences in databases using Multiple Sequence Alignment (Fig 4.11) revealed that these phages were closely related to phages of *E. coli*. The gray areas were indicative of the conserved sequences of the phages while the coloured areas were the non-conserved areas (Jankun-Kelly *et al.*, 2009). Further analysis of these phages indicated that they were highly similar to phages in the family Autographiviridea/Studiervirinae with a similarity of approximately 75% (Hongyu Ren1, 2020).

Of the five bacteriophages, sequences of vB_Eclo_MII_002_1 and vB_Eclo_MII_003 did not give a clear family classification. The study hypothesised that these bacteriophages were prophages containing sections of host genome in their bacteriophage DNA.

5.2 Conclusions and Recommendation

The spread of antibiotic resistant MDR *E. cloacae* bacterial pathogens poses a serious threat to clinicians due to scarcity of accessible treatment options. ESBL and its rising relationship with MDR phenotype in Enterobacteriaceae, including *E. cloacae*, is becoming a significant therapeutic problem. *E. cloacae*, as a significant opportunistic microbe, is capable of causing nosocomial epidemics and invasive infections such as septicaemia, bacteraemia, lower respiratory tract infections, skin and soft tissue infections, UTIs, endocarditis and intraabdominal infections (Kuai *et al.*, 2014).

This research, has described lytic bacteriophages with lytic activity against *E. cloacae*. The isolated phages are widely distributed within the environment, with rich sources of isolation being sewage water. The isolated phages had a wide host range to *E. cloacae* bacterial isolate with no lysis experience outside the host species, a clear indication of phage specificity. Thermal and pH stability testing results add to our understanding of these unique viruses. These characteristics, combined with host specificity, close genetic relatedness to the purely lytic genus Autographiviridea/ Studiervirinae phages, and the lack of associated genes involved in lysogeny, make the isolated phages attractive candidates for possible therapeutic uses such as decontamination or treatment of MDR bacteria. Phylogenetic analysis using previously validated markers (Ackermann *et al.*, 2011; Cheepudom *et al.*, 2015) revealed that it belongs to the unique genus Autographiviridea/ Studiervirinae.

The sequenced bacteriophages had no AMR genes as well as virulence genes. Phage therapy has been fronted as the next frontier in dealing with MDR bacteria. These findings reveal that vB_Eclo_MII_002 and vB_Eclo_MII_004 are good candidates for phage therapy.

5.3 Recommendations

1. A large proportion of the predicted genes were unknown or ‘hypothetical’ and therefore require characterization in order to determine their gene functions which in turn will not only help in understanding of bacteriophage biology but also add value to the virome data.
2. It’s also a recommendation of this study that the isolated lytic phages be tested in animal models to ascertain the efficacy *in vivo*.
3. It is also this study’s recommendation that additional screening be done to cover all endemic strains

5.4 Limitations of the Study

1. This study proposes to isolate phages from various different environments which are fresh water lake and sewage. This is a limitation as bacteriophages from these environments are not exhaustive of the natural diversity of bacteriophages.
2. The study also incorporates only a few *E. cloacae* MDR isolates due to the limited number in the parent study at the time. This will be mitigated by expanded research in the parent protocol.

REFERENCES

- Abedon, S. T. (2015). Bacteriophage exploitation of bacterial biofilms: Phage preference for less mature targets? *FEMS Microbiology Letters*, 363(3), 1–5. <https://doi.org/10.1093/femsle/fnv246>
- Abedon, S. T. (2017). Information phage therapy research should report. *Pharmaceuticals*, 10(2), 1–17. <https://doi.org/10.3390/ph10020043>
- Abedon, S. T., Kuhl, S. J., Blasdel, B. G., & Kutter, E. M. (2011). Phage treatment of human infections. *Bacteriophage*, 1(2), 66–85. <https://doi.org/10.4161/bact.1.2.15845>
- Addy, H. S., Ahmad, A. A., & Huang, Q. (2019). Molecular and biological characterization of ralstonia phage RsoM1USA, a new species of P2virus, isolated in the United States. *Frontiers in Microbiology*, 10(FEB), 1–14. <https://doi.org/10.3389/fmicb.2019.00267>
- Adler, A., Khabra, E., Paikin, S., & Carmeli, Y. (n.d.). *Dissemination of the bla KPC gene by clonal spread and horizontal gene transfer: comparative study of incidence and molecular mechanisms*. <https://doi.org/10.1093/jac/dkw106>
- Alves, D. R., Perez-Esteban, P., Kot, W., Bean, J. E., Arnot, T., Hansen, L. H., ... Jenkins, A. T. A. (2016). A novel bacteriophage cocktail reduces and disperses *Pseudomonas aeruginosa* biofilms under static and flow conditions. *Microbial Biotechnology*, 9(1), 61–74. <https://doi.org/10.1111/1751-7915.12316>
- Aminov, R., Hyman, P., Maresso, A. W., Trautner, B. W., Ramig, R. F., Sb, G., ... Kaplan, H. B. (2019). *Constructing and Characterizing Bacteriophage Libraries for Phage Therapy of Human Infections*. <https://doi.org/10.3389/fmicb.2019.02537>
- Anand, T., Virmani, N., Kumar, S., Mohanty, A. K., Pavulraj, S., Bera, B. C., ... Tripathi, B. N. (2020). Phage therapy for treatment of virulent *Klebsiella pneumoniae* infection in a mouse model. *Journal of Global Antimicrobial Resistance*, 21, 34–41. <https://doi.org/10.1016/j.jgar.2019.09.018>
- Annavajhala, M. K., Gomez-Simmonds, A., & Uhlemann, A. C. (2019a). Multidrug-

- resistant *Enterobacter cloacae* complex emerging as a global, diversifying threat. *Frontiers in Microbiology*, 10(JAN), 1–8. <https://doi.org/10.3389/fmicb.2019.00044>
- Annavaiah, M. K., Gomez-Simmonds, A., & Uhlemann, A. C. (2019b). Multidrug-Resistant *Enterobacter cloacae* Complex Emerging as a Global, Diversifying Threat. *Frontiers in Microbiology*, 10(JAN). <https://doi.org/10.3389/FMICB.2019.00044>
- Bao, L., Peng, R., Ren, X., Ma, R., Li, J., & Wang, Y. (2012). Analysis of some common pathogens and their drug resistance to antibiotics. *Pakistan Journal of Medical Sciences*, 29(1), 135–139. <https://doi.org/10.12669/pjms.291.2744>
- Baroness, J. J., & Beckwith, J. (1990). A bacterial virulence determinant encoded by lysogenic coliphage lambda. *Nature*, 346(6287), 871–874. <https://doi.org/10.1038/346871A0>
- Barrangou, R., & Oost, J. (2015). Bacteriophage exclusion, a new defense system. *The EMBO Journal*, 34(2), 134–135. <https://doi.org/10.15252/EMBJ.201490620>
- Bauernfeind, A. (1986). Classification of beta-lactamases. *Reviews of Infectious Diseases*, 8 Suppl 5.
- Buckling, A., & Brockhurst, M. (2012). Bacteria-virus coevolution. *Advances in Experimental Medicine and Biology*, 751, 347–370. https://doi.org/10.1007/978-1-4614-3567-9_16
- Capelo, J. L., Sahl, J., Uhlemann, A.-C., Annavaiah, M. K., & Gomez-Simmonds, A. (2019). Multidrug-Resistant *Enterobacter cloacae* Complex Emerging as a Global, Diversifying Threat. <https://doi.org/10.3389/fmicb.2019.00044>
- Chanishvili, N. (2012). Phage Therapy—History from Twort and d’Herelle Through Soviet Experience to Current Approaches. *Advances in Virus Research*, 83, 3–40. <https://doi.org/10.1016/B978-0-12-394438-2.00001-3>
- Chavda, K. D., Chen, L., Fouts, D. E., Sutton, G., Brinkac, L., Jenkins, S. G., ... Kreiswirth, B. N. (2016). Comprehensive genome analysis of carbapenemase-producing *Enterobacter* spp.: New insights into phylogeny, population structure, and resistance mechanisms. *MBio*, 7(6). <https://doi.org/10.1128/MBIO.02093->

16/ASSET/8C29E16C-D597-4791-98DC-

1262A26B1C17/ASSETS/GRAPHIC/MBO0061631110007.JPEG

- Chen, C. H., & Huang, C. C. (2013). Risk factor analysis for extended-spectrum β -lactamase-producing *Enterobacter cloacae* bloodstream infections in central Taiwan. *BMC Infectious Diseases*, *13*(1), 417. <https://doi.org/10.1186/1471-2334-13-417>
- Chen, Y., Batra, H., Dong, J., Chen, C., Rao, V. B., & Tao, P. (2019). Genetic Engineering of Bacteriophages Against Infectious Diseases. *Frontiers in Microbiology*, *10*(May), 1–12. <https://doi.org/10.3389/fmicb.2019.00954>
- Clokier, M. R. J., Millard, A. D., Letarov, A. V., & Heaphy, S. (2011). Phages in nature. *Bacteriophage*, *1*(1), 31–45. <https://doi.org/10.4161/BACT.1.1.14942>
- Codjoe, F. S., & Donkor, E. S. (n.d.). *medical sciences Review Carbapenem Resistance: A Review*. <https://doi.org/10.3390/medsci6010001>
- Criscuolo, E., Spadini, S., Lamanna, J., Ferro, M., & Burioni, R. (2017). Bacteriophages and Their Immunological Applications against Infectious Threats. *Journal of Immunology Research*, *2017*. <https://doi.org/10.1155/2017/3780697>
- De Melo, A. C. C., Da Mata Gomes, A., Melo, F. L., Ardisson-Araújo, D. M. P., De Vargas, A. P. C., Ely, V. L., ... Wolff, J. L. C. (2019). Characterization of a bacteriophage with broad host range against strains of *Pseudomonas aeruginosa* isolated from domestic animals. *BMC Microbiology*, *19*(1), 1–15. <https://doi.org/10.1186/S12866-019-1481-Z/FIGURES/5>
- Detection of NDM-1-Producing *Klebsiella pneumoniae* in Kenya. (n.d.). Retrieved August 26, 2022, from <https://journals.asm.org/doi/epdf/10.1128/AAC.01247-10?src=getfr>
- Dramowski, A., Cotton, M. F., & Whitelaw, A. (2017). Surveillance of healthcare-associated infection in hospitalised South African children: Which method performs best? *South African Medical Journal*, *107*(1), 56–63. <https://doi.org/10.7196/SAMJ.2017.v107i1.11431>
- Dugleux, G., Le Coutour, X., Hecquard, C., & Oblin, I. (1991). Septicemia Caused by

- Contaminated Parenteral Nutrition Pouches: The Refrigerator as an Unusual Cause. *Journal of Parenteral and Enteral Nutrition*, 15(4), 474–475. <https://doi.org/10.1177/0148607191015004474>
- Eichenberger, E. M., & Thaden, J. T. (n.d.). *antibiotics Epidemiology and Mechanisms of Resistance of Extensively Drug Resistant Gram-Negative Bacteria*. <https://doi.org/10.3390/antibiotics8020037>
- Endersen, L., & Coffey, A. (2020). The use of bacteriophages for food safety. *Current Opinion in Food Science*, 36, 1–8. <https://doi.org/10.1016/J.COFS.2020.10.006>
- Essack, S. Y. (2000). MiniReview Treatment options for extended-spectrum L-lactamase-producers. In *FEMS Microbiology Letters* (Vol. 190). <https://doi.org/10.1111/j.1574-6968.2000.tb09283.x>
- Feng, Y. Y., Ong, S. L., Hu, J. Y., Tan, X. L., & Ng, W. J. (2003). Effects of pH and temperature on the survival of coliphages MS2 and Q β . *Journal of Industrial Microbiology and Biotechnology*, 30(9), 549–552. <https://doi.org/10.1007/S10295-003-0080-Y>
- Fernández-Baca, V., Ballesteros, F., Hervás, J. A., Villalón, P., Domínguez, M. A., Benedí, V. J., & Albertí, S. (2001). Molecular epidemiological typing of *Enterobacter cloacae* isolates from a neonatal intensive care unit: three-year prospective study. *Journal of Hospital Infection*, 49(3), 173–182. <https://doi.org/10.1053/JHIN.2001.1053>
- Fernández, L., Gutiérrez, D., Rodríguez, A., & García, P. (2018). Application of bacteriophages in the agro-food sector: A long way toward approval. *Frontiers in Cellular and Infection Microbiology*, 8(AUG), 296. <https://doi.org/10.3389/FCIMB.2018.00296/BIBTEX>
- Founou, R. C., Founou, L. L., & Essack, S. Y. (2017). Clinical and economic impact of antibiotic resistance in developing countries: A systematic review and meta-analysis. *PLOS ONE*, 12(12), e0189621. <https://doi.org/10.1371/JOURNAL.PONE.0189621>
- Furfaro, L. L., Chang, B. J., & Payne, M. S. (2018). Applications for bacteriophage

- therapy during pregnancy and the perinatal period. *Frontiers in Microbiology*, 8(JAN), 1–14. <https://doi.org/10.3389/fmicb.2017.02660>
- Ghosh, C., Sarkar, P., Issa, R., & Haldar, J. (2019). Alternatives to Conventional Antibiotics in the Era of Antimicrobial Resistance. *Trends in Microbiology*, 27(4), 323–338. <https://doi.org/10.1016/J.TIM.2018.12.010>
- Global Action Plan on Antimicrobial Resistance. (2015). *Microbe Magazine*, 10(9), 354–355. <https://doi.org/10.1128/microbe.10.354.1>
- Goldfarb, T., Sberro, H., Weinstock, E., Cohen, O., Doron, S., Charpak-Amikam, Y., ... Sorek, R. (2015). BREX is a novel phage resistance system widespread in microbial genomes. *The EMBO Journal*, 34(2), 169–183. <https://doi.org/10.15252/EMBJ.201489455>
- Govind, R., Vedyappan, G., Rolfe, R. D., Dupuy, B., & Fralick, J. A. (2009). Bacteriophage-Mediated Toxin Gene Regulation in *Clostridium difficile*. *Journal of Virology*, 83(23), 12037–12045. <https://doi.org/10.1128/JVI.01256-09/FORMAT/EPUB>
- Gutiérrez-Gutiérrez, B., & Rodríguez-Baño, J. (2019). Current options for the treatment of infections due to extended-spectrum beta-lactamase-producing Enterobacteriaceae in different groups of patients. *Clinical Microbiology and Infection*, 25(8), 932–942. <https://doi.org/10.1016/j.cmi.2019.03.030>
- Hall, A. R., Scanlan, P. D., Morgan, A. D., & Buckling, A. (2011). Host-parasite coevolutionary arms races give way to fluctuating selection. *Ecology Letters*, 14(7), 635–642. <https://doi.org/10.1111/J.1461-0248.2011.01624.X>
- Haney, E. F., & Hancock, R. E. W. (n.d.). *Addressing Antibiotic Failure-Beyond Genetically Encoded Antimicrobial Resistance*. <https://doi.org/10.3389/fddsv.2022.892975>
- Häuser, R., Blasche, S., Dokland, T., Haggård-Ljungquist, E., von Brunn, A., Salas, M., ... Uetz, P. (2012). Bacteriophage Protein–Protein Interactions. *Advances in Virus Research*, 83, 219. <https://doi.org/10.1016/B978-0-12-394438-2.00006-2>

- Holmes, A. H., Moore, L. S. P., Sundsfjord, A., Steinbakk, M., Regmi, S., Karkey, A., ... Piddock, L. J. V. (2016). Understanding the mechanisms and drivers of antimicrobial resistance. *The Lancet*, 387(10014), 176–187. [https://doi.org/10.1016/S0140-6736\(15\)00473-0](https://doi.org/10.1016/S0140-6736(15)00473-0)
- Hyman, P., & Abedon, S. T. (2010). Bacteriophage host range and bacterial resistance. *Advances in Applied Microbiology*, 70, 217–248. [https://doi.org/10.1016/S0065-2164\(10\)70007-1](https://doi.org/10.1016/S0065-2164(10)70007-1)
- Izdebski, R., Baraniak, A., Herda, M., Fiett, J., Bonten, M. J. M., Carmeli, Y., ... Lerman, Y. (2015). MLST reveals potentially high-risk international clones of *Enterobacter cloacae*. *Journal of Antimicrobial Chemotherapy*, 70(1), 48–56. <https://doi.org/10.1093/JAC/DKU359>
- Jankun-Kelly, T. J., Lindeman, A. D., & Bridges, S. M. (2009). Exploratory visual analysis of conserved domains on multiple sequence alignments. *BMC Bioinformatics*, 10(SUPPL. 11), 1–9. <https://doi.org/10.1186/1471-2105-10-S11-S7/FIGURES/6>
- Jeśman, C., Młudzik, A., & Cybulska, M. (2011). [History of antibiotics and sulphonamides discoveries]. *Polski Merkurusz Lekarski: Organ Polskiego Towarzystwa Lekarskiego*, 30(179), 320–322. Retrieved from <https://europepmc.org/article/med/21675132>
- Jończyk, E., Kłak, M., Międzybrodzki, R., & Górski, A. (2011). The influence of external factors on bacteriophages-review. *Folia Microbiologica*, 56(3), 191–200. <https://doi.org/10.1007/S12223-011-0039-8>
- Kakasis, A., & Panitsa, G. (2019). Bacteriophage therapy as an alternative treatment for human infections. A comprehensive review. *International Journal of Antimicrobial Agents*, 53(1), 16–21. <https://doi.org/10.1016/J.IJANTIMICAG.2018.09.004>
- Kutter, E., De Vos, D., Gvasalia, G., Alavidze, Z., Gogokhia, L., Kuhl, S., & Abedon, S. (2010). Phage Therapy in Clinical Practice: Treatment of Human Infections. *Current Pharmaceutical Biotechnology*, 11(1), 69–86.

<https://doi.org/10.2174/138920110790725401>

- Laanto, E., Hoikkala, V., Ravantti, J., & Sundberg, L. R. (2017). Long-term genomic coevolution of host-parasite interaction in the natural environment. *Nature Communications*, 8(1). <https://doi.org/10.1038/S41467-017-00158-7>
- Labrie, S. J., Samson, J. E., & Moineau, S. (2010). Bacteriophage resistance mechanisms. *Nature Reviews Microbiology* 2010 8:5, 8(5), 317–327. <https://doi.org/10.1038/nrmicro2315>
- Lehman, S. M., & Donlan, R. M. (2015). Bacteriophage-mediated control of a two-species biofilm formed by microorganisms causing catheter-associated urinary tract infections in an in vitro urinary catheter model. *Antimicrobial Agents and Chemotherapy*, 59(2), 1127–1137. <https://doi.org/10.1128/AAC.03786-14>
- Levy, S. B., & Marshall, B. (2004). *Antibacterial resistance worldwide : causes , challenges and responses* REVIEW. 10(12), 122–129. <https://doi.org/10.1038/nm1145>
- Li, E., Wei, X., Ma, Y., Yin, Z., Li, H., Lin, W., ... Zhao, X. (2016). Isolation and characterization of a bacteriophage phiEap-2 infecting multidrug resistant *Enterobacter aerogenes*. *Scientific Reports*, 6(June), 1–11. <https://doi.org/10.1038/srep28338>
- Lin, D. M., Koskella, B., & Lin, H. C. (2017). Phage therapy: An alternative to antibiotics in the age of multi-drug resistance. *World Journal of Gastrointestinal Pharmacology and Therapeutics*, 8(3), 162. <https://doi.org/10.4292/WJGPT.V8.I3.162>
- Liu, X., Zhang, J., Li, Y., Shen, Q., Jiang, W., Zhao, K., ... Zhou, Y. (2019). Diversity and frequency of resistance and virulence genes in blaKPC and blaNDM co-producing *Klebsiella pneumoniae* strains from China. *Infection and Drug Resistance*, 12. <https://doi.org/10.2147/IDR.S214960>
- Loh, B., Chen, J., Manohar, P., Yu, Y., Hua, X., & Leptihn, S. (2020). A Biological Inventory of Prophages in *A. baumannii* Genomes Reveal Distinct Distributions in Classes, Length, and Genomic Positions. *Frontiers in Microbiology*, 11(December),

- 1–13. <https://doi.org/10.3389/fmicb.2020.579802>
- Malik, D. J., Sokolov, I. J., Vinner, G. K., Mancuso, F., Cinquerrui, S., Vladislavljevic, G. T., ... Kirpichnikova, A. (2017). Formulation, stabilisation and encapsulation of bacteriophage for phage therapy. *Advances in Colloid and Interface Science*, 249(May), 100–133. <https://doi.org/10.1016/j.cis.2017.05.014>
- Manohar, P., Nachimuthu, R., & Lopes, B. S. (2018). The therapeutic potential of bacteriophages targeting gram-negative bacteria using *Galleria mellonella* infection model. *BMC Microbiology*, 18(1), 1–11. <https://doi.org/10.1186/s12866-018-1234-4>
- Martínez, L., Martínez-Martínez, M., Martínez, M., Pascual, A., Hernández, S., Hernández-Allé, H., ... Jacoby, G. A. (1999). Roles of β -Lactamases and Porins in Activities of Carbapenems and Cephalosporins against *Klebsiella pneumoniae*. *Antimicrobial Agents and Chemotherapy*, 43(7), 1669–1673. <https://doi.org/10.1128/AAC.43.7.1669>
- Melo, L. D. R., Ferreira, R., Costa, A. R., Oliveira, H., & Azeredo, J. (2019). Efficacy and safety assessment of two enterococci phages in an in vitro biofilm wound model. *Scientific Reports*, 9(1), 1–12. <https://doi.org/10.1038/s41598-019-43115-8>
- Mezzatesta, M. L., Gona, F., & Stefani, S. (2012). Enterobacter cloacae complex: Clinical impact and emerging antibiotic resistance. *Future Microbiology*, 7(7), 887–902. <https://doi.org/10.2217/fmb.12.61>
- Moye, Z. D., Woolston, J., & Sulakvelidze, A. (2018). Bacteriophage Applications for Food Production and Processing. *Viruses*, 10(4). <https://doi.org/10.3390/V10040205>
- Mushi, M. F., Mshana, S. E., Imirzalioglu, C., & Bwanga, F. (2014). Carbapenemase genes among multidrug resistant gram negative clinical isolates from a tertiary hospital in Mwanza, Tanzania. *BioMed Research International*, 2014. <https://doi.org/10.1155/2014/303104>
- Musila, L., Kyany'a, C., Maybank, R., Stam, J., Oundo, V., & Sang, W. (2021). Detection of diverse carbapenem and multidrug resistance genes and high-risk strain types among carbapenem non-susceptible clinical isolates of target gram-negative bacteria

- in Kenya. *PLoS ONE*, *16*(2). <https://doi.org/10.1371/JOURNAL.PONE.0246937>
- Nagel, T. E., Chan, B. K., De Vos, D., El-Shibiny, A., Kang'ethe, E. K., Makumi, A., & Pirnay, J. P. (2016). The developing world urgently needs phages to combat pathogenic bacteria. *Frontiers in Microbiology*, *7*(JUN), 1–4. <https://doi.org/10.3389/fmicb.2016.00882>
- Okoche, D., Asiimwe, B. B., Katabazi, F. A., Kato, L., & Najjuka, C. F. (2015). Prevalence and Characterization of Carbapenem-Resistant Enterobacteriaceae Isolated from Mulago National Referral Hospital, Uganda. *PloS One*, *10*(8). <https://doi.org/10.1371/JOURNAL.PONE.0135745>
- Pestourie, N., Garnier, F., Barraud, O., Bedu, A., Ploy, M. C., & Mounier, M. (2014). Outbreak of AmpC β -lactamase-hyper-producing *Enterobacter cloacae* in a neonatal intensive care unit in a French teaching hospital. *American Journal of Infection Control*, *42*(4), 456–458. <https://doi.org/10.1016/J.AJIC.2013.11.005>
- Pfaller, M. A., & Segreti, J. (2006). Overview of the epidemiological profile and laboratory detection of extended-spectrum β -lactamases. *Clinical Infectious Diseases*, *42*(SUPPL. 4), 153–163. <https://doi.org/10.1086/500662>
- Pires, D. P., Melo, L. D. R., Vilas Boas, D., Sillankorva, S., & Azeredo, J. (2017). Phage therapy as an alternative or complementary strategy to prevent and control biofilm-related infections. *Current Opinion in Microbiology*, *39*, 48–56. <https://doi.org/10.1016/J.MIB.2017.09.004>
- Potron, A., Poirel, L., Rondinaud, E., & Nordmann, P. (2013). Intercontinental spread of OXA-48 beta-lactamase-producing enterobacteriaceae over a 11-year period, 2001 to 2011. *Eurosurveillance*, *18*(31), 20549. <https://doi.org/10.2807/1560-7917.ES2013.18.31.20549/CITE/PLAINTEXT>
- Principi, N., Silvestri, E., & Esposito, S. (2019a). Advantages and limitations of bacteriophages for the treatment of bacterial infections. *Frontiers in Pharmacology*, *10*(MAY), 513. <https://doi.org/10.3389/FPHAR.2019.00513/XML/NLM>
- Principi, N., Silvestri, E., & Esposito, S. (2019b). Advantages and limitations of

- bacteriophages for the treatment of bacterial infections. *Frontiers in Pharmacology*, 10(MAY), 513. <https://doi.org/10.3389/FPHAR.2019.00513/BIBTEX>
- Principi, N., Silvestri, E., & Esposito, S. (2019c). Advantages and Limitations of Bacteriophages for the Treatment of Bacterial Infections. *Frontiers in Pharmacology*, 10(May), 1–9. <https://doi.org/10.3389/fphar.2019.00513>
- Rawat, D., & Nair, D. (2010). Extended-spectrum β -lactamases in gram negative bacteria. *Journal of Global Infectious Diseases*, 2(3), 263. <https://doi.org/10.4103/0974-777x.68531>
- Raya, R. R., Varey, P., Oot, R. A., Dyen, M. R., Callaway, T. R., Edrington, T. S., ... Brabban, A. D. (2006). Isolation and characterization of a new T-even bacteriophage, CEV1, and determination of its potential to reduce *Escherichia coli* O157:H7 levels in sheep. *Applied and Environmental Microbiology*, 72(9), 6405–6410. <https://doi.org/10.1128/AEM.03011-05>
- Reidl, J., & Mekalanos, J. J. (1995). Characterization of *Vibrio cholerae* bacteriophage K139 and use of a novel mini-transposon to identify a phage-encoded virulence factor. *Molecular Microbiology*, 18(4), 685–701. https://doi.org/10.1111/J.1365-2958.1995.MMI_18040685.X
- Reindel, R., & Fiore, C. R. (2017). Phage therapy: Considerations and challenges for development. *Clinical Infectious Diseases*, 64(11), 1589–1590. <https://doi.org/10.1093/cid/cix188>
- Rohde, C., Resch, G., Pirnay, J. P., Blasdel, B. G., Debarbieux, L., Gelman, D., ... Chanishvili, N. (2018). Expert Opinion on Three Phage Therapy Related Topics: Bacterial Phage Resistance, Phage Training and Prophages in Bacterial Production Strains. *Viruses* 2018, Vol. 10, Page 178, 10(4), 178. <https://doi.org/10.3390/V10040178>
- Rottman, M., Benzerara, Y., Hanau-Berçot, B., Bizet, C., Philippon, A., & Arlet, G. (2002). Chromosomal ampC genes in *Enterobacter* species other than *Enterobacter cloacae*, and ancestral association of the ACT-1 plasmid-encoded cephalosporinase

- to *Enterobacter asburiae*. *FEMS Microbiology Letters*, 210(1), 87–92.
[https://doi.org/10.1016/S0378-1097\(02\)00613-4](https://doi.org/10.1016/S0378-1097(02)00613-4)
- Royer, S., Morais, A. P., & da Fonseca Batistão, D. W. (2021). Phage therapy as strategy to face post-antibiotic era: a guide to beginners and experts. *Archives of Microbiology*, 203(4), 1271–1279. <https://doi.org/10.1007/S00203-020-02167-5/METRICS>
- Salmond, G. P. C., & Fineran, P. C. (2015). A century of the phage: Past, present and future. *Nature Reviews Microbiology*, 13(12), 777–786.
<https://doi.org/10.1038/nrmicro3564>
- Scallan, E., Hoekstra, R. M., Angulo, F. J., Tauxe, R. V., Widdowson, M. A., Roy, S. L., ... Griffin, P. M. (2011). Foodborne Illness Acquired in the United States—Major Pathogens - Volume 17, Number 1—January 2011 - Emerging Infectious Diseases journal - CDC. *Emerging Infectious Diseases*, 17(1), 7–15.
<https://doi.org/10.3201/EID1701.P11101>
- Shang, J., Jiang, J., & Sun, Y. (2021). Bacteriophage classification for assembled contigs using graph convolutional network. *Bioinformatics*, 37, I25–I33.
<https://doi.org/10.1093/bioinformatics/btab293>
- Sköld, O. (2000). Sulfonamide resistance: mechanisms and trends. *Drug Resistance Updates*, 3(3), 155–160. <https://doi.org/10.1054/DRUP.2000.0146>
- Stern, A., & Sorek, R. (2011). The phage-host arms race: Shaping the evolution of microbes. *BioEssays*, 33(1), 43–51. <https://doi.org/10.1002/BIES.201000071>
- Steward, K. (2018). Lytic vs Lysogenic-Understanding Bacteriophage Life Cycles. *Technology Networks*, (Figure 1).
- Strockbine, N. A., Jackson, M. P., Sung, L. M., Holmes, R. K., & O'Brien, A. D. (1988). Cloning and sequencing of the genes for shiga toxin from *Shigella dysenteriae* type 1. *Journal of Bacteriology*, 170(3), 1116–1122.
<https://doi.org/10.1128/JB.170.3.1116-1122.1988>
- Tamma, P. D., Doi, Y., Bonomo, R. A., Johnson, J. K., & Simner, P. J. (2019). A Primer

- on AmpC β -Lactamases: Necessary Knowledge for an Increasingly Multidrug-resistant World. *Clinical Infectious Diseases*, Vol. 69, pp. 1446–1455. <https://doi.org/10.1093/cid/ciz173>
- Thung, T. Y., Lee, E., Premarathne, J. M. K. J. K., Nurzafirah, M., Kuan, C. H., Elexson, N., ... Son, R. (2018). Bacteriophages and their applications. *Food Research*, 2(5), 404–414. [https://doi.org/10.26656/FR.2017.2\(5\).082](https://doi.org/10.26656/FR.2017.2(5).082)
- Torres-Barceló, C. (2018). Phage therapy faces evolutionary challenges. *Viruses*, 10(6). <https://doi.org/10.3390/v10060323>
- Torres-Barceló, C., & Hochberg, M. E. (2016). Evolutionary Rationale for Phages as Complements of Antibiotics. *Trends in Microbiology*, 24(4), 249–256. <https://doi.org/10.1016/J.TIM.2015.12.011>
- Turner, D., Wand, M. E., Briers, Y., Lavigne, R., Sutton, J. M., & Reynolds, D. M. (2017). Characterisation and genome sequence of the lytic *Acinetobacter baumannii* bacteriophage vB-AbaS-Loki. *PLoS ONE*, 12(2), 1–19. <https://doi.org/10.1371/journal.pone.0172303>
- Turner, D., Wand, M. E., Sutton, J. M., Centron, D., Kropinski, A. M., & Reynolds, D. M. (2016). Genome sequence of vB_AbaS_TRS1, a viable prophage isolated from *Acinetobacter baumannii* strain A118. *Genome Announcements*, 4(5), 2015–2016. <https://doi.org/10.1128/genomeA.01051-16>
- Ul Haq, I., Chaudhry, W. N., Akhtar, M. N., Andleeb, S., & Qadri, I. (2012a). Bacteriophages and their implications on future biotechnology: A review. *Virology Journal*, 9(1), 1–8. <https://doi.org/10.1186/1743-422X-9-9/FIGURES/2>
- Ul Haq, I., Chaudhry, W. N., Akhtar, M. N., Andleeb, S., & Qadri, I. (2012b). Bacteriophages and their implications on future biotechnology: A review. *Virology Journal*, 9(1), 1–8. <https://doi.org/10.1186/1743-422X-9-9/FIGURES/2>
- Vilchèze, C., & Jacobs, W. R. (2015). Resistance to isoniazid and ethionamide in *Mycobacterium tuberculosis*: Genes, mutations, and causalities. *Molecular Genetics of Mycobacteria*, 2(4), 431–453. <https://doi.org/10.1128/9781555818845.ch22>

- Waldor, M. K., & Mekalanos, J. J. (1996). Lysogenic conversion by a filamentous phage encoding cholera toxin. *Science (New York, N.Y.)*, 272(5270), 1910–1913. <https://doi.org/10.1126/SCIENCE.272.5270.1910>
- Wang, S. A., Tokars, J. I., Bianchine, P. J., Carson, L. A., Arduino, M. J., Smith, A. L., ... Jarvis, W. R. (2000). Enterobacter cloacae bloodstream infections traced to contaminated human albumin. *Clinical Infectious Diseases*, 30(1), 35–40. <https://doi.org/10.1086/313585/2/30-1-35-FIG002.GIF>
- WHO. (2014). Antimicrobial resistance. Global report on surveillance. *World Health Organization*, 61(3), 12–28. <https://doi.org/10.1007/s13312-014-0374-3>
- Xia, F., Li, X., Wang, B., Gong, P., Xiao, F., Yang, M., ... Hana, W. (2016). Combination therapy of LysGH15 and apigenin as 1new strategy for treating pneumonia caused by Staphylococcus aureus. *Applied and Environmental Microbiology*, 82(1), 87–94. <https://doi.org/10.1128/AEM.02581-15>
- Yang, Y. S., Ku, C. H., Lin, J. C., Shang, S. T., Chiu, C. H., Yeh, K. M., ... Chang, F. Y. (2010). Impact of Extended-spectrum β -lactamase-producing Escherichia coli and Klebsiella pneumoniae on the Outcome of Community-onset Bacteremic Urinary Tract Infections. *Journal of Microbiology, Immunology and Infection*, 43(3), 194–199. [https://doi.org/10.1016/S1684-1182\(10\)60031-X](https://doi.org/10.1016/S1684-1182(10)60031-X)
- Yin, H., Lam, P., Lai, M.-J., Chen, T.-Y., Wu, W.-J., Peng, S.-Y., & Chang, K.-C. (2021). Therapeutic Effect of a Newly Isolated Lytic Bacteriophage against Multi-Drug-Resistant Cutibacterium acnes Infection in Mice. *International Journal of Molecular Sciences Article*. <https://doi.org/10.3390/ijms22137031>
- Zhao, J., Zhang, Z., Tian, C., Chen, X., Hu, L., Wei, X., ... Zhao, X. (2019). Characterizing the Biology of Lytic Bacteriophage vB_EaeM_φEap-3 Infecting Multidrug-Resistant Enterobacter aerogenes. *Frontiers in Microbiology*, Vol. 10. <https://doi.org/10.3389/fmicb.2019.00420>

APPENDICES

APPENDIX 1: Annotated Genome features of bacteriophage vB_Eclo_MII_001

	Feature Type	Start	End	Length	Strand	Genus-specific families (PLfams)	Cross-genus families (PGfams)	AA Length	Product
vB_Eclo_MII_001	CDS	10244	10609	366	-	PLF_547_00014275	PGF_01624602	121	Phage antitermination protein N
vB_Eclo_MII_001	CDS	10560	10769	210	-			69	hypothetical protein
vB_Eclo_MII_001	CDS	1098	1244	147	-	PLF_547_00003174	PGF_00072365	48	Bactoprenol glucosyl transferase
vB_Eclo_MII_001	CDS	10997	11356	360	-	PLF_547_00099107	PGF_00091980	119	Phage repressor protein cI
vB_Eclo_MII_001	CDS	11269	11646	378	-	PLF_547_00099107	PGF_00091980	125	Phage repressor protein cI
vB_Eclo_MII_001	CDS	11730	11915	186	+	PLF_547_00040876	PGF_06330746	61	Phage repressor protein
vB_Eclo_MII_001	CDS	12034	12297	264	+	PLF_547_00017230	PGF_05008693	87	Phage activator protein cII
vB_Eclo_MII_001	CDS	12354	12512	159	+	PLF_547_00031287	PGF_00139736	52	Phage protein
vB_Eclo_MII_001	CDS	1241	1384	144	-	PLF_547_00003953	PGF_07561028	47	Bactoprenol-linked glucose translocase
vB_Eclo_MII_001	CDS	12499	13398	900	+	PLF_547_00014299	PGF_08225224	299	hypothetical protein
vB_Eclo_MII_001	CDS	13398	14735	1338	+	PLF_547_00012070	PGF_03375877	445	DNA helicase (EC 3.6.4.12), phage-associated
vB_Eclo_MII_001	CDS	1428	1604	177	-			58	Bactoprenol-linked glucose translocase
vB_Eclo_MII_001	CDS	14735	15013	279	+	PLF_547_00066360	PGF_04560094	92	Phage protein
vB_Eclo_MII_001	CDS	15010	15462	453	+	PLF_547_00015114	PGF_02925889	150	Arginine/ornithine ABC transporter, periplasmic arginine/ornithine binding protein
vB_Eclo_MII_001	CDS	15465	15611	147	+			48	hypothetical protein
vB_Eclo_MII_001	CDS	15674	15967	294	+			97	hypothetical protein
vB_Eclo_MII_001	CDS	15983	16288	306	+	PLF_547_00099314	PGF_09847607	101	unknown protein encoded by bacteriophage BP-933W
vB_Eclo_MII_001	CDS	161	334	174	-	PLF_547_00021056	PGF_08225224	57	hypothetical protein
vB_Eclo_MII_001	CDS	1613	1765	153	-			50	hypothetical protein
vB_Eclo_MII_001	CDS	16304	16753	450	+	PLF_547_00028330	PGF_00095584	149	Phage protein (ACLAME 414)
vB_Eclo_MII_001	CDS	16761	17345	585	+		PGF_01388171	194	HNH homing endonuclease # Phage intron
vB_Eclo_MII_001	CDS	17326	17547	222	+	PLF_547_00055199		73	hypothetical protein
vB_Eclo_MII_001	CDS	17550	17777	228	+	PLF_547_00029886	PGF_01570190	75	hypothetical protein
vB_Eclo_MII_001	CDS	17743	18138	396	+		PGF_09108661	131	Phage NinX
vB_Eclo_MII_001	CDS	1807	2106	300	+	PLF_547_00004337	PGF_07518314	99	Error-prone repair protein UmuD
vB_Eclo_MII_001	CDS	18131	18307	177	+	PLF_547_00040904		58	Phage NinF (ACLAME 467)
vB_Eclo_MII_001	CDS	18297	18575	279	+			92	hypothetical protein
vB_Eclo_MII_001	CDS	18568	19164	597	+	PLF_547_00043127	PGF_03977074	198	Phage recombination protein NinG

vB_Eclo_MII_001	CDS	19161	19427	267	+	PLF_547_00043031	PGF_01386880	88	hypothetical protein
vB_Eclo_MII_001	CDS	19415	19600	186	+	PLF_547_00012893	PGF_01564596	61	hypothetical protein
vB_Eclo_MII_001	CDS	19597	19785	189	+			62	hypothetical protein
vB_Eclo_MII_001	CDS	19785	20303	519	+	PLF_547_00066045	PGF_06294679	172	Phage antitermination protein Q
vB_Eclo_MII_001	CDS	20331	20486	156	+			51	hypothetical protein
vB_Eclo_MII_001	CDS	20555	20668	114	+			37	hypothetical protein
vB_Eclo_MII_001	CDS	2060	2287	228	-			75	hypothetical protein
vB_Eclo_MII_001	CDS	20748	21074	327	+		PGF_08840140	108	Phage protein
vB_Eclo_MII_001	CDS	21116	21352	237	+		PGF_12845924	78	hypothetical protein
vB_Eclo_MII_001	CDS	21327	21794	468	+			155	Phage lysozyme R (EC 3.2.1.17)
vB_Eclo_MII_001	CDS	21791	22021	231	+			76	hypothetical protein
vB_Eclo_MII_001	CDS	22018	22305	288	+	PLF_547_00026404	PGF_06943569	95	hypothetical protein
vB_Eclo_MII_001	CDS	22282	22464	183	-			60	hypothetical protein
vB_Eclo_MII_001	CDS	22461	22667	207	-			68	hypothetical protein
vB_Eclo_MII_001	CDS	22697	23386	690	+	PLF_547_00069559	PGF_08225224	229	hypothetical protein
vB_Eclo_MII_001	CDS	2292	2561	270	-		PGF_01615525	89	Phage integrase
vB_Eclo_MII_001	CDS	23665	23931	267	+			88	hypothetical protein
vB_Eclo_MII_001	CDS	24010	24339	330	+	PLF_547_00065985	PGF_06359935	109	hypothetical protein
vB_Eclo_MII_001	CDS	24336	25895	1560	+	PLF_547_00018406	PGF_00032804	519	Phage terminase, large subunit
vB_Eclo_MII_001	CDS	2530	2625	96	-			31	hypothetical protein
vB_Eclo_MII_001	CDS	25904	27160	1257	+	PLF_547_00014262	PGF_00352574	418	hypothetical protein
vB_Eclo_MII_001	CDS	27153	27959	807	+	PLF_547_00045083	PGF_08225224	268	plasmid-related protein
vB_Eclo_MII_001	CDS	2746	3225	480	-	PLF_547_00004314	PGF_01615525	159	Phage integrase
vB_Eclo_MII_001	CDS	27972	29072	1101	+	PLF_547_00020461	PGF_00894049	366	hypothetical protein
vB_Eclo_MII_001	CDS	29072	29581	510	+		PGF_00103577	169	hypothetical protein
vB_Eclo_MII_001	CDS	29591	30529	939	+	PLF_547_00014741	PGF_05590037	312	Phage protein (ACLAME 194)
vB_Eclo_MII_001	CDS	3	161	159	-			53	hypothetical protein
vB_Eclo_MII_001	CDS	30562	30765	204	+	PLF_547_00035875		67	hypothetical protein
vB_Eclo_MII_001	CDS	30829	30921	93	+			30	hypothetical protein
vB_Eclo_MII_001	CDS	31036	31623	588	+	PLF_547_00015200	PGF_04110214	195	hypothetical protein
vB_Eclo_MII_001	CDS	31620	31967	348	+	PLF_547_00018837		115	hypothetical protein
vB_Eclo_MII_001	CDS	31960	32499	540	+	PLF_547_00014743	PGF_01565096	179	hypothetical protein
vB_Eclo_MII_001	CDS	32519	33859	1341	+	PLF_547_00012525	PGF_02933321	446	hypothetical protein
vB_Eclo_MII_001	CDS	3310	3681	372	-	PLF_547_00077625	PGF_05857080	123	Phage excisionase
vB_Eclo_MII_001	CDS	33862	34308	447	+	PLF_547_00014746	PGF_00157766	148	FIG00696183: hypothetical protein
vB_Eclo_MII_001	CDS	34344	34781	438	+	PLF_547_00014744	PGF_08225224	145	hypothetical protein
vB_Eclo_MII_001	CDS	34823	34942	120	+	PLF_547_00050280	PGF_05733706	39	hypothetical protein
vB_Eclo_MII_001	CDS	34943	36514	1572	+	PLF_547_00014206	PGF_00294625	523	hypothetical protein
vB_Eclo_MII_001	CDS	36516	37232	717	+	PLF_547_00014205	PGF_00355427	238	hypothetical protein
vB_Eclo_MII_001	CDS	3693	4049	357	-			118	hypothetical protein
vB_Eclo_MII_001	CDS	37229	37570	342	+	PLF_547_00066372	PGF_05509249	113	hypothetical protein
vB_Eclo_MII_001	CDS	374	511	138	-	PLF_547_00003174	PGF_00072365	45	Bactoprenol glucosyl transferase
vB_Eclo_MII_001	CDS	37545	38159	615	+	PLF_547_00014745	PGF_00201822	204	hypothetical protein
vB_Eclo_MII_001	CDS	38156	38479	324	+	PLF_547_00014745	PGF_00201822	107	hypothetical protein
vB_Eclo_MII_001	CDS	38479	39153	675	+		PGF_12855838	224	hypothetical protein
vB_Eclo_MII_001	CDS	39163	39399	237	+			78	hypothetical protein
vB_Eclo_MII_001	CDS	39440	39808	369	+	PLF_547_00050970	PGF_06193476	122	hypothetical protein
vB_Eclo_MII_001	CDS	39874	41292	1419	+	PLF_547_00014204	PGF_00239204	472	hypothetical protein
vB_Eclo_MII_001	CDS	4112	4453	342	-		PGF_10827763	113	hypothetical protein

vB_Eclo_MII_001	CDS	41270	42040	771	+	PLF_547_00018543	PGF_00390561	256	hypothetical protein
vB_Eclo_MII_001	CDS	42049	42285	237	+	PLF_547_00058236	PGF_01813040	78	hypothetical protein
vB_Eclo_MII_001	CDS	42285	42929	645	+	PLF_547_00061555	PGF_05184720	214	hypothetical protein
vB_Eclo_MII_001	CDS	42999	44369	1371	+	PLF_547_00042278	PGF_08225224	456	hypothetical protein
vB_Eclo_MII_001	CDS	44469	44579	111	-			36	hypothetical protein
vB_Eclo_MII_001	CDS	4459	4659	201	-	PLF_547_00041345	PGF_02922518	66	hypothetical protein
vB_Eclo_MII_001	CDS	44705	45346	642	+	PLF_547_00022145	PGF_08225224	213	hypothetical protein
vB_Eclo_MII_001	CDS	45376	46833	1458	-	PLF_547_00021056	PGF_08225224	485	hypothetical protein
vB_Eclo_MII_001	CDS	4632	4748	117	-			38	hypothetical protein
vB_Eclo_MII_001	CDS	46830	47747	918	-	PLF_547_00003174	PGF_00072365	305	Bactoprenol glucosyl transferase
vB_Eclo_MII_001	CDS	47744	48106	363	-	PLF_547_00003953	PGF_07561028	120	Bactoprenol-linked glucose translocase
vB_Eclo_MII_001	CDS	4813	4917	105	-			34	hypothetical protein
vB_Eclo_MII_001	CDS	48220	48609	390	+	PLF_547_00004337	PGF_07518314	129	Error-prone repair protein UmuD
vB_Eclo_MII_001	CDS	48793	49956	1164	-	PLF_547_00004314	PGF_01615525	387	Phage integrase
vB_Eclo_MII_001	CDS	4911	5093	183	-			60	hypothetical protein
vB_Eclo_MII_001	CDS	49988	50158	171	-			56	hypothetical protein
vB_Eclo_MII_001	CDS	50195	50551	357	-			118	hypothetical protein
vB_Eclo_MII_001	CDS	50614	50955	342	-		PGF_10827763	113	hypothetical protein
vB_Eclo_MII_001	CDS	508	906	399	-	PLF_547_00003174	PGF_00072365	132	Bactoprenol glucosyl transferase
vB_Eclo_MII_001	CDS	50961	51161	201	-	PLF_547_00041345	PGF_02922518	66	hypothetical protein
vB_Eclo_MII_001	CDS	51134	51250	117	-			38	hypothetical protein
vB_Eclo_MII_001	CDS	51308	51406	99	-			32	hypothetical protein
vB_Eclo_MII_001	CDS	51437	51565	129	-			42	hypothetical protein
vB_Eclo_MII_001	CDS	5147	5716	570	-	PLF_547_00099025	PGF_08225224	189	hypothetical protein
vB_Eclo_MII_001	CDS	51510	52217	708	-	PLF_547_00099025	PGF_08225224	235	hypothetical protein
vB_Eclo_MII_001	CDS	52221	52508	288	-	PLF_547_00040851	PGF_12916126	95	FIG00640186: hypothetical protein
vB_Eclo_MII_001	CDS	52511	52912	402	-	PLF_547_00090948	PGF_08225224	133	Phage EaA protein
vB_Eclo_MII_001	CDS	52909	53100	192	-			63	hypothetical protein
vB_Eclo_MII_001	CDS	53084	53299	216	-	PLF_547_00015263	PGF_01248310	71	hypothetical protein
vB_Eclo_MII_001	CDS	53296	53754	459	-		PGF_00031654	152	Phage EaE protein
vB_Eclo_MII_001	CDS	53751	53924	174	-	PLF_547_00030859	PGF_12752565	57	Phage protein (ACLAME 770)
vB_Eclo_MII_001	CDS	53921	54223	303	-	PLF_547_00072806	PGF_06320551	100	hypothetical protein
vB_Eclo_MII_001	CDS	54293	54514	222	+			73	hypothetical protein
vB_Eclo_MII_001	CDS	54571	54813	243	+			80	hypothetical protein
vB_Eclo_MII_001	CDS	54847	54957	111	-			36	Phage protein
vB_Eclo_MII_001	CDS	55020	55334	315	-	PLF_547_00007843	PGF_00031622	104	Phage DNA binding ATPase
vB_Eclo_MII_001	CDS	55353	55469	117	-			38	hypothetical protein
vB_Eclo_MII_001	CDS	55502	55597	96	-			31	hypothetical protein
vB_Eclo_MII_001	CDS	55573	55779	207	-			68	hypothetical protein
vB_Eclo_MII_001	CDS	55890	56141	252	-			83	hypothetical protein
vB_Eclo_MII_001	CDS	56233	56430	198	-			65	hypothetical protein
vB_Eclo_MII_001	CDS	56488	56685	198	-			65	hypothetical protein
vB_Eclo_MII_001	CDS	56715	57080	366	-	PLF_547_00014275	PGF_01624602	121	Phage antitermination protein N
vB_Eclo_MII_001	CDS	57031	57240	210	-			69	hypothetical protein
vB_Eclo_MII_001	CDS	5720	6007	288	-	PLF_547_00040851	PGF_12916126	95	FIG00640186: hypothetical protein
vB_Eclo_MII_001	CDS	57468	57689	222	-	PLF_547_00099107	PGF_00091980	73	Phage repressor protein cI

vB_Eclo_MII_001	CDS	57702	57839	138	-	PLF_547_00099107	PGF_00091980	45	Phage repressor protein cI
vB_Eclo_MII_001	CDS	57913	58014	102	-			33	hypothetical protein
vB_Eclo_MII_001	CDS	58052	58147	96	+			31	hypothetical protein
vB_Eclo_MII_001	CDS	58188	58373	186	+			61	Phage repressor protein
vB_Eclo_MII_001	CDS	58493	58771	279	+	PLF_547_00017230	PGF_05008693	92	Phage activator protein cII
vB_Eclo_MII_001	CDS	58814	58969	156	+	PLF_547_00031287	PGF_00139736	51	Phage protein
vB_Eclo_MII_001	CDS	59026	59490	465	+	PLF_547_00014299	PGF_08225224	154	hypothetical protein
vB_Eclo_MII_001	CDS	59540	59707	168	+	PLF_547_00014299	PGF_08225224	55	hypothetical protein
vB_Eclo_MII_001	CDS	59834	59953	120	+			39	Replicative DNA helicase (EC 3.6.1.-)
vB_Eclo_MII_001	CDS	59959	60060	102	+			33	hypothetical protein
vB_Eclo_MII_001	CDS	6010	6411	402	-	PLF_547_00090948	PGF_08225224	133	Phage EaA protein
vB_Eclo_MII_001	CDS	60128	60289	162	+	PLF_547_00012070	PGF_03375877	53	DNA helicase (EC 3.6.4.12), phage-associated
vB_Eclo_MII_001	CDS	60289	60405	117	+			38	hypothetical protein
vB_Eclo_MII_001	CDS	60535	60957	423	+	PLF_547_00012070	PGF_03375877	140	DNA helicase (EC 3.6.4.12), phage-associated
vB_Eclo_MII_001	CDS	61001	61147	147	+	PLF_547_00012070	PGF_03375877	48	DNA helicase (EC 3.6.4.12), phage-associated
vB_Eclo_MII_001	CDS	61166	61435	270	+	PLF_547_00066360	PGF_04560094	89	hypothetical protein
vB_Eclo_MII_001	CDS	61438	61617	180	+			59	Arginine/ornithine ABC transporter, periplasmic arginine/ornithine binding protein
vB_Eclo_MII_001	CDS	61718	61828	111	+	PLF_547_00015114	PGF_02925889	36	Arginine/ornithine ABC transporter, periplasmic arginine/ornithine binding protein
vB_Eclo_MII_001	CDS	61809	61952	144	+			47	hypothetical protein
vB_Eclo_MII_001	CDS	6408	6599	192	-			63	hypothetical protein
vB_Eclo_MII_001	CDS	6596	6799	204	-	PLF_547_00015263	PGF_01248310	67	hypothetical protein
vB_Eclo_MII_001	CDS	6796	7254	459	-		PGF_00031654	152	Phage EaE protein
vB_Eclo_MII_001	CDS	7251	7424	174	-	PLF_547_00030859	PGF_12752565	57	Phage protein (ACLAME 770)
vB_Eclo_MII_001	CDS	7421	7636	216	-	PLF_547_00072806	PGF_06320551	71	hypothetical protein
vB_Eclo_MII_001	CDS	7600	7722	123	-			40	hypothetical protein
vB_Eclo_MII_001	CDS	7789	8370	582	-		PGF_00291087	193	Putative phage repair nuclease (ACLAME 1137)
vB_Eclo_MII_001	CDS	8367	9047	681	-	PLF_547_00007843	PGF_00031622	226	Phage DNA binding ATPase
vB_Eclo_MII_001	CDS	9055	9225	171	-	PLF_547_00019122	PGF_01566815	56	Phage protein (ACLAME 697)
vB_Eclo_MII_001	CDS	9301	9447	147	-			48	hypothetical protein
vB_Eclo_MII_001	CDS	9463	9627	165	-			54	hypothetical protein
vB_Eclo_MII_001	CDS	969	1094	126	-			41	hypothetical protein
vB_Eclo_MII_001	CDS	9769	9963	195	-	PLF_547_00099625	PGF_01601748	64	Phage protein
vB_Eclo_MII_001	CDS	9963	10214	252	-			83	hypothetical protein

APPENDIX 2: Annotated Genome features of bacteriophage vB_Eclo_MII_002

Genome	Feature Type	Start	End	Length	Strand	PATRIC genus-specific families (PLfams)	Cross-genus families (PGfams)	AA Length	Product
vB_Eclo_MII_002	CDS	100097	100396	300	-		PGF_00387812	99	hypothetical protein
vB_Eclo_MII_002	CDS	100410	101027	618	-		PGF_00270247	205	hypothetical protein
vB_Eclo_MII_002	CDS	101174	101404	231	-		PGF_00270247	76	hypothetical protein
vB_Eclo_MII_002	CDS	101509	102192	684	-	PLF_547_00010043	PGF_06196706	227	Phage serine/threonine protein phosphatase NinI
vB_Eclo_MII_002	CDS	102189	102416	228	-		PGF_07448952	75	Phage protein
vB_Eclo_MII_002	CDS	102394	102612	219	-		PGF_12710107	72	hypothetical protein
vB_Eclo_MII_002	CDS	102684	103394	711	-		PGF_08225224	236	hypothetical protein
vB_Eclo_MII_002	CDS	103485	104300	816	-		PGF_08225224	271	hypothetical protein
vB_Eclo_MII_002	CDS	104378	104887	510	-	PLF_547_00099264	PGF_10331201	169	Phage eae protein
vB_Eclo_MII_002	CDS	104877	105161	285	-		PGF_08225224	94	hypothetical protein
vB_Eclo_MII_002	CDS	105191	105814	624	-		PGF_08225224	207	hypothetical protein
vB_Eclo_MII_002	CDS	105814	105966	153	-		PGF_01626306	50	hypothetical protein
vB_Eclo_MII_002	CDS	106087	106665	579	+		PGF_08225224	192	hypothetical protein
vB_Eclo_MII_002	CDS	106633	10797	165	-			54	Phage protein
vB_Eclo_MII_002	CDS	106695	106913	219	+			72	hypothetical protein
vB_Eclo_MII_002	CDS	106910	106999	90	+			29	hypothetical protein
vB_Eclo_MII_002	CDS	106996	107163	168	+		PGF_10515476	55	hypothetical protein
vB_Eclo_MII_002	CDS	107333	107434	102	-			33	hypothetical protein
vB_Eclo_MII_002	CDS	107540	107941	402	-		PGF_10392456	133	hypothetical protein
vB_Eclo_MII_002	CDS	10775	11068	294	-		PGF_12710107	97	hypothetical protein
vB_Eclo_MII_002	CDS	107962	108108	147	-			48	hypothetical protein
vB_Eclo_MII_002	CDS	108108	108584	477	-		PGF_08225224	158	hypothetical protein
vB_Eclo_MII_002	CDS	108759	108899	141	-			46	hypothetical protein
vB_Eclo_MII_002	CDS	108896	109102	207	-			68	hypothetical protein
vB_Eclo_MII_002	CDS	109133	109504	372	+		PGF_00254986	123	hypothetical protein
vB_Eclo_MII_002	CDS	109501	109599	99	+			32	hypothetical protein
vB_Eclo_MII_002	CDS	109669	109821	153	+			50	hypothetical protein
vB_Eclo_MII_002	CDS	109833	110162	330	+		PGF_00394224	109	hypothetical protein
vB_Eclo_MII_002	CDS	110199	110288	90	+			29	hypothetical protein
vB_Eclo_MII_002	CDS	110457	110999	543	+	PLF_547_00068339	PGF_08225224	180	Phage protein
vB_Eclo_MII_002	CDS	110944	111348	405	+		PGF_08225224	134	hypothetical protein
vB_Eclo_MII_002	CDS	111369	111491	123	-		PGF_10301412	40	hypothetical protein
vB_Eclo_MII_002	CDS	111499	112110	612	-		PGF_10301412	203	hypothetical protein
vB_Eclo_MII_002	CDS	11156	11347	192	-		PGF_08225224	63	hypothetical protein
vB_Eclo_MII_002	CDS	1119	1730	612	+		PGF_00193827	203	hypothetical protein
vB_Eclo_MII_002	CDS	112174	112533	360	-	PLF_547_00008269	PGF_00011199	119	Helix-turn-helix motif
vB_Eclo_MII_002	CDS	112537	112674	138	-			45	putative membrane protein
vB_Eclo_MII_002	CDS	112757	112897	141	-			46	hypothetical protein
vB_Eclo_MII_002	CDS	112944	113234	291	+			96	hypothetical protein
vB_Eclo_MII_002	CDS	113336	113689	354	+		PGF_00906157	117	hypothetical protein
vB_Eclo_MII_002	CDS	11344	11601	258	-		PGF_08225224	85	hypothetical protein
vB_Eclo_MII_002	CDS	113673	113771	99	+			32	hypothetical protein
vB_Eclo_MII_002	CDS	113803	114024	222	+			74	hypothetical protein
vB_Eclo_MII_002	CDS	11612	11770	159	-		PGF_08225224	52	hypothetical protein
vB_Eclo_MII_002	CDS	11861	12676	816	-		PGF_08225224	271	hypothetical protein
vB_Eclo_MII_002	CDS	12754	13263	510	-	PLF_547_00099264	PGF_10331201	169	Phage eae protein
vB_Eclo_MII_002	CDS	13297	13536	240	-		PGF_08225224	79	hypothetical protein
vB_Eclo_MII_002	CDS	13566	14189	624	-		PGF_08225224	207	hypothetical protein
vB_Eclo_MII_002	CDS	14189	14341	153	-		PGF_01626306	50	hypothetical protein
vB_Eclo_MII_002	CDS	14408	14563	156	-			51	hypothetical protein

vB Eclo MII 002	CDS	14566	14946	381	-			126	hypothetical protein
vB Eclo MII 002	CDS	15088	15204	117	-			38	hypothetical protein
vB Eclo MII 002	CDS	15292	15510	219	-			72	hypothetical protein
vB Eclo MII 002	CDS	15708	15809	102	-			33	hypothetical protein
vB Eclo MII 002	CDS	15925	16317	393	-		PGF_10392456	130	hypothetical protein
vB Eclo MII 002	CDS	16338	16484	147	-			48	hypothetical protein
vB Eclo MII 002	CDS	16484	16960	477	-		PGF_08225224	158	hypothetical protein
vB Eclo MII 002	CDS	17004	17096	93	-			30	hypothetical protein
vB Eclo MII 002	CDS	17162	17260	99	-			32	hypothetical protein
vB Eclo MII 002	CDS	17229	17882	654	+		PGF_00254986	217	hypothetical protein
vB Eclo MII 002	CDS	17883	18017	135	-		PGF_00257396	44	hypothetical protein
vB Eclo MII 002	CDS	1806	1982	177	-	PLF_547_00047022	PGF_00267476	58	Phage protein
vB Eclo MII 002	CDS	18210	18539	330	+		PGF_00394224	109	hypothetical protein
vB Eclo MII 002	CDS	18532	19725	1194	+	PLF_547_00068339	PGF_08225224	397	hypothetical protein
vB_Eclo_MII_002	CDS	1966	2346	381	-	PLF_547_00020646	PGF_00422625	126	Death on curing protein, Doc toxin
vB Eclo MII 002	CDS	19746	20486	741	-		PGF_10301412	246	hypothetical protein
vB Eclo MII 002	CDS	20549	20908	360	-	PLF_547_00008269	PGF_00011199	119	Helix-turn-helix motif
vB Eclo MII 002	CDS	20912	21214	303	-	PLF_547_00010771	PGF_00409249	100	putative membrane protein
vB Eclo MII 002	CDS	21318	22151	834	+		PGF_00906157	277	hypothetical protein
vB Eclo MII 002	CDS	22148	22537	390	+		PGF_00080373	129	hypothetical protein
vB Eclo MII 002	CDS	22486	22914	429	+		PGF_00080373	142	hypothetical protein
vB Eclo MII 002	CDS	22918	23466	549	+		PGF_08225224	182	hypothetical protein
vB Eclo MII 002	CDS	23427	23897	471	+		PGF_08225224	156	hypothetical protein
vB Eclo MII 002	CDS	23894	24547	654	+	PLF_547_00055795	PGF_00214149	217	hypothetical protein
vB_Eclo_MII_002	CDS	24607	25512	906	+	PLF_547_00000182	PGF_02296690	301	DNA recombinationdependent growth factor RdgC
vB Eclo MII 002	CDS	2467	2565	99	-			32	hypothetical protein
vB Eclo MII 002	CDS	25427	26035	609	+		PGF_08225224	202	hypothetical protein
vB Eclo MII 002	CDS	2607	2699	93	-			30	hypothetical protein
vB_Eclo_MII_002	CDS	26072	27073	1002	+		PGF_08354915	333	Type II, 5-methylcytosine DNA methyltransferase
vB_Eclo_MII_002	CDS	27122	28783	1662	-	PLF_547_00000829	PGF_00008326	553	Glutaminyl-tRNA synthetase (EC 6.1.1.18)
vB_Eclo_MII_002	CDS	2768	2935	168	-	PLF_547_00004337	PGF_07518314	55	Error-prone repair protein UmuD
vB Eclo MII 002	CDS	277	534	258	-			85	hypothetical protein
vB Eclo MII 002	CDS	28862	29017	156	-			51	hypothetical protein
vB Eclo MII 002	CDS	29052	29339	288	-		PGF_00321127	95	hypothetical protein
vB Eclo MII 002	CDS	29332	29973	642	-		PGF_04757817	213	ParA-like protein
vB Eclo MII 002	CDS	30085	30195	111	-			36	hypothetical protein
vB Eclo MII 002	CDS	30261	30605	345	-		PGF_00351954	114	hypothetical protein
vB Eclo MII 002	CDS	3036	3125	90	-			29	hypothetical protein
vB_Eclo_MII_002	CDS	30613	30831	219	-		PGF_00476202	72	Putative stability/partitioning protein encoded within prophage CP-933T
vB Eclo MII 002	CDS	30890	30979	90	-			29	hypothetical protein
vB_Eclo_MII_002	CDS	30954	31568	615	-		PGF_00476202	204	Putative stability/partitioning protein encoded within prophage CP-933T
vB_Eclo_MII_002	CDS	3122	3394	273	-	PLF_547_00017970	PGF_08970263	90	DNA polymerase III theta subunit (EC 2.7.7.7)
vB Eclo MII 002	CDS	31727	31993	267	-			88	hypothetical protein

vB Eclo MII 002	CDS	32082	32243	162	-			53	hypothetical protein
vB Eclo MII 002	CDS	32330	32926	597	+		PGF_08225224	198	hypothetical protein
vB Eclo MII 002	CDS	32983	33456	474	+		PGF_08225224	157	hypothetical protein
vB Eclo MII 002	CDS	33473	33622	150	+		PGF_05235730	49	hypothetical protein
vB Eclo MII 002	CDS	33610	34068	459	-		PGF_00299192	152	hypothetical protein
vB Eclo MII 002	CDS	3397	3771	375	-		PGF_01625400	124	hypothetical protein
vB Eclo MII 002	CDS	34085	34477	393	-		PGF_01632454	130	hypothetical protein
vB Eclo MII 002	CDS	34485	34589	105	+			34	hypothetical protein
vB Eclo MII 002	CDS	34681	35349	669	+	PLF_547_00057410	PGF_08225224	222	hypothetical protein
vB Eclo MII 002	CDS	35383	35553	171	+			56	hypothetical protein
vB Eclo MII 002	CDS	35574	36368	795	+	PLF_547_00057410	PGF_08225224	264	Unclassified head protein
vB Eclo MII 002	CDS	36331	36435	105	+		PGF_01635494	34	hypothetical protein
vB Eclo MII 002	CDS	36479	36757	279	+		PGF_08225224	92	hypothetical protein
vB Eclo MII 002	CDS	36825	38483	1659	+		PGF_08225224	552	Phage tail sheath protein
vB Eclo MII 002	CDS	3707	4480	774	-		PGF_04008137	257	Phage EaA protein
vB Eclo MII 002	CDS	38526	39263	738	+		PGF_08225224	245	Unclassified tail protein
vB Eclo MII 002	CDS	39	215	177	-			58	hypothetical protein
vB_Eclo_MII_002	CDS	39327	39899	573	+		PGF_00203217	190	putative morphogenetic function
vB Eclo MII 002	CDS	39908	40111	204	+		PGF_12668369	67	Phage baseplate protein
vB Eclo MII 002	CDS	40108	40398	291	+		PGF_12668369	96	Phage baseplate protein
vB Eclo MII 002	CDS	40452	41003	552	+		PGF_00386528	183	hypothetical protein
vB Eclo MII 002	CDS	41019	41726	708	+		PGF_00374990	235	Phage protein
vB Eclo MII 002	CDS	41758	41871	114	-			37	hypothetical protein
vB Eclo MII 002	CDS	41886	42029	144	-			47	hypothetical protein
vB_Eclo_MII_002	CDS	42107	42862	756	-		PGF_00047577	251	Replication initiation protein RepE
vB Eclo MII 002	CDS	42922	43122	201	-			66	hypothetical protein
vB Eclo MII 002	CDS	43206	43307	102	-			33	hypothetical protein
vB Eclo MII 002	CDS	43392	44072	681	+		PGF_02914608	226	PmgB
vB Eclo MII 002	CDS	44087	44767	681	+		PGF_08225224	226	hypothetical protein
vB Eclo MII 002	CDS	4462	4836	375	-		PGF_00077482	124	hypothetical protein
vB Eclo MII 002	CDS	44776	45198	423	+		PGF_08225224	140	hypothetical protein
vB Eclo MII 002	CDS	45188	45373	186	+			61	hypothetical protein
vB Eclo MII 002	CDS	45494	45790	297	+		PGF_08225224	98	Phage internal (core) protein
vB Eclo MII 002	CDS	45769	47691	1923	+		PGF_08225224	640	hypothetical protein
vB Eclo MII 002	CDS	47754	48017	264	+		PGF_08225224	87	hypothetical protein
vB Eclo MII 002	CDS	48057	48185	129	+			42	hypothetical protein
vB Eclo MII 002	CDS	48172	48396	225	+		PGF_00373118	74	hypothetical protein
vB Eclo MII 002	CDS	48483	49823	1341	+		PGF_09421096	446	Phage baseplate
vB Eclo MII 002	CDS	4865	5137	273	-		PGF_00153550	90	Phage protein
vB Eclo MII 002	CDS	49834	50385	552	+			183	hypothetical protein
vB Eclo MII 002	CDS	50352	50678	327	+		PGF_08225224	108	hypothetical protein
vB Eclo MII 002	CDS	50773	51195	423	+		PGF_01625812	140	hypothetical protein
vB_Eclo_MII_002	CDS	51221	53488	2268	+		PGF_10378329	755	Phage tail fiber Mup49, S
vB Eclo MII 002	CDS	5150	5578	429	-		PGF_04005792	142	hypothetical protein
vB_Eclo_MII_002	CDS	53379	55244	1866	+	PLF_547_00099655	PGF_10378329	621	Phage tail fiber Mup49, S
vB Eclo MII 002	CDS	545	655	111	-			36	hypothetical protein
vB_Eclo_MII_002	CDS	55247	55393	147	+		PGF_02875915	48	Phage tail fiber assembly protein
vB_Eclo_MII_002	CDS	55429	55779	351	+	PLF_547_00092452	PGF_00090969	116	Phage tail fiber assembly protein Mup50, U
vB Eclo MII 002	CDS	5571	5807	237	-	PLF_547_00092553	PGF_01524160	78	Phage protein
vB_Eclo_MII_002	CDS	55807	56334	528	-	PLF_547_00021062	PGF_10148872	175	Phage tail fiber assembly protein GpG

vB_Eclo_MII_002	CDS	56338	57213	876	-	PLF_547_00004152	PGF_06366833	291	Phage tail fiber, side tail fiber protein Stf
vB_Eclo_MII_002	CDS	57164	57466	303	+			100	hypothetical protein
vB_Eclo_MII_002	CDS	57516	57617	102	+			33	hypothetical protein
vB_Eclo_MII_002	CDS	57614	57706	93	+			30	hypothetical protein
vB_Eclo_MII_002	CDS	57777	57866	90	+			29	hypothetical protein
vB_Eclo_MII_002	CDS	57900	58052	153	-			50	hypothetical protein
vB_Eclo_MII_002	CDS	58049	58321	273	-		PGF_06366833	90	Phage tail fiber, side tail fiber protein Stf
vB_Eclo_MII_002	CDS	58413	58508	96	-			31	hypothetical protein
vB_Eclo_MII_002	CDS	5845	6015	171	-		PGF_08086784	56	Phage ea22 protein
vB_Eclo_MII_002	CDS	58573	59133	561	-	PLF_547_00005679	PGF_04069129	186	Phage DNA invertase
vB_Eclo_MII_002	CDS	59238	59564	327	+		PGF_04887537	108	hypothetical protein
vB_Eclo_MII_002	CDS	59564	60010	447	+		PGF_00388771	148	hypothetical protein
vB_Eclo_MII_002	CDS	60000	60620	621	+		PGF_00309152	206	hypothetical protein
vB_Eclo_MII_002	CDS	6020	6652	633	-		PGF_08086784	210	Phage ea22 protein
vB_Eclo_MII_002	CDS	60613	62538	1926	+		PGF_00351963	641	hypothetical protein
vB_Eclo_MII_002	CDS	62538	62906	369	+		PGF_00236580	122	hypothetical protein
vB_Eclo_MII_002	CDS	62922	63047	126	+			41	hypothetical protein
vB_Eclo_MII_002	CDS	63199	64386	1188	+	PLF_547_00050444	PGF_01543848	395	Phage protein
vB_Eclo_MII_002	CDS	64451	64828	378	+		PGF_12801660	125	hypothetical protein
vB_Eclo_MII_002	CDS	64864	66132	1269	+		PGF_08736726	422	Phage portal (connector) protein
vB_Eclo_MII_002	CDS	66146	67009	864	+	PLF_547_00091783	PGF_03918565	287	Phage protein
vB_Eclo_MII_002	CDS	67049	67168	120	+			39	hypothetical protein
vB_Eclo_MII_002	CDS	6708	6860	153	-		PGF_00032198	50	Phage protein
vB_Eclo_MII_002	CDS	67343	67477	135	+			44	hypothetical protein
vB_Eclo_MII_002	CDS	67527	67853	327	+			108	hypothetical protein
vB_Eclo_MII_002	CDS	67825	68229	405	+		PGF_00189209	134	hypothetical protein
vB_Eclo_MII_002	CDS	68239	68328	90	+			29	hypothetical protein
vB_Eclo_MII_002	CDS	68423	68710	288	+			95	hypothetical protein
vB_Eclo_MII_002	CDS	6862	7050	189	-	PLF_547_00035426	PGF_07843775	62	Phage protein
vB_Eclo_MII_002	CDS	68713	68937	225	+		PGF_00394055	74	Icd protein
vB_Eclo_MII_002	CDS	68937	69644	708	+		PGF_00031627	235	Phage DNA binding protein Roi
vB_Eclo_MII_002	CDS	69644	69814	171	+			56	hypothetical protein
vB_Eclo_MII_002	CDS	69767	70357	591	-	PLF_547_00014476	PGF_08225224	196	Phage tail fiber protein (long tail fiber)
vB_Eclo_MII_002	CDS	70433	73738	3306	+	PLF_547_00024073	PGF_02798643	1101	Phage protein
vB_Eclo_MII_002	CDS	7047	7223	177	-		PGF_01627595	58	hypothetical protein
vB_Eclo_MII_002	CDS	709	885	177	+		PGF_00290329	58	hypothetical protein
vB_Eclo_MII_002	CDS	7220	7396	177	-		PGF_00685215	58	hypothetical protein
vB_Eclo_MII_002	CDS	73729	77346	3618	+	PLF_547_00024073	PGF_02798643	1205	Phage protein
vB_Eclo_MII_002	CDS	7396	7566	171	-		PGF_08225224	56	hypothetical protein
vB_Eclo_MII_002	CDS	7627	7827	201	-		PGF_08086784	66	Phage ea22 protein
vB_Eclo_MII_002	CDS	77383	77817	435	+		PGF_00273608	144	Ulx
vB_Eclo_MII_002	CDS	77820	78080	261	+		PGF_05973039	86	hypothetical protein
vB_Eclo_MII_002	CDS	78221	78712	492	+		PGF_00239349	163	Phage protein (ACLAME 766)
vB_Eclo_MII_002	CDS	78727	78927	201	+		PGF_00208569	66	hypothetical protein
vB_Eclo_MII_002	CDS	7881	7997	117	-		PGF_00031654	38	Phage EaE protein
vB_Eclo_MII_002	CDS	79053	79223	171	+			56	hypothetical protein
vB_Eclo_MII_002	CDS	79327	79590	264	+			87	hypothetical protein
vB_Eclo_MII_002	CDS	79668	80546	879	+		PGF_06182504	292	hypothetical protein
vB_Eclo_MII_002	CDS	7994	8155	162	-		PGF_00031654	53	Phage EaE protein
vB_Eclo_MII_002	CDS	80598	80690	93	-			30	hypothetical protein
vB_Eclo_MII_002	CDS	80707	80823	117	-			38	hypothetical protein

vB Eclo MII 002	CDS	80801	80926	126	-			41	hypothetical protein
vB Eclo MII 002	CDS	80926	81081	156	-			51	hypothetical protein
vB Eclo MII 002	CDS	81128	81241	114	-			37	hypothetical protein
vB Eclo MII 002	CDS	81259	81657	399	-			132	hypothetical protein
vB Eclo MII 002	CDS	8164	8496	333	-		PGF_08225224	110	hypothetical protein
vB Eclo MII 002	CDS	82063	82512	450	-		PGF_08225224	149	Lipoprotein, phageassociated
vB Eclo MII 002	CDS	82548	82646	99	-			32	hypothetical protein
vB Eclo MII 002	CDS	82709	82819	111	-			36	hypothetical protein
vB Eclo MII 002	CDS	82810	83070	261	-			86	hypothetical protein
vB Eclo MII 002	CDS	83222	83380	159	+			52	hypothetical protein
vB Eclo MII 002	CDS	83463	83558	96	+			31	hypothetical protein
vB Eclo MII 002	CDS	83628	84098	471	+		PGF_00255582	156	hypothetical protein
vB Eclo MII 002	CDS	84098	84202	105	+			34	hypothetical protein
vB Eclo MII 002	CDS	84202	84594	393	+		PGF_01632868	130	hypothetical protein
vB Eclo MII 002	CDS	84703	85095	393	+		PGF_00314481	130	hypothetical protein
vB Eclo MII 002	CDS	8483	8782	300	-		PGF_00387812	99	hypothetical protein
vB Eclo MII 002	CDS	85092	85250	159	+		PGF_01643850	52	hypothetical protein
vB Eclo MII 002	CDS	85235	85351	117	+			38	hypothetical protein
vB Eclo MII 002	CDS	85383	86453	1071	+		PGF_01643850	356	hypothetical protein
vB_Eclo_MII_002	CDS	86453	86944	492	+		PGF_12821453	163	Phage terminase, large subunit
vB_Eclo_MII_002	CDS	86989	87960	972	+	PLF_547_00082022	PGF_09464755	323	Phage terminase, large subunit
vB Eclo MII 002	CDS	88032	89069	1038	-		PGF_01631233	345	hypothetical protein
vB Eclo MII 002	CDS	8855	9412	558	-		PGF_00270247	185	hypothetical protein
vB Eclo MII 002	CDS	89117	89218	102	-			33	hypothetical protein
vB Eclo MII 002	CDS	89231	89320	90	+			29	hypothetical protein
vB Eclo MII 002	CDS	89454	90482	1029	+	PLF_547_00016853	PGF_04687495	342	hypothetical protein
vB Eclo MII 002	CDS	90556	90900	345	+		PGF_00081660	114	hypothetical protein
vB Eclo MII 002	CDS	90897	91085	189	+		PGF_01626853	62	hypothetical protein
vB Eclo MII 002	CDS	91139	91372	234	+		PGF_01626853	77	hypothetical protein
vB_Eclo_MII_002	CDS	91369	91863	495	+		PGF_01430214	164	Deoxyuridine 5'triphosphate nucleotidohydrolase (EC 3.6.1.23)
vB Eclo MII 002	CDS	91878	92555	678	+		PGF_00290329	225	hypothetical protein
vB Eclo MII 002	CDS	92562	93338	777	+		PGF_00193827	258	hypothetical protein
vB Eclo MII 002	CDS	93371	93589	219	-	PLF_547_00047022	PGF_00267476	72	Phage protein
vB_Eclo_MII_002	CDS	93573	93953	381	-	PLF_547_00020646	PGF_00422625	126	Death on curing protein, Doc toxin
vB_Eclo_MII_002	CDS	93953	94174	222	-	PLF_547_00081325	PGF_00272408	73	RelB/StbD replicon stabilization protein (antitoxin to RelE/StbE)
vB_Eclo_MII_002	CDS	94247	94636	390	-	PLF_547_00004337	PGF_07518314	129	Error-prone repair protein UmuD
vB_Eclo_MII_002	CDS	94732	95007	276	-	PLF_547_00017970	PGF_08970263	91	DNA polymerase III theta subunit (EC 2.7.7.7)
vB Eclo MII 002	CDS	95010	95276	267	-		PGF_01625400	88	hypothetical protein
vB Eclo MII 002	CDS	95322	96095	774	-		PGF_04008137	257	Phage EaA protein
vB Eclo MII 002	CDS	955	1047	93	+		PGF_00193827	30	hypothetical protein
vB Eclo MII 002	CDS	9559	9789	231	-		PGF_00270247	76	hypothetical protein
vB Eclo MII 002	CDS	96077	96451	375	-		PGF_00077482	124	hypothetical protein
vB Eclo MII 002	CDS	96458	96751	294	-		PGF_00153550	97	Phage protein
vB Eclo MII 002	CDS	96764	97192	429	-		PGF_04005792	142	hypothetical protein
vB Eclo MII 002	CDS	97185	97421	237	-	PLF_547_00092553	PGF_01524160	78	Phage protein
vB Eclo MII 002	CDS	97459	98265	807	-		PGF_08086784	268	Phage ea22 protein
vB Eclo MII 002	CDS	98262	98471	210	-		PGF_00032198	69	Phage protein

vB_Eclo_MII_002	CDS	98473	98661	189	-	PLF_547_00035426	PGF_07843775	62	Phage protein
vB_Eclo_MII_002	CDS	98658	98834	177	-		PGF_01627595	58	hypothetical protein
vB_Eclo_MII_002	CDS	98831	99007	177	-		PGF_00685215	58	hypothetical protein
vB_Eclo_MII_002	CDS	99007	99438	432	-		PGF_08086784	143	Phage ea22 protein
vB_Eclo_MII_002	CDS	9925	10575	651	-	PLF_547_00010043	PGF_06196706	216	Phage serine/threonine protein phosphatase NinI (EC 3.1.3.16)
vB_Eclo_MII_002	CDS	99492	99608	117	-		PGF_00031654	38	Phage EaE protein
vB_Eclo_MII_002	CDS	99605	99766	162	-		PGF_00031654	53	Phage EaE protein
vB_Eclo_MII_002	CDS	99775	100110	336	-			111	hypothetical protein
vB_Eclo_MII_002	CDS	10355	10561	207	+		PGF_05437948	68	Phage protein
vB_Eclo_MII_002	CDS	10632	12335	1704	+		PGF_00421723	567	Phage primase/helicase protein Gp4A
vB_Eclo_MII_002	CDS	1073	1261	189	+			62	hypothetical protein
vB_Eclo_MII_002	CDS	12380	12562	183	+			60	Phage protein
vB_Eclo_MII_002	CDS	12621	13016	396	+			131	T7-like phage DNA Polymerase (EC 2.7.7.7)
vB_Eclo_MII_002	CDS	127	234	108	-			35	hypothetical protein
vB_Eclo_MII_002	CDS	1272	1799	528	+		PGF_06014785	175	hypothetical protein
vB_Eclo_MII_002	CDS	13018	14808	1791	+		PGF_08740592	596	Phage DNA-directed DNA polymerase (EC 2.7.7.7)
vB_Eclo_MII_002	CDS	14808	14969	162	+			53	hypothetical protein
vB_Eclo_MII_002	CDS	14969	15259	291	+			96	Phage HNS binding protein
vB_Eclo_MII_002	CDS	15256	15465	210	+		PGF_04070011	69	Phage protein Gp5.7
vB_Eclo_MII_002	CDS	15449	15679	231	+			76	Phage protein
vB_Eclo_MII_002	CDS	15679	16548	870	+		PGF_00031762	289	Phage exonuclease (EC 3.1.11.3)
vB_Eclo_MII_002	CDS	16530	16619	90	+			29	hypothetical protein
vB_Eclo_MII_002	CDS	16754	17026	273	+			90	hypothetical protein
vB_Eclo_MII_002	CDS	17037	17258	222	+		PGF_05140785	73	Phage protein (ACLAME 1292)
vB_Eclo_MII_002	CDS	17262	17666	405	+		PGF_06150282	134	Phage protein
vB_Eclo_MII_002	CDS	17659	17910	252	+			83	Phage host specificity protein (ACLAME 1293)
vB_Eclo_MII_002	CDS	17922	19490	1569	+		PGF_08466151	522	Phage collar, head-tail connector protein Gp8
vB_Eclo_MII_002	CDS	1793	1942	150	+			49	hypothetical protein
vB_Eclo_MII_002	CDS	1945	2070	126	+			41	hypothetical protein
vB_Eclo_MII_002	CDS	19598	20479	882	+		PGF_12668281	293	Phage capsid and scaffold
vB_Eclo_MII_002	CDS	20606	21655	1050	+		PGF_08799475	349	Phage major capsid protein Gp10A
vB_Eclo_MII_002	CDS	2141	2245	105	+			34	hypothetical protein
vB_Eclo_MII_002	CDS	21712	21918	207	+			68	hypothetical protein
vB_Eclo_MII_002	CDS	21978	22544	567	+		PGF_04874775	188	Phage tail fiber protein / T7-like tail tubular protein A
vB_Eclo_MII_002	CDS	2245	2442	198	+			65	Phage protein
vB_Eclo_MII_002	CDS	22544	22771	228	+			75	Phage protein
vB_Eclo_MII_002	CDS	22783	24201	1419	+		PGF_07801391	472	Phage non-contractile tail tubular protein Gp12
vB_Eclo_MII_002	CDS	24294	25139	846	+		PGF_07801391	281	Phage non-contractile tail tubular protein Gp12
vB_Eclo_MII_002	CDS	2442	2654	213	+			70	hypothetical protein
vB_Eclo_MII_002	CDS	25226	25519	294	+		PGF_04145078	97	Phage internal (core) protein
vB_Eclo_MII_002	CDS	25519	25695	177	+		PGF_04145078	58	Phage internal (core) protein

vB_Eclo_MII_002	CDS	25680	26285	606	+		PGF_12760961	201	Phage internal (core) protein
vB_Eclo_MII_002	CDS	26278	27054	777	+		PGF_05947970	258	Phage DNA ejectosome component, internal virion protein Gp15
vB_Eclo_MII_002	CDS	26957	28513	1557	+			518	hypothetical protein
vB_Eclo_MII_002	CDS	2752	5418	2667	+		PGF_08961762	888	Phage DNA-directed RNA polymerase (EC 2.7.7.6)
vB_Eclo_MII_002	CDS	28565	32014	3450	+		PGF_04695520	1149	Phage DNA ejectosome component Gp16, peptidoglycan lytic exotransglycosylase (EC 4.2.2.n1)
vB_Eclo_MII_002	CDS	32035	32220	186	+			61	hypothetical protein
vB_Eclo_MII_002	CDS	32220	32453	234	+		PGF_12880186	77	Phage internal (core) protein
vB_Eclo_MII_002	CDS	32512	33348	837	+			278	hypothetical protein
vB_Eclo_MII_002	CDS	33577	33699	123	+			40	hypothetical protein
vB_Eclo_MII_002	CDS	33718	33843	126	+			41	hypothetical protein
vB_Eclo_MII_002	CDS	33957	34499	543	+			180	hypothetical protein
vB_Eclo_MII_002	CDS	34535	35215	681	+			226	hypothetical protein
vB_Eclo_MII_002	CDS	35320	35514	195	+			64	Phage holin, class II Gp17.5
vB_Eclo_MII_002	CDS	35511	35774	264	+		PGF_05281019	87	DNA packaging protein A, T7-like gp18
vB_Eclo_MII_002	CDS	35775	35864	90	+			29	hypothetical protein
vB_Eclo_MII_002	CDS	35876	36319	444	+		PGF_06297248	147	Phage Rz-like lysis protein Gp18.5
vB_Eclo_MII_002	CDS	36319	36705	387	+			128	hypothetical protein
vB_Eclo_MII_002	CDS	36748	38541	1794	+		PGF_07972002	597	Phage terminase large subunit Gp19, DNA packaging
vB_Eclo_MII_002	CDS	38542	38649	108	+			35	hypothetical protein
vB_Eclo_MII_002	CDS	38683	38775	93	+			30	hypothetical protein
vB_Eclo_MII_002	CDS	38867	38998	132	+			43	hypothetical protein
vB_Eclo_MII_002	CDS	39	143	105	-			34	hypothetical protein
vB_Eclo_MII_002	CDS	39205	39309	105	+			34	hypothetical protein
vB_Eclo_MII_002	CDS	39397	39528	132	+			43	hypothetical protein
vB_Eclo_MII_002	CDS	39534	39641	108	+			35	hypothetical protein
vB_Eclo_MII_002	CDS	39723	39839	117	+			38	hypothetical protein
vB_Eclo_MII_002	CDS	40034	40288	255	+			84	Phage protein
vB_Eclo_MII_002	CDS	40357	40545	189	+			62	hypothetical protein
vB_Eclo_MII_002	CDS	40556	41080	525	+		PGF_06014785	174	hypothetical protein
vB_Eclo_MII_002	CDS	41074	41223	150	+			49	hypothetical protein
vB_Eclo_MII_002	CDS	41226	41351	126	+			41	hypothetical protein
vB_Eclo_MII_002	CDS	41422	41526	105	+			34	hypothetical protein
vB_Eclo_MII_002	CDS	41526	41723	198	+			65	Phage protein
vB_Eclo_MII_002	CDS	41723	41935	213	+			70	hypothetical protein
vB_Eclo_MII_002	CDS	42033	44699	2667	+		PGF_08961762	888	Phage DNA-directed RNA polymerase (EC 2.7.7.6)
vB_Eclo_MII_002	CDS	439	570	132	-			43	hypothetical protein
vB_Eclo_MII_002	CDS	44712	44912	201	+			66	Phage protein
vB_Eclo_MII_002	CDS	44935	45168	234	+		PGF_05697581	77	Phage protein
vB_Eclo_MII_002	CDS	45173	45457	285	+			94	hypothetical protein
vB_Eclo_MII_002	CDS	45423	46526	1104	+		PGF_05993939	367	Phage-associated ATPdependent DNA ligase (EC 6.5.1.1)
vB_Eclo_MII_002	CDS	46639	46893	255	+			84	Phage protein (ACLAME 1535)

vB_Eclo_MII_002	CDS	46893	47213	321	+		PGF_09934437	106	Phage nucleotide kinase Gp1.7, phosphorylates dGMP to dGDP and dTMP to dTDP
vB_Eclo_MII_002	CDS	47200	47295	96	+			31	Phage protein
vB_Eclo_MII_002	CDS	47292	47465	174	+			57	hypothetical protein
vB_Eclo_MII_002	CDS	47574	48269	696	+		PGF_02997548	231	Phage single-stranded DNA-binding protein Gp2.5
vB_Eclo_MII_002	CDS	48305	48724	420	+		PGF_06491438	139	Phage endonuclease I (EC 3.1.21.2), four-way DNA junctions resolving
vB_Eclo_MII_002	CDS	48721	49173	453	+			150	Phage protein
vB_Eclo_MII_002	CDS	49163	49621	459	+		PGF_06446683	152	Phage endolysin
vB_Eclo_MII_002	CDS	49636	49848	213	+		PGF_05437948	70	Phage protein
vB_Eclo_MII_002	CDS	49919	51622	1704	+		PGF_00421723	567	Phage primase/helicase protein Gp4A
vB_Eclo_MII_002	CDS	51667	51831	165	+			54	Phage protein
vB_Eclo_MII_002	CDS	51903	54089	2187	+		PGF_08740592	728	Phage DNA-directed DNA polymerase (EC 2.7.7.7)
vB_Eclo_MII_002	CDS	54089	54250	162	+			53	hypothetical protein
vB_Eclo_MII_002	CDS	54250	54411	162	+			53	Phage HNS binding protein
vB_Eclo_MII_002	CDS	5431	5631	201	+			66	Phage protein
vB_Eclo_MII_002	CDS	54408	54539	132	+			43	Phage HNS binding protein
vB_Eclo_MII_002	CDS	54536	54745	210	+		PGF_04070011	69	Phage protein Gp5.7
vB_Eclo_MII_002	CDS	54742	54912	171	+			56	Phage protein
vB_Eclo_MII_002	CDS	54958	55824	867	+		PGF_00031762	288	Phage exonuclease (EC 3.1.11.3)
vB_Eclo_MII_002	CDS	55806	55940	135	+			44	hypothetical protein
vB_Eclo_MII_002	CDS	56031	56303	273	+			90	hypothetical protein
vB_Eclo_MII_002	CDS	56314	56535	222	+		PGF_05140785	73	Phage protein (ACLAME 1292)
vB_Eclo_MII_002	CDS	56539	56928	390	+		PGF_06150282	129	Phage protein
vB_Eclo_MII_002	CDS	5654	5887	234	+		PGF_05697581	77	Phage protein
vB_Eclo_MII_002	CDS	56931	57182	252	+			83	Phage host specificity protein (ACLAME 1293)
vB_Eclo_MII_002	CDS	57194	58762	1569	+		PGF_08466151	522	Phage collar, head-tail connector protein Gp8
vB_Eclo_MII_002	CDS	58870	59751	882	+		PGF_12668281	293	Phage capsid and scaffold
vB_Eclo_MII_002	CDS	5892	6050	159	+			52	hypothetical protein
vB_Eclo_MII_002	CDS	59878	60435	558	+		PGF_08799475	185	Phage major capsid protein Gp10A
vB_Eclo_MII_002	CDS	60534	60938	405	+		PGF_08799475	134	Phage major capsid protein Gp10A
vB_Eclo_MII_002	CDS	60985	61191	207	+			68	hypothetical protein
vB_Eclo_MII_002	CDS	61251	61817	567	+		PGF_04874775	188	Phage tail fiber protein / T7-like tail tubular protein A
vB_Eclo_MII_002	CDS	6142	7245	1104	+		PGF_05993939	367	Phage-associated ATPdependent DNA ligase (EC 6.5.1.1)
vB_Eclo_MII_002	CDS	61817	62044	228	+			75	Phage protein
vB_Eclo_MII_002	CDS	62056	63471	1416	+		PGF_07801391	471	Phage non-contractile tail tubular protein Gp12
vB_Eclo_MII_002	CDS	63560	64411	852	+		PGF_07801391	283	Phage non-contractile tail tubular protein Gp12

vB_Eclo_MII_002	CDS	64490	64960	471	+		PGF_04145078	156	Phage internal (core) protein
vB_Eclo_MII_002	CDS	64945	65532	588	+		PGF_12760961	195	Phage internal (core) protein
vB_Eclo_MII_002	CDS	65544	67115	1572	+		PGF_05947970	523	Phage DNA ejectosome component, internal virion protein Gp15
vB_Eclo_MII_002	CDS	67010	67828	819	+			272	Phage internal (core) protein
vB_Eclo_MII_002	CDS	67834	70383	2550	+		PGF_04695520	849	Phage DNA ejectosome component Gp16, peptidoglycan lytic exotransglycosylase (EC 4.2.2.n1)
vB_Eclo_MII_002	CDS	70392	70886	495	+		PGF_04695520	164	Phage DNA ejectosome component Gp16, peptidoglycan lytic exotransglycosylase (EC 4.2.2.n1)
vB_Eclo_MII_002	CDS	70975	71487	513	+		PGF_12880186	170	Phage internal (core) protein
vB_Eclo_MII_002	CDS	71487	71720	234	+		PGF_12880186	77	Phage internal (core) protein
vB_Eclo_MII_002	CDS	71779	72615	837	+			278	hypothetical protein
vB_Eclo_MII_002	CDS	72844	72966	123	+			40	hypothetical protein
vB_Eclo_MII_002	CDS	72985	73110	126	+			41	hypothetical protein
vB_Eclo_MII_002	CDS	73224	74489	1266	+			421	hypothetical protein
vB_Eclo_MII_002	CDS	7358	7612	255	+			84	Phage protein (ACLAME 1535)
vB_Eclo_MII_002	CDS	74594	74788	195	+			64	Phage holin, class II Gp17.5
vB_Eclo_MII_002	CDS	74785	75048	264	+		PGF_05281019	87	DNA packaging protein A, T7-like gp18
vB_Eclo_MII_002	CDS	75049	75138	90	+			29	hypothetical protein
vB_Eclo_MII_002	CDS	75150	75593	444	+		PGF_06297248	147	Phage Rz-like lysis protein Gp18.5
vB_Eclo_MII_002	CDS	752	1006	255	+			84	Phage protein
vB_Eclo_MII_002	CDS	75593	76030	438	+			145	Phage HNH homing endonuclease (ACLAME 27)
vB_Eclo_MII_002	CDS	76023	77789	1767	+		PGF_07972002	588	Phage terminase large subunit Gp19, DNA packaging
vB_Eclo_MII_002	CDS	7612	7932	321	+		PGF_09934437	106	Phage nucleotide kinase Gp1.7, phosphorylates dGMP to dGDP and dTMP to dTDP
vB_Eclo_MII_002	CDS	77815	77937	123	+			40	hypothetical protein
vB_Eclo_MII_002	CDS	77957	78049	93	+			30	hypothetical protein
vB_Eclo_MII_002	CDS	78141	78272	132	+			43	hypothetical protein
vB_Eclo_MII_002	CDS	78478	78582	105	+			34	hypothetical protein
vB_Eclo_MII_002	CDS	7919	8014	96	+			31	Phage protein
vB_Eclo_MII_002	CDS	8011	8250	240	+			79	Host RNA polymerase inhibitor, T7-like gp2
vB_Eclo_MII_002	CDS	8294	8632	339	+			112	hypothetical protein
vB_Eclo_MII_002	CDS	8566	8988	423	+			140	T7-like phage ssDNA binding protein
vB_Eclo_MII_002	CDS	9024	9443	420	+		PGF_06491438	139	Phage endonuclease I (EC 3.1.21.2), four-way DNA junctions resolving
vB_Eclo_MII_002	CDS	9440	9892	453	+			150	Phage protein
vB_Eclo_MII_002	CDS	9882	10340	459	+		PGF_06446683	152	Phage endolysin
vB_Eclo_MII_002	CDS	1425	2417	993	-		PGF_07972002	330	Phage terminase large subunit Gp19, DNA packaging
vB_Eclo_MII_002	CDS	158	286	129	+			42	hypothetical protein
vB_Eclo_MII_002	CDS	2468	2674	207	-			68	Phage DNA packaging protein

vB_Eclo_MII_002	CDS	2667	3107	441	-			146	Phage HNH homing endonuclease (ACLAME 27)
vB_Eclo_MII_002	CDS	300	419	120	+			39	hypothetical protein
vB_Eclo_MII_002	CDS	3104	3547	444	-		PGF_06297248	147	Phage Rz-like lysis protein Gp18.5
vB_Eclo_MII_002	CDS	3559	3648	90	-			29	hypothetical protein
vB_Eclo_MII_002	CDS	3649	3912	264	-		PGF_05281019	87	DNA packaging protein A, T7-like gp18
vB_Eclo_MII_002	CDS	3909	4103	195	-			64	Phage holin, class II Gp17.5
vB_Eclo_MII_002	CDS	40	144	105	+			34	hypothetical protein
vB_Eclo_MII_002	CDS	4208	5467	1260	-			419	hypothetical protein
vB_Eclo_MII_002	CDS	463	621	159	-		PGF_04272194	52	Phage protein
vB_Eclo_MII_002	CDS	5581	5706	126	-			41	hypothetical protein
vB_Eclo_MII_002	CDS	5725	5847	123	-			40	hypothetical protein
vB_Eclo_MII_002	CDS	6076	6912	837	-			278	hypothetical protein
vB_Eclo_MII_002	CDS	652	744	93	-			30	hypothetical protein
vB_Eclo_MII_002	CDS	6971	7204	234	-		PGF_12880186	77	Phage internal (core) protein
vB_Eclo_MII_002	CDS	7204	8700	1497	-		PGF_04695520	498	Phage DNA ejection component Gp16, peptidoglycan lytic exotransglycosylase (EC 4.2.2.n1)
vB_Eclo_MII_002	CDS	778	885	108	-			35	hypothetical protein
vB_Eclo_MII_002	CDS	8726	9454	729	-		PGF_04695520	242	Phage DNA ejection component Gp16, peptidoglycan lytic exotransglycosylase (EC 4.2.2.n1)
vB_Eclo_MII_002	CDS	934	1401	468	-		PGF_07972002	155	Phage terminase large subunit Gp19, DNA packaging
vB_Eclo_MII_002	CDS	9451	9600	150	-			49	hypothetical protein
vB_Eclo_MII_002	CDS	9594	9800	207	-			68	Phage internal (core) protein
vB_Eclo_MII_002	CDS	11343	11744	402	+	PLF_547_00098321	PGF_00249446	133	hypothetical protein
vB_Eclo_MII_002	CDS	11810	12292	483	+	PLF_547_00076579	PGF_06765199	160	hypothetical protein
vB_Eclo_MII_002	CDS	12302	12682	381	+	PLF_547_00091372	PGF_08225224	126	hypothetical protein
vB_Eclo_MII_002	CDS	12601	13161	561	+	PLF_547_00009259	PGF_08225224	186	hypothetical protein
vB_Eclo_MII_002	CDS	13173	13526	354	+	PLF_547_00009259	PGF_08225224	117	hypothetical protein
vB_Eclo_MII_002	CDS	13616	15391	1776	+	PLF_547_00009259	PGF_08225224	591	hypothetical protein
vB_Eclo_MII_002	CDS	15441	17816	2376	+	PLF_547_00019953	PGF_08225224	791	hypothetical protein
vB_Eclo_MII_002	CDS	17856	19301	1446	-	PLF_547_00034708	PGF_03091987	481	hypothetical protein
vB_Eclo_MII_002	CDS	19288	19872	585	-	PLF_547_00003174	PGF_00072365	194	Bactoprenol glucosyl transferase
vB_Eclo_MII_002	CDS	19899	20213	315	-	PLF_547_00003174	PGF_00072365	104	Bactoprenol glucosyl transferase
vB_Eclo_MII_002	CDS	20210	20572	363	-	PLF_547_00003953	PGF_07561028	120	Bactoprenol-linked glucose translocase
vB_Eclo_MII_002	CDS	20685	20924	240	+	PLF_547_00012948	PGF_06288013	79	hypothetical protein
vB_Eclo_MII_002	CDS	20924	21244	321	+	PLF_547_00081676	PGF_08225224	106	hypothetical protein
vB_Eclo_MII_002	CDS	21229	21321	93	+			30	hypothetical protein
vB_Eclo_MII_002	CDS	21370	21492	123	+	PLF_547_00009796	PGF_01575442	40	hypothetical protein
vB_Eclo_MII_002	CDS	21623	22765	1143	-	PLF_547_00005531	PGF_01615525	380	Phage integrase
vB_Eclo_MII_002	CDS	22740	23003	264	-	PLF_547_00074693	PGF_06529909	87	hypothetical protein
vB_Eclo_MII_002	CDS	2287	3591	1305	+	PLF_547_00004621	PGF_12722937	434	Phage head, portal protein B
vB_Eclo_MII_002	CDS	23121	23564	444	-	PLF_547_00099025	PGF_08225224	147	hypothetical protein
vB_Eclo_MII_002	CDS	23561	24073	513	-	PLF_547_00092657	PGF_08225224	170	hypothetical protein
vB_Eclo_MII_002	CDS	24075	24533	459	-	PLF_547_00090948	PGF_08225224	152	Phage EaA protein
vB_Eclo_MII_002	CDS	24530	24826	297	-	PLF_547_00034785	PGF_04025082	98	hypothetical protein

vB_Eclo_MII_002	CDS	24807	25055	249	-	PLF_547_00011650	PGF_01958888	82	hypothetical protein
vB_Eclo_MII_002	CDS	25052	25552	501	-	PLF_547_00091215	PGF_00031654	166	Phage EaE protein
vB_Eclo_MII_002	CDS	25549	26376	828	-	PLF_547_00004365	PGF_00037001	275	Probable chromosome partitioning protein parB
vB_Eclo_MII_002	CDS	26376	26735	360	-	PLF_547_00005091	PGF_09008356	119	hypothetical protein
vB_Eclo_MII_002	CDS	26752	26877	126	-			41	hypothetical protein
vB_Eclo_MII_002	CDS	27090	27179	90	-			29	hypothetical protein
vB_Eclo_MII_002	CDS	27170	27322	153	-			50	hypothetical protein
vB_Eclo_MII_002	CDS	27488	28138	651	-	PLF_547_00011846	PGF_00835539	216	Phage repressor protein C2
vB_Eclo_MII_002	CDS	28244	28441	198	+	PLF_547_00041625	PGF_12866849	65	hypothetical protein
vB_Eclo_MII_002	CDS	28467	28994	528	+	PLF_547_00081674	PGF_12906257	175	Orf33
vB_Eclo_MII_002	CDS	28998	29336	339	+	PLF_547_00051758	PGF_05434849	112	hypothetical protein
vB_Eclo_MII_002	CDS	29346	30272	927	+	PLF_547_00041326	PGF_08048965	308	Hypothetical protein, PV83 orf 20 homolog [SA bacteriophages 11, Mu50B]
vB_Eclo_MII_002	CDS	30269	30763	495	+	PLF_547_00005911	PGF_01574617	164	hypothetical protein
vB_Eclo_MII_002	CDS	30763	31422	660	+	PLF_547_00005140	PGF_00018449	219	MT-A70 family protein
vB_Eclo_MII_002	CDS	31419	31646	228	+	PLF_547_00004993	PGF_01574497	75	hypothetical protein
vB_Eclo_MII_002	CDS	31643	31963	321	+	PLF_547_00005177	PGF_00396182	106	SOS-response repressor and protease LexA
vB_Eclo_MII_002	CDS	31960	32349	390	+	PLF_547_00081925	PGF_00012266	129	Holliday junction resolvase / Crossover junction endodeoxyribonuclease rusA (EC 3.1.22.-)
vB_Eclo_MII_002	CDS	32379	33335	957	+	PLF_547_00004342	PGF_12951569	318	Phage protein YdfU family
vB_Eclo_MII_002	CDS	33348	33926	579	+	PLF_547_00005076	PGF_08274576	192	Phage antitermination protein Q
vB_Eclo_MII_002	CDS	34058	34336	279	+	PLF_547_00072305	PGF_05818861	92	hypothetical protein
vB_Eclo_MII_002	CDS	34320	34427	108	+			35	hypothetical protein
vB_Eclo_MII_002	CDS	34428	34832	405	+	PLF_547_00081438	PGF_00290579	134	hypothetical protein
vB_Eclo_MII_002	CDS	34829	35110	282	+	PLF_547_00011714	PGF_08048396	93	hypothetical protein
vB_Eclo_MII_002	CDS	35059	35736	678	+	PLF_547_00099657	PGF_05639308	225	FIG101079: Lytic enzyme
vB_Eclo_MII_002	CDS	35741	35956	216	+			71	hypothetical protein
vB_Eclo_MII_002	CDS	35953	36225	273	+	PLF_547_00003493	PGF_08225224	90	hypothetical protein
vB_Eclo_MII_002	CDS	3605	4453	849	+	PLF_547_00004688	PGF_12755283	282	Phage major head subunit Mup34, T
vB_Eclo_MII_002	CDS	36230	36367	138	+			45	hypothetical protein
vB_Eclo_MII_002	CDS	36379	36477	99	+			32	hypothetical protein
vB_Eclo_MII_002	CDS	36470	37108	639	+			212	hypothetical protein
vB_Eclo_MII_002	CDS	37213	38670	1458	+	PLF_547_00003713	PGF_08225224	485	hypothetical protein
vB_Eclo_MII_002	CDS	38652	39242	591	+	PLF_547_00005589	PGF_08225224	196	Phage protein
vB_Eclo_MII_002	CDS	39242	39592	351	+	PLF_547_00072515	PGF_06492536	116	Phage-associated homing endonuclease
vB_Eclo_MII_002	CDS	4463	5674	1212	+	PLF_547_00004620	PGF_03696163	403	Phage major capsid protein
vB_Eclo_MII_002	CDS	551	2287	1737	+	PLF_547_00004166	PGF_12848885	578	Phage head, terminase DNA packaging protein A
vB_Eclo_MII_002	CDS	5717	6043	327	+	PLF_547_00004748	PGF_08225224	108	hypothetical protein
vB_Eclo_MII_002	CDS	6046	6537	492	+	PLF_547_00022143	PGF_08892219	163	Phage head-tail adapter
vB_Eclo_MII_002	CDS	6534	6650	117	+	PLF_547_00022143	PGF_08892219	38	Phage head-tail adapter
vB_Eclo_MII_002	CDS	6643	7182	540	+	PLF_547_00012865	PGF_12765584	179	hypothetical protein
vB_Eclo_MII_002	CDS	7179	7544	366	+	PLF_547_00012579	PGF_10503178	121	Phage protein (ACLAME 276)
vB_Eclo_MII_002	CDS	7600	8091	492	+	PLF_547_00099014	PGF_08225224	163	hypothetical protein
vB_Eclo_MII_002	CDS	78	551	474	+	PLF_547_00004211	PGF_00037261	157	Phage terminase, small subunit

vB_Eclo_MII_002	CDS	8143	8520	378	+	PLF_547_00011679	PGF_00265381	125	tail protein
vB_Eclo_MII_002	CDS	8631	8786	156	+	PLF_547_00099389	PGF_12712735	51	Phage protein
vB_Eclo_MII_002	CDS	8788	11343	2556	+	PLF_547_00012488	PGF_09123954	851	Phage tail, tail length tape-measure protein H
vB_Eclo_MII_002	CDS	10438	11856	1419	-	PLF_547_00014204	PGF_00239204	472	hypothetical protein
vB_Eclo_MII_002	CDS	1175	1534	360	+			119	hypothetical protein
vB_Eclo_MII_002	CDS	11922	12290	369	-	PLF_547_00050970	PGF_06193476	122	hypothetical protein
vB_Eclo_MII_002	CDS	12331	12567	237	-			78	hypothetical protein
vB_Eclo_MII_002	CDS	12577	13284	708	-		PGF_12855838	235	hypothetical protein
vB_Eclo_MII_002	CDS	13251	14186	936	-	PLF_547_00014745	PGF_00201822	311	hypothetical protein
vB_Eclo_MII_002	CDS	14161	14502	342	-	PLF_547_00066372	PGF_05509249	113	hypothetical protein
vB_Eclo_MII_002	CDS	14499	15215	717	-	PLF_547_00014205	PGF_00355427	238	hypothetical protein
vB_Eclo_MII_002	CDS	15217	16788	1572	-	PLF_547_00014206	PGF_00294625	523	hypothetical protein
vB_Eclo_MII_002	CDS	1571	1741	171	+			56	hypothetical protein
vB_Eclo_MII_002	CDS	16789	16908	120	-	PLF_547_00050280	PGF_05733706	39	hypothetical protein
vB_Eclo_MII_002	CDS	16950	17387	438	-	PLF_547_00014744	PGF_08225224	145	hypothetical protein
vB_Eclo_MII_002	CDS	17423	17869	447	-	PLF_547_00014746	PGF_00157766	148	FIG00696183: hypothetical protein
vB_Eclo_MII_002	CDS	1773	2936	1164	+	PLF_547_00004314	PGF_01615525	387	Phage integrase
vB_Eclo_MII_002	CDS	17872	19212	1341	-	PLF_547_00012525	PGF_02933321	446	hypothetical protein
vB_Eclo_MII_002	CDS	19232	19771	540	-	PLF_547_00014743	PGF_01565096	179	hypothetical protein
vB_Eclo_MII_002	CDS	19764	20111	348	-	PLF_547_00018837		115	hypothetical protein
vB_Eclo_MII_002	CDS	2	217	216	+		PGF_08225224	71	hypothetical protein
vB_Eclo_MII_002	CDS	20108	20575	468	-	PLF_547_00015200	PGF_04110214	155	hypothetical protein
vB_Eclo_MII_002	CDS	20595	20966	372	-	PLF_547_00044354	PGF_01813316	123	hypothetical protein
vB_Eclo_MII_002	CDS	20966	21169	204	-	PLF_547_00035875		67	hypothetical protein
vB_Eclo_MII_002	CDS	21202	22140	939	-	PLF_547_00014741	PGF_05590037	312	Phage protein (ACLAME 194)
vB_Eclo_MII_002	CDS	217	414	198	+	PLF_547_00019012	PGF_04020803	65	hypothetical protein
vB_Eclo_MII_002	CDS	22150	22659	510	-		PGF_00103577	169	hypothetical protein
vB_Eclo_MII_002	CDS	22659	23759	1101	-	PLF_547_00020461	PGF_00894049	366	hypothetical protein
vB_Eclo_MII_002	CDS	23772	24578	807	-	PLF_547_00045083	PGF_08225224	268	plasmid-related protein
vB_Eclo_MII_002	CDS	24571	25827	1257	-	PLF_547_00014262	PGF_00352574	418	hypothetical protein
vB_Eclo_MII_002	CDS	25836	27395	1560	-	PLF_547_00018406	PGF_00032804	519	Phage terminase, large subunit
vB_Eclo_MII_002	CDS	27392	27721	330	-	PLF_547_00065985	PGF_06359935	109	hypothetical protein
vB_Eclo_MII_002	CDS	27800	28066	267	-			88	hypothetical protein
vB_Eclo_MII_002	CDS	3120	3509	390	-	PLF_547_00004337	PGF_07518314	129	Error-prone repair protein UmuD
vB_Eclo_MII_002	CDS	3623	3985	363	+	PLF_547_00003953	PGF_07561028	120	Bactoprenol-linked glucose translocase
vB_Eclo_MII_002	CDS	3982	4899	918	+	PLF_547_00003174	PGF_00072365	305	Bactoprenol glucosyl transferase
vB_Eclo_MII_002	CDS	479	595	117	+			38	hypothetical protein
vB_Eclo_MII_002	CDS	4896	6353	1458	+	PLF_547_00021056	PGF_08225224	485	hypothetical protein
vB_Eclo_MII_002	CDS	568	768	201	+	PLF_547_00041345	PGF_02922518	66	hypothetical protein
vB_Eclo_MII_002	CDS	6383	8800	2418	-	PLF_547_00022145	PGF_08225224	805	hypothetical protein
vB_Eclo_MII_002	CDS	774	1115	342	+		PGF_10827763	113	hypothetical protein
vB_Eclo_MII_002	CDS	8802	9446	645	-	PLF_547_00061555	PGF_05184720	214	hypothetical protein
vB_Eclo_MII_002	CDS	9439	9681	243	-	PLF_547_00058236	PGF_01813040	80	hypothetical protein
vB_Eclo_MII_002	CDS	9690	10460	771	-	PLF_547_00018543	PGF_00390561	256	hypothetical protein

APPENDIX 3: Annotated Genome features of bacteriophage vB_Eclo_MII_003

Genome	Feature Type	Start	End	Length	Strand	Cross-genus families (PGfams)	AA Length	Product
vB_Eclo_MII_003	CDS	10033	10194	162	+		53	Phage lysin, N-acetylmuramoyl-L-alanine amidase (EC 3.5.1.28)
vB_Eclo_MII_003	CDS	10397	10609	213	+	PGF_05437948	70	Phage protein
vB_Eclo_MII_003	CDS	10680	11231	552	+	PGF_00421723	183	Phage primase/helicase protein Gp4A
vB_Eclo_MII_003	CDS	11296	11667	372	+		123	T7-like phage primase/helicase protein
vB_Eclo_MII_003	CDS	1136	1324	189	+		62	hypothetical protein
vB_Eclo_MII_003	CDS	11697	12587	891	+	PGF_00421723	296	Phage primase/helicase protein Gp4A
vB_Eclo_MII_003	CDS	12659	13594	936	+	PGF_08740592	311	Phage DNA-directed DNA polymerase (EC 2.7.7.7)
vB_Eclo_MII_003	CDS	13630	13947	318	+		105	T7-like phage DNA Polymerase (EC 2.7.7.7)
vB_Eclo_MII_003	CDS	14101	14916	816	+	PGF_08740592	271	Phage DNA-directed DNA polymerase (EC 2.7.7.7)
vB_Eclo_MII_003	CDS	1430	1858	429	+	PGF_06014785	142	hypothetical protein
vB_Eclo_MII_003	CDS	14879	14998	120	+		39	hypothetical protein
vB_Eclo_MII_003	CDS	14998	15087	90	+		29	hypothetical protein
vB_Eclo_MII_003	CDS	15257	15490	234	+	PGF_04070011	77	Phage protein Gp5.7
vB_Eclo_MII_003	CDS	15487	15705	219	+		72	Phage protein
vB_Eclo_MII_003	CDS	15705	15794	90	+		29	hypothetical protein
vB_Eclo_MII_003	CDS	15844	16569	726	+	PGF_00031762	241	Phage exonuclease (EC 3.1.11.3)
vB_Eclo_MII_003	CDS	16551	16640	90	+		29	hypothetical protein
vB_Eclo_MII_003	CDS	16773	17021	249	+		82	hypothetical protein
vB_Eclo_MII_003	CDS	17055	17276	222	+	PGF_05140785	73	Phage protein (ACLAME 1292)
vB_Eclo_MII_003	CDS	17279	17581	303	+		100	Phage protein
vB_Eclo_MII_003	CDS	17674	17931	258	+		85	Phage host specificity protein (ACLAME 1293)
vB_Eclo_MII_003	CDS	17935	18624	690	+	PGF_08466151	229	Phage collar, head-to-tail connector protein Gp8
vB_Eclo_MII_003	CDS	182	307	126	+		41	hypothetical protein
vB_Eclo_MII_003	CDS	1852	2001	150	+		49	hypothetical protein
vB_Eclo_MII_003	CDS	18684	18914	231	+	PGF_08466151	76	Phage collar, head-to-tail connector protein Gp8
vB_Eclo_MII_003	CDS	19044	19133	90	+		29	hypothetical protein
vB_Eclo_MII_003	CDS	19103	19498	396	+	PGF_08466151	131	Phage collar, head-to-tail connector protein Gp8
vB_Eclo_MII_003	CDS	19605	20399	795	+	PGF_12668281	264	Phage capsid and scaffold
vB_Eclo_MII_003	CDS	2004	2129	126	+		41	hypothetical protein
vB_Eclo_MII_003	CDS	20396	20485	90	+		29	hypothetical protein
vB_Eclo_MII_003	CDS	20611	21660	1050	+	PGF_08799475	349	Phage major capsid protein Gp10A
vB_Eclo_MII_003	CDS	21715	21870	156	+		51	hypothetical protein
vB_Eclo_MII_003	CDS	22032	22544	513	+	PGF_04874775	170	Phage tail fiber protein / T7-like tail tubular protein A
vB_Eclo_MII_003	CDS	22544	22771	228	+		75	Phage protein
vB_Eclo_MII_003	CDS	22783	22956	174	+	PGF_07801391	57	Phage non-contractile tail tubular protein Gp12
vB_Eclo_MII_003	CDS	2302	2499	198	+		65	Phage protein
vB_Eclo_MII_003	CDS	23036	23131	96	+		31	hypothetical protein
vB_Eclo_MII_003	CDS	23161	23901	741	+	PGF_07801391	246	Phage non-contractile tail tubular protein Gp12

vB_Eclo_MII_003	CDS	23939	24112	174	+	PGF_07801391	57	Phage non-contractile tail tubular protein Gp12
vB_Eclo_MII_003	CDS	24078	24191	114	+		37	hypothetical protein
vB_Eclo_MII_003	CDS	24284	24808	525	+		174	Phage tail fiber protein / T7-like tail tubular protein A
vB_Eclo_MII_003	CDS	24811	24909	99	+		32	hypothetical protein
vB_Eclo_MII_003	CDS	2499	2711	213	+		70	hypothetical protein
vB_Eclo_MII_003	CDS	25006	25128	123	+		40	hypothetical protein
vB_Eclo_MII_003	CDS	25207	25308	102	+		33	hypothetical protein
vB_Eclo_MII_003	CDS	25348	25497	150	+		49	Phage internal (core) protein
vB_Eclo_MII_003	CDS	25497	25664	168	+	PGF_04145078	55	Phage internal (core) protein
vB_Eclo_MII_003	CDS	25657	26262	606	+	PGF_12760961	201	Phage internal (core) protein
vB_Eclo_MII_003	CDS	26255	26491	237	+		78	Phage internal (core) protein
vB_Eclo_MII_003	CDS	26507	26605	99	+		32	hypothetical protein
vB_Eclo_MII_003	CDS	26658	26813	156	+		51	hypothetical protein
vB_Eclo_MII_003	CDS	26834	28225	1392	+	PGF_12832054	463	hypothetical protein
vB_Eclo_MII_003	CDS	2809	3447	639	+		212	T7-like phage DNA-directed RNA polymerase (EC 2.7.7.6)
vB_Eclo_MII_003	CDS	28222	28530	309	+		102	Phage internal (core) protein
vB_Eclo_MII_003	CDS	28536	28820	285	+	PGF_12725872	94	Phage internal (core) protein
vB_Eclo_MII_003	CDS	28830	28958	129	+		42	hypothetical protein
vB_Eclo_MII_003	CDS	29044	29388	345	+		114	Phage internal (core) protein
vB_Eclo_MII_003	CDS	29523	29672	150	+		49	hypothetical protein
vB_Eclo_MII_003	CDS	29669	30478	810	+	PGF_04695520	269	Phage DNA ejectosome component Gp16, peptidoglycan lytic exotransglycosylase (EC 4.2.2.n1)
vB_Eclo_MII_003	CDS	30475	30933	459	+	PGF_04695520	152	Phage DNA ejectosome component Gp16, peptidoglycan lytic exotransglycosylase (EC 4.2.2.n1)
vB_Eclo_MII_003	CDS	30930	31604	675	+	PGF_04695520	224	Phage DNA ejectosome component Gp16, peptidoglycan lytic exotransglycosylase (EC 4.2.2.n1)
vB_Eclo_MII_003	CDS	313	420	108	+		35	hypothetical protein
vB_Eclo_MII_003	CDS	31670	32182	513	+	PGF_12880186	170	Phage internal (core) protein
vB_Eclo_MII_003	CDS	32182	32415	234	+	PGF_12880186	77	Phage internal (core) protein
vB_Eclo_MII_003	CDS	32474	33007	534	+		177	Phage tail fiber protein
vB_Eclo_MII_003	CDS	33001	33186	186	+		61	hypothetical protein
vB_Eclo_MII_003	CDS	33189	33290	102	+		33	hypothetical protein
vB_Eclo_MII_003	CDS	33324	33566	243	+		80	hypothetical protein
vB_Eclo_MII_003	CDS	33551	33802	252	+		83	hypothetical protein
vB_Eclo_MII_003	CDS	33916	34209	294	+		97	hypothetical protein
vB_Eclo_MII_003	CDS	34228	34458	231	+		76	hypothetical protein
vB_Eclo_MII_003	CDS	3425	3715	291	+		96	T7-like phage DNA-directed RNA polymerase (EC 2.7.7.6)
vB_Eclo_MII_003	CDS	34446	34574	129	+		42	hypothetical protein
vB_Eclo_MII_003	CDS	34590	34931	342	+		113	hypothetical protein
vB_Eclo_MII_003	CDS	34971	35168	198	+		65	hypothetical protein
vB_Eclo_MII_003	CDS	35273	35467	195	+		64	Phage holin, class II Gp17.5
vB_Eclo_MII_003	CDS	35464	35727	264	+	PGF_05281019	87	DNA packaging protein A, T7like gp18
vB_Eclo_MII_003	CDS	35847	36269	423	+	PGF_06297248	140	Phage Rz-like lysis protein Gp18.5
vB_Eclo_MII_003	CDS	36269	36376	108	+		35	hypothetical protein
vB_Eclo_MII_003	CDS	36451	37425	975	+	PGF_07972002	324	Phage terminase large subunit Gp19, DNA packaging

vB_Eclo_MII_003	CDS	3715	5472	1758	+	PGF_08961762	585	Phage DNA-directed RNA polymerase (EC 2.7.7.6)
vB_Eclo_MII_003	CDS	37422	38438	1017	+	PGF_07972002	338	Phage terminase large subunit Gp19, DNA packaging
vB_Eclo_MII_003	CDS	38486	38593	108	+		35	hypothetical protein
vB_Eclo_MII_003	CDS	38604	38714	111	+		36	hypothetical protein
vB_Eclo_MII_003	CDS	38750	38908	159	+	PGF_04272194	52	Phage protein
vB_Eclo_MII_003	CDS	39106	39213	108	+		35	hypothetical protein
vB_Eclo_MII_003	CDS	39285	39419	135	+		44	hypothetical protein
vB_Eclo_MII_003	CDS	502	618	117	+		38	hypothetical protein
vB_Eclo_MII_003	CDS	5485	5613	129	+		42	Phage protein
vB_Eclo_MII_003	CDS	5707	5940	234	+	PGF_05697581	77	Phage protein
vB_Eclo_MII_003	CDS	5945	6229	285	+		94	hypothetical protein
vB_Eclo_MII_003	CDS	6195	6749	555	+	PGF_12773210	184	DNA ligase, phage-associated
vB_Eclo_MII_003	CDS	6938	7063	126	+		41	hypothetical protein
vB_Eclo_MII_003	CDS	7057	7299	243	+		80	hypothetical protein
vB_Eclo_MII_003	CDS	7408	7662	255	+		84	Phage protein (ACLAME 1535)
vB_Eclo_MII_003	CDS	7662	7817	156	+		51	hypothetical protein
vB_Eclo_MII_003	CDS	7814	7981	168	+	PGF_09934437	55	Phage nucleotide kinase Gp1.7, phosphorylates dGMP to dGDP and dTMP to dTDP
vB_Eclo_MII_003	CDS	7968	8063	96	+		31	Phage protein
vB_Eclo_MII_003	CDS	8060	8233	174	+		57	hypothetical protein
vB_Eclo_MII_003	CDS	813	1067	255	+		84	Phage protein
vB_Eclo_MII_003	CDS	8342	9037	696	+	PGF_02997548	231	Phage single-stranded DNA-binding protein Gp2.5
vB_Eclo_MII_003	CDS	8901	9491	591	+	PGF_06491438	196	Phage endonuclease I (EC 3.1.21.2), four-way DNA junctions resolving
vB_Eclo_MII_003	CDS	9488	9940	453	+		150	Phage protein

APPENDIX 4: Annotated Genome features of bacteriophage vB_Eclo_MII_004

Genome	Feature Type	Start	End	Length	Strand	Cross-genus families (PGfams)	AA Length	Product
vB_Eclo_MII_004	CDS	10052	10183	132	+		43	Phage lysin, N-acetylmuramoyl-L-alanine amidase (EC 3.5.1.28)
vB_Eclo_MII_004	CDS	10249	10404	156	+	PGF_06446683	51	Phage endolysin
vB_Eclo_MII_004	CDS	10419	10613	195	+		64	hypothetical protein
vB_Eclo_MII_004	CDS	10707	10823	117	+		38	hypothetical protein
vB_Eclo_MII_004	CDS	10804	11637	834	+	PGF_00421723	277	Phage primase/helicase protein Gp4A
vB_Eclo_MII_004	CDS	1157	1345	189	+		62	hypothetical protein
vB_Eclo_MII_004	CDS	11580	12044	465	+		154	T7-like phage primase/helicase protein
vB_Eclo_MII_004	CDS	12128	12460	333	+		110	Phage protein
vB_Eclo_MII_004	CDS	12444	12608	165	+		54	Phage protein
vB_Eclo_MII_004	CDS	12680	12937	258	+		85	T7-like phage DNA Polymerase (EC 2.7.7.7)
vB_Eclo_MII_004	CDS	12982	13077	96	+		31	hypothetical protein
vB_Eclo_MII_004	CDS	13074	13409	336	+	PGF_08740592	111	Phage DNA-directed DNA polymerase (EC 2.7.7.7)
vB_Eclo_MII_004	CDS	13390	13686	297	+		98	T7-like phage DNA Polymerase (EC 2.7.7.7)
vB_Eclo_MII_004	CDS	1356	1502	147	+		48	hypothetical protein
vB_Eclo_MII_004	CDS	13649	13966	318	+		105	T7-like phage DNA Polymerase (EC 2.7.7.7)
vB_Eclo_MII_004	CDS	14083	14184	102	+		33	hypothetical protein
vB_Eclo_MII_004	CDS	14198	14893	696	+	PGF_08740592	231	Phage DNA-directed DNA polymerase (EC 2.7.7.7)
vB_Eclo_MII_004	CDS	14899	15018	120	+		39	hypothetical protein
vB_Eclo_MII_004	CDS	1499	1879	381	+	PGF_06014785	126	hypothetical protein
vB_Eclo_MII_004	CDS	14996	15106	111	+		36	hypothetical protein
vB_Eclo_MII_004	CDS	15301	15417	117	+		38	hypothetical protein
vB_Eclo_MII_004	CDS	15506	15724	219	+		72	Phage protein
vB_Eclo_MII_004	CDS	15780	16373	594	+	PGF_00031762	197	Phage exonuclease (EC 3.1.11.3)
vB_Eclo_MII_004	CDS	16454	16588	135	+	PGF_00031762	44	Phage exonuclease (EC 3.1.11.3)
vB_Eclo_MII_004	CDS	16570	16659	90	+		29	hypothetical protein
vB_Eclo_MII_004	CDS	16794	17063	270	+		89	hypothetical protein
vB_Eclo_MII_004	CDS	170	328	159	+		52	hypothetical protein
vB_Eclo_MII_004	CDS	17074	17217	144	+	PGF_05140785	47	Phage protein (ACLAME 1292)
vB_Eclo_MII_004	CDS	17265	17369	105	+		34	hypothetical protein
vB_Eclo_MII_004	CDS	17332	17457	126	+		41	Phage protein
vB_Eclo_MII_004	CDS	17450	17596	147	+		48	hypothetical protein
vB_Eclo_MII_004	CDS	17689	17940	252	+		83	Phage host specificity protein (ACLAME 1293)
vB_Eclo_MII_004	CDS	17952	18131	180	+	PGF_08466151	59	Phage collar, head-to-tail connector protein Gp8
vB_Eclo_MII_004	CDS	18167	18640	474	+	PGF_08466151	157	Phage collar, head-to-tail connector protein Gp8
vB_Eclo_MII_004	CDS	18700	18972	273	+	PGF_08466151	90	Phage collar, head-to-tail connector protein Gp8
vB_Eclo_MII_004	CDS	1873	2022	150	+		49	hypothetical protein
vB_Eclo_MII_004	CDS	18965	19078	114	+		37	Phage portal (connector) protein (T7-like gp8)
vB_Eclo_MII_004	CDS	19104	19199	96	+		31	hypothetical protein
vB_Eclo_MII_004	CDS	19274	19561	288	+		95	Phage portal (connector) protein (T7-like gp8)
vB_Eclo_MII_004	CDS	19639	19737	99	+		32	hypothetical protein
vB_Eclo_MII_004	CDS	19737	19919	183	+		60	hypothetical protein
vB_Eclo_MII_004	CDS	19960	20502	543	+	PGF_04925984	180	Phage capsid and scaffold

vB_Eclo_MII_004	CDS	2025	2150	126	+		41	hypothetical protein
vB_Eclo_MII_004	CDS	20513	20608	96	-		31	hypothetical protein
vB_Eclo_MII_004	CDS	20659	20787	129	-		42	hypothetical protein
vB_Eclo_MII_004	CDS	20788	21612	825	-		274	hypothetical protein
vB_Eclo_MII_004	CDS	2151	2270	120	+		39	hypothetical protein
vB_Eclo_MII_004	CDS	21597	21743	147	+		48	hypothetical protein
vB_Eclo_MII_004	CDS	21800	21937	138	+		45	hypothetical protein
vB_Eclo_MII_004	CDS	21888	22025	138	+		45	hypothetical protein
vB_Eclo_MII_004	CDS	22113	22556	444	+		147	Phage tail fiber protein / T7-like tail tubular protein A
vB_Eclo_MII_004	CDS	22556	22783	228	+		75	Phage protein
vB_Eclo_MII_004	CDS	23045	23140	96	+		31	hypothetical protein
vB_Eclo_MII_004	CDS	2322	2519	198	+		65	Phage protein
vB_Eclo_MII_004	CDS	23294	23911	618	+		205	Phage tail fiber protein / T7-like tail tubular protein A
vB_Eclo_MII_004	CDS	23949	24203	255	+	PGF_07801391	84	Phage non-contractile tail tubular protein Gp12
vB_Eclo_MII_004	CDS	24205	24462	258	+		85	Phage tail fiber protein / T7-like tail tubular protein A
vB_Eclo_MII_004	CDS	24520	24726	207	+		68	hypothetical protein
vB_Eclo_MII_004	CDS	24735	24878	144	+		47	hypothetical protein
vB_Eclo_MII_004	CDS	24871	25017	147	+		48	hypothetical protein
vB_Eclo_MII_004	CDS	25014	25148	135	+		44	Phage tail fiber protein / T7-like tail tubular protein A
vB_Eclo_MII_004	CDS	2519	2731	213	+		70	hypothetical protein
vB_Eclo_MII_004	CDS	25213	25314	102	+		33	Phage internal (core) protein
vB_Eclo_MII_004	CDS	25287	25682	396	+	PGF_04145078	131	Phage internal (core) protein
vB_Eclo_MII_004	CDS	25667	25846	180	+	PGF_12760961	59	Phage internal (core) protein
vB_Eclo_MII_004	CDS	25885	26064	180	+		59	hypothetical protein
vB_Eclo_MII_004	CDS	26131	26268	138	+		45	hypothetical protein
vB_Eclo_MII_004	CDS	26261	26731	471	+	PGF_05947970	156	Phage DNA ejection component, internal virion protein Gp15
vB_Eclo_MII_004	CDS	26841	27164	324	+	PGF_12832054	107	Phage internal (core) protein
vB_Eclo_MII_004	CDS	27174	27293	120	+		39	hypothetical protein
vB_Eclo_MII_004	CDS	27290	27520	231	+		76	Phage internal (core) protein
vB_Eclo_MII_004	CDS	27517	27822	306	+		101	Phage internal (core) protein
vB_Eclo_MII_004	CDS	27819	28061	243	+		80	Phage internal (core) protein
vB_Eclo_MII_004	CDS	28115	28534	420	+		139	Phage internal (core) protein
vB_Eclo_MII_004	CDS	2829	3491	663	+		220	T7-like phage DNA-directed RNA polymerase (EC 2.7.7.6)
vB_Eclo_MII_004	CDS	28540	28653	114	+	PGF_12725872	37	Phage internal (core) protein
vB_Eclo_MII_004	CDS	28707	29051	345	+		114	Phage internal (core) protein
vB_Eclo_MII_004	CDS	29048	29677	630	+	PGF_06226557	209	Phage internal (core) protein
vB_Eclo_MII_004	CDS	29674	29904	231	+		76	Phage internal (core) protein
vB_Eclo_MII_004	CDS	3	173	171	+		56	hypothetical protein
vB_Eclo_MII_004	CDS	30052	30480	429	+		142	Phage internal (core) protein
vB_Eclo_MII_004	CDS	30692	31609	918	+	PGF_04695520	305	Phage DNA ejection component Gp16, peptidoglycan lytic exotransglycosylase (EC 4.2.2.n1)
vB_Eclo_MII_004	CDS	31675	32088	414	+		137	Phage internal (core) protein
vB_Eclo_MII_004	CDS	32085	32186	102	+		33	hypothetical protein
vB_Eclo_MII_004	CDS	32186	32431	246	+	PGF_12880186	81	Phage internal (core) protein
vB_Eclo_MII_004	CDS	32564	33349	786	+		261	Phage tail fiber protein
vB_Eclo_MII_004	CDS	33396	33803	408	+		135	hypothetical protein
vB_Eclo_MII_004	CDS	334	441	108	+		35	hypothetical protein
vB_Eclo_MII_004	CDS	33917	34210	294	+		97	hypothetical protein
vB_Eclo_MII_004	CDS	34189	34458	270	+		89	hypothetical protein

vB_Eclo_MII_004	CDS	34446	34574	129	+		42	hypothetical protein
vB_Eclo_MII_004	CDS	34590	35036	447	+		148	hypothetical protein
vB_Eclo_MII_004	CDS	3494	3922	429	+	PGF_08961762	142	Phage DNA-directed RNA polymerase (EC 2.7.7.6)
vB_Eclo_MII_004	CDS	35017	35232	216	+		71	hypothetical protein
vB_Eclo_MII_004	CDS	35275	35469	195	+		64	Phage holin, class II Gp17.5
vB_Eclo_MII_004	CDS	35466	35663	198	+	PGF_05281019	65	DNA packaging protein A, T7-like gp18
vB_Eclo_MII_004	CDS	35729	35818	90	+		29	hypothetical protein
vB_Eclo_MII_004	CDS	35850	36272	423	+	PGF_06297248	140	Phage Rz-like lysis protein Gp18.5
vB_Eclo_MII_004	CDS	36272	36658	387	+		128	Phage HNH homing endonuclease (ACLAME 27)
vB_Eclo_MII_004	CDS	36701	37027	327	+	PGF_07972002	108	Phage terminase large subunit Gp19, DNA packaging
vB_Eclo_MII_004	CDS	37027	37176	150	+	PGF_07972002	49	Phage terminase large subunit Gp19, DNA packaging
vB_Eclo_MII_004	CDS	37245	37427	183	+	PGF_07972002	60	Phage terminase large subunit Gp19, DNA packaging
vB_Eclo_MII_004	CDS	37424	38110	687	+	PGF_07972002	228	Phage terminase large subunit Gp19, DNA packaging
vB_Eclo_MII_004	CDS	38194	38463	270	+	PGF_07972002	89	Phage terminase large subunit Gp19, DNA packaging
vB_Eclo_MII_004	CDS	38489	38596	108	+		35	hypothetical protein
vB_Eclo_MII_004	CDS	38607	38717	111	+		36	hypothetical protein
vB_Eclo_MII_004	CDS	38814	38945	132	+		43	hypothetical protein
vB_Eclo_MII_004	CDS	39159	39281	123	+		40	hypothetical protein
vB_Eclo_MII_004	CDS	3919	4032	114	+		37	hypothetical protein
vB_Eclo_MII_004	CDS	39278	39424	147	+		48	hypothetical protein
vB_Eclo_MII_004	CDS	4095	5492	1398	+	PGF_08961762	465	Phage DNA-directed RNA polymerase (EC 2.7.7.6)
vB_Eclo_MII_004	CDS	523	639	117	+		38	hypothetical protein
vB_Eclo_MII_004	CDS	5505	5705	201	+		66	Phage protein
vB_Eclo_MII_004	CDS	5728	5961	234	+	PGF_05697581	77	Phage protein
vB_Eclo_MII_004	CDS	5966	6250	285	+		94	hypothetical protein
vB_Eclo_MII_004	CDS	6216	6935	720	+	PGF_12773210	239	DNA ligase, phage-associated
vB_Eclo_MII_004	CDS	7002	7319	318	+	PGF_05993939	105	Phage-associated ATPdependent DNA ligase (EC 6.5.1.1)
vB_Eclo_MII_004	CDS	7432	7686	255	+		84	Phage protein (ACLAME 1535)
vB_Eclo_MII_004	CDS	7686	8006	321	+	PGF_09934437	106	Phage nucleotide kinase Gp1.7, phosphorylates dGMP to dGDP and dTMP to dTDP
vB_Eclo_MII_004	CDS	7993	8088	96	+		31	Phage protein
vB_Eclo_MII_004	CDS	8085	8258	174	+		57	hypothetical protein
vB_Eclo_MII_004	CDS	834	1088	255	+		84	Phage protein
vB_Eclo_MII_004	CDS	8366	9451	1086	+	PGF_02997548	361	Phage single-stranded DNA-binding protein Gp2.5
vB_Eclo_MII_004	CDS	9507	9959	453	+		150	Phage protein
vB_Eclo_MII_004	CDS	1318	1464	147	-	PGF_04881348	48	hypothetical protein
vB_Eclo_MII_004	CDS	140	262	123	-		40	hypothetical protein
vB_Eclo_MII_004	CDS	1491	1580	90	-		29	hypothetical protein
vB_Eclo_MII_004	CDS	1614	1790	177	-		58	hypothetical protein
vB_Eclo_MII_004	CDS	1781	1885	105	-		34	hypothetical protein
vB_Eclo_MII_004	CDS	276	536	261	+		86	hypothetical protein
vB_Eclo_MII_004	CDS	533	742	210	-		69	hypothetical protein
vB_Eclo_MII_004	CDS	749	859	111	-		36	hypothetical protein
vB_Eclo_MII_004	CDS	75	164	90	-		29	hypothetical protein
vB_Eclo_MII_004	CDS	983	1192	210	-		69	hypothetical protein